1-1-2003

Thermal method for measuring perfusion in transplanted organs

Fredericka Delores Brown
University of Nevada, Las Vegas

THERMAL METHOD FOR MEASURING PERFUSION IN TRANSPLANTED ORGANS

by

Fredericka Delores Brown

Bachelor of Science
Xavier University of Louisiana
1996

Master of Science
University of Nevada, Las Vegas
1998

A dissertation submitted in partial fulfillment
of the requirements for the

Doctor of Philosophy Degree in Mechanical Engineering
Howard R. Hughes Department of Mechanical Engineering
Howard R. Hughes College of Engineering

Graduate College
University of Nevada, Las Vegas
August 2003

UNLV
UNIVERSITY OF NEVADA LAS VEGAS

Dissertation Approval

The Graduate College
University of Nevada, Las Vegas

Friday, August 1, 2003

The Dissertation prepared by

FREDERICKA D. BROWN

Entitled

Thermal Method for Measuring Perfusion in Transplanted Organs

is approved in partial fulfillment of the requirements for the degree of

Doctor of Philosophy

Examination Committee Chair

Examination Committee Member

Dean of the Graduate College

Examination Committee Member

Examination Committee Member

Graduate College Faculty Representative

PR/1017-52/1-00

ABSTRACT

Thermal Method for Measuring Perfusion in Transplanted Organs

by

Fredericka Delores Brown

Dr. Robert F. Boehm, Examination Committee Chair
Professor of Mechanical Engineering
University of Nevada, Las Vegas

Adequate blood flow to the graft kidney is critical in the postoperative care of the transplant patient. Many factors can lead to disturbance in blood flow to the kidney, including the various effects of medication or volume status of the patient. Current methods to monitor blood flow depend on either duplex ultrasound or nuclear medicine renal flow scan. These modalities do not provide continuous monitoring of renal blood flow.

A non-invasive technique to the organ is developed that will allow for the continuous qualitative and quantitative monitoring of blood perfusion in a kidney during postoperative periods utilizing an easily extracted thermistor probe. The continuous assessment of blood perfusion in the kidney may allow timely therapeutic maneuvers to correct any abnormality in blood flow and prevent graft thrombosis and loss.

The technique involves the use of a thermistor heating/measurement system. Results of the measurements are used with numerical calculations to infer qualitative levels of perfusion.

A two-dimensional axisymmetric finite difference model for predicting regional blood perfusion is presented. The system consists of two semi-infinite bodies, the kidney and a specified adjacent medium, and a spherical thermistor. The thermistor is treated as a point source and located adjacent to both media. The initial temperature of the system is taken as the baseline temperature. At $t=0^{+}$, the temperature of the thermistor is increased by 0.5°C of the baseline temperature and a transient, constant temperature heating is imposed at the heat source surface. Heating is induced for a predetermined amount of time and terminated. The system is allowed to return to baseline temperatures and the process is repeated. The "bioheat equation" is used in the development of the governing equations for the system. Different perfusion situations within the two media are simulated to assess the sensitivity of the technique to a variety of possibilities that might be found in actual surgery. The method yields temperature field distributions along with a qualitative and quantitative measurement of regional blood perfusion. Results of the numerical model are then validated with analytical and experimental results.

TABLE OF CONTENTS

LIST OF FIGURES

LIST OF TABLES

ACKNOWLEDGEMENTS

It is with pleasure that I acknowledge the support and inspiration of Dr. Robert F. Boehm, my thesis and dissertation advisor, who has supplied me with technical ideas, friendship and encouragement since my early years at the University of Nevada Las Vegas. He has been a great mentor and an even greater role model.

I would also like to acknowledge Mrs. Marcia Boehm for being like a mother to me. Her guidance, support and understanding helped me through the turbulent times.

My special thanks goes to Bill O'Donnell for his electrical engineering design assistance. He volunteered his free time to help with the design of the control box.

I wish to give an extra special thanks to Robert Brown, Olive Brown, Byron Brown, Derek Brown and Jasmine Brown for their love and constant support throughout the years.

I would like to thank the Bill and Melinda Gates Foundation, NIH and MGE@MSA for their support over the last few years.

CHAPTER 1

INTRODUCTION

1.1 Bioheat Transfer

Temperature is the principal controlling factor in everyday physiological phenomena occurring in biological systems. The innate survival of the biological system depends on its ability to maintain and control body temperature. If the body temperature of the system is altered in response to external conditions, such as temperature variation due to weather or performance of traditional and diagnostic medical procedures, normal occurring physiological functions may be sacrificed. An analysis of many of the major processes occurring in biological systems due to the influences of external factors and physiological processes requires an understanding of heat transfer mechanisms. Therefore, it is evident why the knowledge of how temperature can be monitored and controlled in living systems is of great importance in the assessment of normal and abnormal physiological function, determination of diseased states, and the treatment of diseased states.

The analysis of thermal energy transport in the biological system due to physiological processes and external effects is termed bioheat transfer. Due to the complex interactions between tissue perfusion, conduction, convection, and tissue

metabolism, the physiological processes and temperature variations in the biological system can make for a more grueling analysis than that of the traditional non-living system. This system is further complicated due to the anisotropic and inhomogeneous nature of tissue. These issues lead to differences in thermal properties throughout the biological system. The assessment of thermal properties also allows for the thermal mapping of tissue properties. Applications of bioheat transfer include the thermoregulation process, estimation of tissue blood flow, breast cancer detection, soft tissue trauma, infection, environmental stress, and viability of ischemic or re-implanted tissue, and viability of skin flaps.

Thermal energy transport in a biological system is mainly achieved through conduction and convection modes of heat transfer. Thermal conduction is a measure of the ability of a system to transport heat from a region of higher temperature to that of a lower temperature. Convection heat transfer is energy transfer due to random molecular motion where energy transfer occurs due to bulk, or macroscopic, motion of the fluid. In the system, conduction heat transfer is proportional to the local temperature gradient and the intrinsic tissue thermal conductivity. The convection heat transfer is related to the analysis of fluid movement through vascular channels, ducts, or interstitial spaces. The most important properties needed for heat transfer analyses are thermal conductivity, k, and the thermal diffusivity, α.

1.2 Tissue Perfusion

Some of the most important tasks encountered in the fields of medicine and physiological sciences are the analysis and assessment of tissue blood perfusion rates,

blood transmission in the microcirculation, and heat generation rates due to metabolism and external sources in the biological system. Tissue perfusion, measure of blood flow through a capillary bed, is an important factor in tissue and organ transplants, cancer therapy, and the assessment of viable organs. Perfusion analyses occur daily in every intensive care unit, hospital, outpatient care unit, and emergency room throughout the world. Despite the notable importance of perfusion analyses, there is no widely accepted clinical method to ascertain blood perfusion rates. Current clinical methods used to determine tissue perfusion rates are typically highly invasive, exorbitant in cost, lack the ability to provide continuous monitoring of perfusion rates, or lack data accuracy or reproducibility.

The ability to have a non-invasive, inexpensive, continuous monitoring system, in theory, may allow timely therapeutic maneuvers to correct any abnormality in blood flow. Present available assessments of perfusion typically involve the addition of a foreign substance into the biological system. Common substances are dyes, radioactivity, ultrasound, X-rays, electricity, and heat. Microsphere, gas, and dye dilution techniques fall short when data accuracy and reproducibility are a must. The advantage of localized heating when compared to other approaches is that it produces no systemic effects. In addition, low levels of thermal energy are easily tolerated by the biological system. Heat is quickly dissipated in the surrounding tissue, which eliminates problems frequently encountered with re-circulation in other perfusion measurement methods.

1.3 Objective of Research

Sufficient renal blood perfusion is extremely important to successful implantation of the kidney. If insufficient blood perfusion occurs, transplant surgeons have available some means of stimulating perfusion if the need is known. What is critical to this is a minimally invasive method of inferring the presence of satisfactory perfusion.

The objective of this study is to analyze whether the presence of tissue perfusion in an organ can be assessed using a noninvasive self-heated thermal diffusion probe. This involves thermal numerical modeling of the system along with in vivo experimentation. A thermal numerical model is used to characterize the heat transfer processes occurring in the system. Power dissipation will be related to the perfusion rate, higher power dissipation will signify an increase in perfusion.

The experimentation will be carried out in three stages. The first stage involves the determination of sensitivity of thermal conductivity measurements in liquids and plastic. The second stage and third stages, not actually a part of this dissertation, will be carried out when the protocols for animal experimentation and human experimentation have been approved. The second stage will be done to determine perfusion using thermistor measurement in the kidney of small animals and the second phase will involve human test cases. In the second phase of the experimentation, the probe method, described below, will be used on a vital but anesthetized rat. The probe will be inserted adjacent to the kidney. Measurements will be taken. Then perfusion in the kidney is ceased. Measurements will be taken again. Then perfusion in the kidney is ceased. Measurements will be taken again. Finally, the animal is sacrificed and the

measurements will be taken for the third time. Inferences about the sensitivity of the technique to renal blood flow and adjacent tissue blood flow will be made.

A transient, constant temperature technique for a heated thermistor probe is used to determine tissue blood flow. This process is known as the step temperature heating technique. In this technique the spherical thermistor probe is initially in thermal equilibrium with the surrounding tissue and then power is switched on. After the initiation of power, the probe temperature rises to a preset value. The thermistor temperature is maintained at this constant by a feedback controller that constantly adjusts power. The thermistor is forced to undergo a step change from ambient temperature to the set point temperature in a short time period. The baseline values are measured before the power is turned on and during the cooling periods of the step heating technique. The measurement of the power dissipated through the system over a set time period during the process will be related to the perfusion rate.

To evaluate the potential of this experimental approach, the situation is modeled numerically. In this analysis, the system is taken to be two semi-infinite bodies, the kidney and a specified adjacent medium. The thermistor is located between the kidney and the adjacent medium and is the source of heat input to the system in a manner needed to accomplish the experimental measurements. The adjacent medium is characterized with tissue properties different from those of the kidney. Two separate governing equations, one each for the kidney and one for the adjacent medium are developed. A transient, constant temperature heating is imposed at the thermistor surface. Continuity of temperature and heat flux is assumed between the kidney and the adjacent medium. The end result is an assessment of the effectiveness in monitoring blood perfusion with

the thermistor approach. In essence this is determined by the ability to discern kidney perfusion variations from the rate of heating required.

1.3.1 Future Animal Experiments

Male Sprague Dawley outbred rats that have been kept according to accepted animal laboratory standards would be used. A laparotomy incision will be made to expose internal organs including liver and kidneys. The thermistor probe is used to take measurements of surface blood flow in these organs both with the incision open and closed to assess the effect of surrounding tissues. After experimentation animals are euthanized according to accepted methods.

1.3.2 Future Human Experiments

Humans undergoing kidney transplantation will be tested using the thermistor probes. These patients will be treated in the transplant service at University Medical Center, Las Vegas, NV. Prior to the start of human experiments, protocols will be written for the acceptance of the Institutional Review Board. Probes will be inserted at the time of transplant and exit through a small skin incision near the transplant. Measurements will be taken after the transplant. The probe will be removed several days after the transplant.

1.4 Significance of Research

The non-invasive method of blood perfusion determination has implications that affect a significant number of organ transplant procedures. The importance of being able to quantify perfusion after kidney transplant surgery aids the surgeon in making critical decisions concerning the type of anti-rejection protocols to utilize if perfusion problems

are determined early post-operatively. Perfusion rates in the kidneys are among the highest found in mammalian organs due to its filtration and re-absorption functions. Thermal methods are inherently attractive because the deposited thermal energy is typically small enough that the tissue is not damaged during the determination process of perfusion. The capability of some thermal methods to follow and detect temporal variations of blood perfusion "in vivo" and essentially in a continuous manner is significantly beneficial in various fields of physiological and medical practice and research. Complications of organ transplant procedures are greater than other transplant surgeries. The second most common transplant surgery in the United States is the kidney transplant. Kidney transplantation is a life saving procedure when it's done for those with end stage kidney disease. A patient can be treated with dialysis until a kidney donor can be found. The most common cause of kidney failure is diabetes.

Pre-renal causes of kidney failure may include cardiac failure, inadequate volume status of the patient, or mechanical problems with the inflow artery. Intra-renal causes may include afferent arteriole constriction due to cyclosporine, a widely used immunosuppressant, or efferent arteriole dilation, due to an angiotensin-converting enzyme inhibitor, a common anti-hypertensive medication. Post-renal causes may include compression by a hematoma or lymphocele, or mechanical problems with the renal vein, such as thrombosis or loss. All of these can be corrected if properly detected. If not, the problems may lead to prolonged ATN (acute tubular necrosis), and even graft thrombosis and loss.

Maintaining adequate blood flow to the transplanted kidney is critical in the post-operative care of the transplant patient. Many factors can lead to disturbance in blood

flow to the kidney, including volume status of the patient, various effects of medication, or extrinsic compression from hematoma or lymphoccle. Blood flow to the kidney can be entirely disrupted due to arterial or venous thrombosis. Current methods to monitor blood flow depend on either duplex ultrasound or nuclear medicine renal flow scan.

Thus, measurement of tissue perfusion is of obvious importance in clinical situations such as the immediate post-operative period after renal transplantation. Here, maintenance of renal perfusion is crudely correlated with renal function, that is, the production of urine and clearance of metabolic waste. It can also be directly demonstrated with radiological studies. Currently, the duplex ultrasound and the nuclear medicine renal blood flow scan are the two most commonly used modalities for this purpose. These modalities however do not provide continuous monitoring of renal blood flow. Continuous monitoring, at least in theory, may allow timely therapeutic maneuvers to correct any abnormality in blood flow.

This will aid in providing post-operative care following renal transplant surgery. This method will give the surgeon the knowledge needed in determination of means for stimulating tissue perfusion is needed, if any. Previous numerical and analytical studies by numerous researchers to (Adams 1985, Chen 1977, 1980, 1981, Bowman 1985, Chato 1985) show the general applicability of a heated thermistor to the determination of perfusion rates, but this isn't done in the less direct, but surgically more appropriate manner presented here.

The determination of renal flow implicates more than the successful implantation of the transplanted organ. It is can also help in the implication of disease states that are shown to compromise renal function. There are a variety of patho-physical conditions

that are shown to disrupt renal function. The most important of these states are nephrectomy, ureteric obstruction, and renal artery stenosis, diabetes and ischaemia and reperfusion injuries. The interruption of normal renal function has wide range implications. Assessment of total renal blood flow is therefore imperative in the understanding and treatment of these patho-phyiological states.

Currently, there is no ideal method to assess renal blood flow. The microsphere method of renal blood flow deduction is the most widely used technique to date. It is an invasive process in which an injection of a small volume containing radionucletide-labeled microspheres are entered into the left atrium, left ventricle or possibly the root of the aorta.

By monitoring power requirements of the heated thermistor, a measure of both thermal conductivity and perfusion can be obtained. The more perfused the medium the greater the power required.

CHAPTER 2

LITERATURE SURVEY

2.1 Introduction

Many important perfusion problems related to blood flow do not require a mathematical solution of the actual volume flow per unit time, but only require information as to whether flow has increased, decreased, or remained constant. This determination of tissue perfusion is of interest to medical professionals and engineers. Although a quantitative study is not necessary, the ability to determine tissue perfusion while adhering to stringent clinical requirements is always necessary in the engineering and medical environment.

Maintaining stringent clinical requirements can prove to be quite tasking. Techniques for measuring tissue perfusion in clinical situations must be safe for the patient, supply accurate and reproducible results, unlimited availability, and simple to operate. Researchers such as Bowman (1992), Chen (1981), Holmes (1983), Balasubramaniam (1977), and Chato (1985) have developed measuring techniques that meet required clinical standards. These measurement techniques are based on numerical models that access thermal properties, temperature variations, or energy variations as a function of radius and time. The assessment of these values aid in the determination of tissue perfusion. The basis of these mathematical models is the development of the

bioheat equation or energy balance equation involving biological media properties. In the end, a comparison is done between the numerically derived solution with those of the experimental results. The development of numerical and experimental models has helped in improving currently used methods to determine tissue perfusion.

The assessment of tissue perfusion is usually determined indirectly or directly by evaluating thermal properties such as conduction and diffusion for the biological media in question. The best match of the solution of the theoretical model to the experimentally measured temperature is then produced by systematically varying the values thermal properties in the analytical solution until the theoretical and experimental temperature difference is minimized. The history of measuring thermal properties and tissue perfusion using thermal techniques has been investigated and reviewed by a number of researchers including Bowman et al. (1992), Jain (1978), Holmes and Chen (1983), Valvano et al. (1984, 1994), Walsh (1984), Chato (1985), Bowman (1985), and Kress and Roemer (1987).

This chapter discusses various mathematical models and thermal experimental models that have been developed over the previous years. The mathematical models employ a solution of the bioheat equation.

2.2 Evolving Thermal Methods for Tissue Blood Flow Measurements

The use of thermal methods for determining blood flow dates back to 1926 when Gibbs introduced a thermoelectric method. The thermoelectric method utilized a needle that was supplied with a constant amount of heat. This needle was invasively placed into a vessel or tissue in question. There would be a temperature variation in the needle

depending on an increased flow of blood or a decreased flow of blood. The increased flow of blood would cool the needle, whereas a decreased flow in blood would allow the needle to heat up. Therefore, the needle temperature would vary inversely with the flow of blood. By determining the temperature of the needle, a qualitative analysis can be done.

In 1933 Gibbs introduced a probe method for determining blood flow. The probe method of Gibbs utilized a thermocouple that was to be inserted into the tissue or vessel in question. The thermocouple was provided with a constant electrical power. This method involved measuring the temperature difference between a heated and unheated thermo-junction of a thermocouple and relating it to the measure of blood flow in the region. He found that this temperature difference was inversely related to the rate of blood flow. In the end, a quantitative solution related to volume blood flow per minute was given and a determination of variability in flow was made.

Since the thermoelectric needle and thermal probe methods of Gibbs (1933), there have been numerous methods developed on the basis of his theory. In 1952, Grayson improved the probe method of Gibbs (1933) by utilizing the concept of manual feedback. This concept allowed the manual adjustment of heating power in the thermistor bead, which helped maintain a constant temperature increment above baseline conditions within the probe. The amount of heating power required while maintaining this constant temperature is related proportionally to the amount of thermal energy transported from the thermistor bead to the system.

In 1968, Chato utilized the methods of Gibbs and Grayson and developed a single, spherical thermistor bead method that allowed the bead to be used as a sensing

and heating device. This was the development of what is known as the thermal diffusion probe. The thermal diffusion probe consists of an electronic feedback controller used to maintain the thermistor at a specified temperature above the initially measured equilibrium temperature. The thermistor is first used in passive mode to measure the baseline temperature. Next, electrical power is applied to the thermistor at a time varying rate to hold the thermistor at a constant temperature increment above the measured baseline temperature. The electrical energy supplied to the thermistor to maintain a predetermined fixed temperature increment is monitored as a function of time. The electrical power is dissipated by thermal conduction from the probe into the tissue. The measured electrical power required when maintaining a constant temperature increment depends upon the heat transfer characteristics of the tissue surrounding the bead. The presence of blood flow augments the dissipation of heat in the tissue. Thermal conductivity of the media can be determined directly from a measurement of the heat flux per unit area and the temperature gradient.

Since the development of Chato's first practical use of the thermal probe, various probe techniques have been developed. The commonalties in all thermal probe techniques is the use of a thermistor bead to invasively or non-invasively deliver heat as well monitoring heat removal. In all of these techniques heat is introduced into the biological media of interest and is dissipated by conduction through the tissue and by convection with blood perfusion.

Significant developments in the thermal probe method have occurred since Chato reported his method. Balsasubramaniam et al. (1974) were able to apply the thermal probe method to noninvasive surface measurements. Patel (1987) and Walsh (1984)

improved upon the method of Balsasubramaniam (1974) when they devised a way to account for the temperature variation within the thermal measuring bead. Chen (1981) proposed an alternate operational mode with a thermistor of smaller size in relation to previously used beads.

Thermal dilution techniques were also used to measure tissue perfusion (Zajic 1975, Carter and Atkinson 1973, Gisselson and Ericsson 1981). This technique involved the dissection of the vessel of interest. Once the vessel has been dissected, an indicator is injected at a constant speed in the direction opposite blood flow. This occurs until the mixture of blood and indicator reaches an equilibrium temperature. Two thermistors are used in this technique, one to measure the temperature of the indicator, and another to measure the temperature of the blood/indicator mixture.

In addition to the thermal dilution method, heat clearance has been a method used by Muller-Schauenberg et al. (1975) and Coremans et al. (1985). The method utilizes two thermistors, one is used for heating at a predetermined level above ambient tissue temperature, and the other thermistor is unheated and used as a temperature sensor. Two modes of operation occur in this method: non-heated mode and heated mode. In the non-heated mode, both thermistors are used as sensing devices to determine local temperature. In the heated mode, one thermistor remains in sensing mode and the other is used as the heating device by supplying heat to increase equilibrium temperature. Flow alterations are determined by temperature variations within the system.

Thermal clearance techniques can be subdivided into five categories (a) noninvasive vs. invasive, (b) steady state vs. transient, (c) qualitative vs. quantitative, (d) self-heating vs. external, (e) spherical vs. cylindrical measuring bead. Transient

techniques have several advantages over those of steady state. They tend to allow for fast measurements, are unaffected by spatial gradients, and yield more information than the steady state techniques. In the transient techniques only a single thermistor is involved for temperature measuring and sensing functions. In transient techniques, the thermistor is used as a sensing device to measure baseline temperatures. Invasive techniques require the implantation of the device in the tissue of interest. This may lead to blood flow stoppage, etc. The cylindrical geometry has numerous disadvantages when compared with the spherical geometry. In the cylindrical geometry, a relatively long probe is needed to satisfy the assumption of purely radial flow. Also, with the constant heat input technique, the maximum temperature at the probe increases continually creating a burn hazard unless the experiment is terminated in time.

Constant temperature techniques provide a temperature field and measurement volume that is less dependent on the tissue's thermal properties and more uniform in extent and temperature than obtained using constant power techniques. The most widely utilized thermal clearance techniques can be classified into three categories, based on how their method of how heat is diffused within the media. These categories are: (a) thermistor sensing bead with a change in temperature, (b) thermistor sensing bead with a pulse heat input and (c) thermistor measuring bead with a step change in heat input.

Measurement protocols for the determination of tissue blood flow and thermal conductivity may be classified according to continuous versus transient methods and constant power versus constant temperature. Continuous methods employ a separate temperature reference point outside the region of "thermal influence" of the heated element to continuously monitor baseline temperature. Transient methods require only a

single temperature point. Baseline conditions established at the heating point before each measurement, are unaffected by spatial temperature gradients. Constant temperature procedures involve maintaining a constant incremented probe tissue temperature above equilibrium temperature and the determination of tissue blood flow and thermal conductivity by analysis of thermal power. Constant power procedures involve maintaining a constant thermal power into the tissue and the determination of tissue blood flow and thermal conductivity by analysis of probe/tissue temperature. Analysis of computed temperature profiles conducted with constant temperature procedures versus constant power procedures indicate that constant temperature procedures have the advantage of producing a temperature field and measurement volume that are less dependent on medium thermal properties.

Some of the more notable and promising techniques of measuring tissue perfusion are those of the thermal clearance methods (Chen et al. 1980, Chen et al. 1981, Holmes and Chen 1983, Muller-Schauenburg 1975). The most developed and widely used thermal clearance method is that of the self-heated thermistor bead technology. These methods have great potential because all of the necessary stringent clinical requirements are achieved while providing real time measurements of temperature, intrinsic or effective thermal conductivity, thermal diffusivity, and perfusion in small volumes of tissue. Thermal probe techniques are have been widely used to determine the thermal properties and tissue perfusion. The self-heated thermistor bead technology utilizes a thermistor as a point heating source and a temperature sensor. Measurement of temperature at the surface of perfused tissue can lead to the calculation of blood perfusion with in tissue. Numerous researchers have validated the feasibility of this method. The

relationship between the applied thermistor power and the resulting thermistor temperature rise are used in determination of the above properties and perfusion.

2.3 Mathematical Models

The transfer of heat in perfused tissue occurs due to the modes of conduction and convection. Heat is either gained or lost in a tissue due to its interaction with adjacent media at different temperatures or its interaction with circulating fluids. Convection occurs when there is a significant difference between the temperature of blood and the tissue through which it flows. Therefore, the conduction and convection effects occurring in the system can describe the amount of heat energy transfer through a tissue. Conduction and convection effects are related to tissue by the tissue thermal properties, temperature variation, and surface area of the system. Together these factors are fundamental in the assessment of tissue perfusion.

Numerous mathematical models have been developed that provide solutions of temperature distribution, thermal properties, and perfusion of tissue. The most widely used bioheat model to date is that of Pennes (1948). It was the first notable undertaking in quantifying the heat transfer contribution of tissue perfusion. Pennes originally developed his model to describe the transverse temperature profile in the human forearm. Since Pennes' bioheat model, many investigators have used his model as the basis for the development of alternative models. The alternative models included terms that accounted for effects of vessel size (Anderson 1994, Huang et al. 1996, Legendik 1990, and Chato 1980) countercurrent heat exchange (Lemons 1987, Chen and Holmes 1980, Song 1987, Weinbaum and Jiji 1984,1985,1989, and Baish 1986).

Chato (1968) was the first to solve the bioheat equation for the time dependent perfused tissue response to a heated thermistor. Balasubramaniam and Bowman (1974,1977) extended the thermal model to include the spatial variation of temperature within the spherical thermistor. Jain (1978, 1979) developed a thermal model that included a passive glass shell surrounding the active heated thermistor. Valvano et al. (1983) obtained a closed form transient solution which improved the accuracy of the thermal diffusivity measurements. Holmes and Chen (1983) developed a measurement technique, which heated the thermistor with a pulse of power and monitored the temperature decay. Valvano et al. (1987) used finite elements to validate the thermal conductivity measurements with a realistic thermistor geometry and electrical heating pattern.

2.3.1 Pennes Bioheat Model

The most noted investigator in the field of bioheat transfer was Pennes (1948). He presented a mathematical model of heat transfer in a living system that determined the temperature distribution in the human forearm. It has been widely used and has been found valid for tissue situations other than the forearm. In the mathematical model of Pennes, his major assumption was thermal energy transfer between blood vessels and surrounding tissue occurred predominately in the capillaries. Other assumptions in the development of Pennes bioheat equation included the effect of blood perfusion as isotropic and homogeneous and thermal equilibrium occurred in the microcirculatory capillary bed. He described this thermal energy transfer occurring due to perfusion as a non-directional heat source. His model correctly predicted that the intrinsic thermal conductivity could be measured in perfused tissue independent of perfusion rate. When

his mathematical model is used on macroscopic tissue temperature clearance measurements he provided reasonable agreement with experimental results for temperature decay in the vicinity of constant temperature of pulsed overheat probe.

The bioheat equation is described mathematically by

$$(\rho c)_t \frac{\partial T_t}{\partial t} = k_t \nabla^2 T_t + (\rho c \omega)_b (T_a - T_v) + q_m \quad (1)$$

where

T_t is the tissue temperature,

ω_b is the blood perfusion rate,

ρ is the density of blood,

c is the specific heat of blood,

T_a is the arterial blood temperature,

T_v is the venous blood temperature, and

q_m is the metabolic heat generation.

The major advantage of the Pennes model is that the added term to account for heat transfer due to perfusion is linear with temperature, which facilitates the solution of his bioheat equation. A disadvantage of Pennes' is that there is no information concerning vascular geometry (Xu 1991). Its wide usage has been mainly due to its simplicity of implementations, especially in analyses where a closed form analytical solution is sought. Investigators have obtained good temperature predictions for the following circumstances the porcine kidney cortex in the absence of large vessels, the rat liver, and the capillary bleed off from large vessels. Also good agreement has occurred when Pennes' model is used on macroscopic tissue temperature clearance measurements

with experimental results for temperature decay in the vicinity of a constant temperature-heating probe.

2.3.2 Weinbaum and Jiji Bioheat Model

The first to present the countercurrent structure from their observations of large arteries and veins in human limbs was Bazett et al. (1927). Mitchell and Myers presented the first major quantitative analysis of a countercurrent vasculature (1968). They were followed by the work of Keller and Seiler (1971), who were the predecessors to Weinbaum and Jiji (1989).

Weinbaum and Jiji were strong opponents of Pennes' bioheat equation. They stated that Pennes' bioheat equation didn't account for the fact that blood flow enhances heat flow when the velocity and temperature vectors are not orthogonal and heat transfer between blood is not limited to capillary beds. In 1979, Weinbaum and Jiji proposed a model of the artery-vein pair. This model consisted of two parallel cylinders having equal diameters with collateral bleed off in the plane perpendicular to the cylinders. Perfusion in the system was analyzed in a manner similar to that of heat transfer in porous media. It was denoted as a one dimensional convection term normal to the artery-vein pair. In 1984 Weinbaum and Jiji developed a more thorough model than that of their 1979 artery-vein pair model. This newer model analyzed three tissue layers of a limb. These tissue layers were defined as a) deep, b) intermediate, and c) superficial or d) cutaneous. The countercurrent vasculature of the deep tissue layer was described by a system of three coupled equations. These three-coupled equations described the heat transfer of thermally significant artery-vein pair and the tissue surrounding it. Their analysis showed that the major heat transfer is due to the imperfect countercurrent heat

exchange between artery-vein pairs. Weinbaum and Jiji based their bioheat equation on the assumption that the local blood contribution to tissue heat transfer was mainly associated with incomplete countercurrent heat exchange mechanism between paired arteries and veins and capillary heat exchange mechanisms. Their bioheat model was based on perfusion quantification using a detailed vascular architecture in the skin and muscle of a rabbit hind leg. Their model was presented in 1985. They determine the temperature gradients within the tissue by the thermal flux through the region.

Weinbaum and Jiji's bioheat equation is described mathematically by

$$\rho c \frac{\partial T}{\partial t} = \frac{\partial}{\partial x}\left(k_{eff} \frac{\partial T}{\partial x}\right) + q_{met} \qquad (2)$$

where

k_{eff} is the effective blood-tissue conductivity related to local vascular geometry.

It increases quadratically with increasing blood flow. The Weimbaum-Jiji model has been found to be difficult to implement; there have also been issues of concern when implementing this model because the artery and vein diameters must be identical when evaluating the model. Studies using this model have been applied to the peripheral muscle of a limb, and the model is accepted as valid for vasculature with diameters of 300 micrometers. In response to the criticism that their previous model is too difficult and complex to apply, Weinbaum and Jiji simplified the three-equation model to a single equation. They derived an equation based on the temperature of tissue only. The disadvantage of this model is that the local temperatures along the countercurrent artery and vein cannot be calculated.

2.3.3 Chen and Holmes Bioheat Model

The bioheat model of Chen and Holmes is very similar to that of Pennes. They indicated that thermal equilibrium occurs predominantly within the terminal arterioles and venules, and the blood is essentially equilibrated prior to entering the capillaries. The Chen and Holmes bioheat transfer model has been described as the most developed continuum model. Chen and Holmes analyzed large vessels indirectly. Chen and Holmes developed a bioheat equation that accounted for actual equilibration of blood temperature, the contribution of net blood flow velocity within the tissue relative to already thermally equilibrated vessels, and vessels are considered in thermal equilibrium with surrounding tissue. This bioheat equation includes a source term, which is considered proportional to the perfusion rate. Chen and Holmes' bioheat equation is described mathematically by

$$\rho c \frac{\partial T}{\partial t} = k_t \nabla^2 T + (\rho c)_b \omega (T - T_a) - (\rho c)_b \bar{u} \cdot \nabla T + k_p \nabla^2 T + q_m \qquad (3)$$

where

ω is the blood perfusion rate per unit volume of the microvasculature,

ρ is the density of blood,

c is the specific heat of blood,

k_t is the tissue thermal conductivity,

k_p is the thermal conductivity related to blood perfusion,

T_a is the arterial temperature,

T is the tissue temperature, and

$\bar{u}$ is the net blood flow velocity.

The second term on the right hand side is similar to Pennes except the perfusion and the arterial temperature are specific to the volume being considered. The third term is a directional convection term due to the net flux of equilibrated blood. The last term on the right hand side is to account for the contribution of the nearly equilibrated blood in a tissue temperature gradient. This is a continuum formulation of bioheat transfer, the most developed one of them. A disadvantage (Xu 1991) of the model is that given the detail required, the model is not easy to implement. Also the perfusion conductivity term is difficult to evaluate, and distinction within the continuum model is not well defined. Furthermore, the model does not explicitly address the effect of closely spaced countercurrent artery-vein pairs. This model has been applied to the porcine kidney and was found to predict temperatures similar to Pennes' model, thus given the simplicity of the latter, Xu et al. (1991) recommended that Pennes be used. Arkin et al. (1987) claim that the Chen/Holmes model can be essentially applied to the same tissue region as that for Pennes' bioheat model.

2.3.4 KEFF Bioheat Model

This model is similar to Pennes model but tissue blood flow is accounted for with the k_{eff} term. Without perfusion it reduces to the general heat transfer equation. Patel (1987) and Roemer (1989) proposed an effective thermal conductivity model to describe heat transfer occurring in tissue due to perfusion. The perfusion and intrinsic tissue conductivity are lumped together as the k_{eff} term. Patel (1987) and Valvano (1987) assumed the measured steady state thermal conductivity equaled the thermal effective conductivity. They indicate that perfusion will have exactly the same influence on a thermistor bead heated with steady state or sinusoidal power.

$$\rho_m c_m \frac{\partial T_m}{\partial t} = k_{eff} \nabla^2 T_m + Q_{ext} \quad (4)$$

where $k_{eff} = k_m + \omega \Delta^2 c_{bl} / 6$.

k_m is the intrinsic thermal conductivity of the tissue medium,

ω is the perfusion term,

c_{bl} is the specific heat of blood,

T_m is the temperature of the tissue medium,

c_m is the specific heat of the tissue medium,

ρ_m is the density of the tissue medium, and

Q_{ext} is the external distributed heat.

2.4 Experimental Techniques

Investigators have developed experimental methods in an effort to quantify intrinsic and effective thermal conductivity, thermal diffusivity, and tissue perfusion.

2.4.1 Measuring Bead with Step Change in Temperature

Chato (1968), Bowman and Balasubramiam (1974,1977), Jain (1978,1979), and Cooper and Trezek (1970) utilized the thermistor bead sensing method with step change in temperature. Chato (1968) was the first of these researchers to utilize the thermistor bead as a sensor and thermal heat source for the measurement of thermal properties. Chato's method was one that was self-heating, transient, spherical, and invasive. It is the development of this transient method that measured thermal conductivity and inertia led to the solution of the bioheat equation "for the time dependent perfused response to a self heated thermistor." He modeled a spherical thermistor probe that began in thermal

equilibrium with the surrounding tissue while acting as a sensing device. After equilibrium conditions are recorded, power is switched on to allow the thermistor bead to reach a specified increment present value. This preset value of temperature is maintained with a feedback controller that adjusts the power output.

Bowman and Balasubraniam (1974,1977) developed a similar method to extract thermal properties and perfusion as Chato. They were able to improve on Chato's original thermal model. Their advance led to improvements in the accuracy of the thermal gradient within the thermistor probe. In 1977, Balasubraniam developed a simultaneous measurement technique used to measure thermal conductivity and thermal diffusivity in cases of perfused tissue and non-perfused tissue. They extended Chato's thermal model to include spatial temperature distributions within the spherical thermistor and were able to determine thermal values from the time dependent characteristics of the power requirement needed to hold the thermistor bead at a constant increased temperature.

Cooper and Trezek (1970) constructed a pointed cylindrical cooper probe with a thermocouple in the middle. The probe was heated slightly and then suddenly placed into the tissue and the subsequent temperature decay of the probe was fitted to approximate polynomials by computer. The principal advantage of the cylindrical probe method when compared to that of the spherical probe method is that the thermal conductivity can be directly determined as a first power function and independent of probe radius.

2.4.2 Measuring Bead with Pulse Heat Input

Chen (1977) initially proposed this method. In this method, a bead with a known quantity of heat, "q", is applied to the tissue during a short period of time. Later when the

power is off, the thermistor bead acts as a sensor of the temperature decay. Temperature measurements are made with the bead over a specified time interval to enable the determination of tissue properties. Chen used the bead as an electrical heat source. This method provides positive identification of the presence of the non-conduction heat transfer. Measurement of thermal diffusivity and thermal conductivity are determined from an evaluation of the time history of the temperature field surrounding a cylindrical probe. The method is based on comparing the measured and model simulated temperature decay following the insertion of a power pulse through a bead. The numerical model simulated temperature decay is based on the classic bioheat equation proposed by Pennes.

The pulse heating method has been used to measure local tissue blood flow in several animal tissues. Valvano et al. (1984) were able to quantify perfusion in an isolated rat liver utilizing the method of the measuring bead with pulse heat input. Their results were correlated with that of the invasive radiolabeled microsphere method. Anderson et al. (1988,1989,1992,1994) also measured perfusion by applying a combination of steady state and sinusoidal power to a thermistor probe that is inserted into a canine kidney cortex. From experimental results they determined that the temperature response is an indication of effective thermal conductivity. This invasive method of blood perfusion has been proven to be in agreement with those obtained using trapped microspheres and gas washout or uptake methods.

Chen (1980) claimed the advantages of the pulse heating method as (a) the bead can be very small, (b) fast measuring cycles on a quasi-continuous basis, (c) high sensitivity, (d) an increase in sampling volume with time, (e) a temperature time relationship inversely proportional to the thermal conductivity, (f) and results that provide

a clear distinction between a purely conductive, non-perfused tissue and tissue with blood perfusion. Some disadvantages (Chato 1985) of this method are the intrinsic tissue conductivity (no flow) of perfused tissue must be known to calculate the perfusion rate and time course for temperature recovery to equilibrium values are usually relatively slow.

2.4.3 Measuring Bead with Step Change in Heat Input

This method of measuring thermal properties gained popularity in the food industry. It consists of a long, thin heated wire with a temperature sensor or sensors, located at a known distance, r, from the axis of the wire. Initially the system is in equilibrium at a uniform temperature and then a constant heating rate of energy per unit length is applied to the wire. Since this method keeps energy per unit of length constant, the electrical control is simple. Transient data are curved fit to find the values of thermal conductivity and thermal diffusivity. One disadvantage (Chato 1985) of this method is that the overall time required for a single run may be unacceptable long. Another disadvantage (Chato 1985) is the temperature increases without bound in time if the power is left on, creating a potential burn hazard in either the tissue or even in the device itself.

CHAPTER 3

NUMERICAL MODEL: FORMULATION AND ASSUMPTIONS

Nomenclature

a	radius of the thermistor bead	(m)
c	specific heat	(J/kg ^{o}C)
Fo	grid Fourier number	
k	thermal conductivity	(W/m ^{o}C)
m	grid point number in the r-direction	
N	number of iterations	
n	grid point number in the θ-direction	
q	energy generation rate per unit volume	(W/m^3)
R	radius of the spherical region	(m)
r	radial coordinate distance	(m)
T	tissue temperature	(^{o}C)
T'	tissue temperature at new time	(^{o}C)
t	time	(s)
ω	tissue perfusion	(kg/m^3 s)
α	thermal diffusivity	(m^2/s)
ρ	mass density	(kg/m^3)

θ	angle coordinate distance	(radians)

Subscripts

b	thermistor bead
eff	effective (with perfusion)
inf	infinity
k	kidney
kt	kidney and tissue interface
m	intrinsic (without perfusion)
met	metabolic
o	initial condition
p	constant pressure
per	blood perfusion
t	tissue
s	step

3.1 Methodology

The methodology was based upon previously explored thermal diffusion techniques used in the determination of perfusion values, thermal conductivity, and thermal diffusivity. The thermistor probe was the most widely used device in concluding these values. Until 1968, researchers in their thermal studies utilized two or more thermistor probes. Chato (1968) was the first to use a single thermistor technique as a method for determination of thermal values and perfusion. A constant temperature, transient diffusion technique utilizing a single thermistor was employed in this study.

Combining the research done on thermal diffusion techniques and self-heated thermistors, it was determined that a single thermistor probe utilized as a heating and sensing source would be applicable to this study. The thermistor probe was modeled as a continuous point source and sensing device located at the interface of the kidney and an adjacent medium. The thermistor bead functioned as a sensing element when the collection of the basal temperature data was necessary. The thermistor bead functioned as a heating element when it was desired to maintain an incremental fixed temperature above baseline values.

This spherically modeled thermistor bead begins in temperature equilibrium with the surrounding media. A passive period for measuring baseline temperature was needed before the application of electrical energy to the thermistor bead. After the brief baseline temperature determination, heating was initiated in the bead. Electrical heat was dissipated through the media by the thermistor bead at a rate to maintain the bead temperature at that of a predetermined fixed increment above baseline temperature.

The adjacent medium was characterized with tissue properties different from those of the kidney. Two separate governing equations, one for the kidney and one for the adjacent medium were developed. Continuity of temperature and heat flux was assumed between the kidney and the adjacent medium.

The increase in electrical heat dissipation in the media depended on the amount of heat lost to the surrounding media due to the modes of conduction and convection heat transfer. The relation between energy input into the system due to a predetermined fixed increment in temperature was deemed as a function of thermal and flow properties of the surrounding tissue. This allowed for a qualitative determination of an increase or

decrease in tissue perfusion. The end result was an assessment of the effectiveness in monitoring blood perfusion with the thermistor approach. In essence this was determined by the ability to discern kidney perfusion variations from the rate of thermal energy dissipated through the system.

3.2 Model Definition

The thermal model consisted of the thermal diffusion equations of two continuous, homogeneous, infinite tissue media in intimate contact with each other and with a point-heating source between them. This resulted in the temperature and energy dissipation fields of the system.

3.3 Governing Equations

The mathematical model was based on Pennes' bioheat equation (1948) and the conservation principles of energy. The model was used to determine the effects of perfusion on heat distribution and dissipation. The equation is

$$(\rho c)_t \frac{\partial T}{\partial t} = k_t \nabla^2 T_t + q_{perfusion} + q_{metabolic}. \quad (5)$$

The explicit finite difference method was chosen to numerically determine temperatures throughout the model at discrete points. This method is an efficient way for solving ordinary differential equations in problems. The method requires the construction of a nodal network defining local coordinate surfaces. For each node of this network, the unknown function values are found, replacing the differential equations by

the appropriate finite difference equations for each node. The unknown function values are found by utilizing a step method in an iterative procedure.

A finite difference model was developed based on equation (5) to simulate the thermal aspects in three case, (a) a perfused kidney and perfused tissue, (b) a non-perfused kidney and perfused tissue, and (c) a non-perfused kidney and non-perfused tissue.

The following energy balance equations were derived for an interior node, exterior node, and interface node using the energy balance approach. The system consists of second-order partial differential equations and therefore requires four boundary conditions and two initial conditions to solve for the heat dissipation and temperature distribution of the system.

3.4 Model Geometry

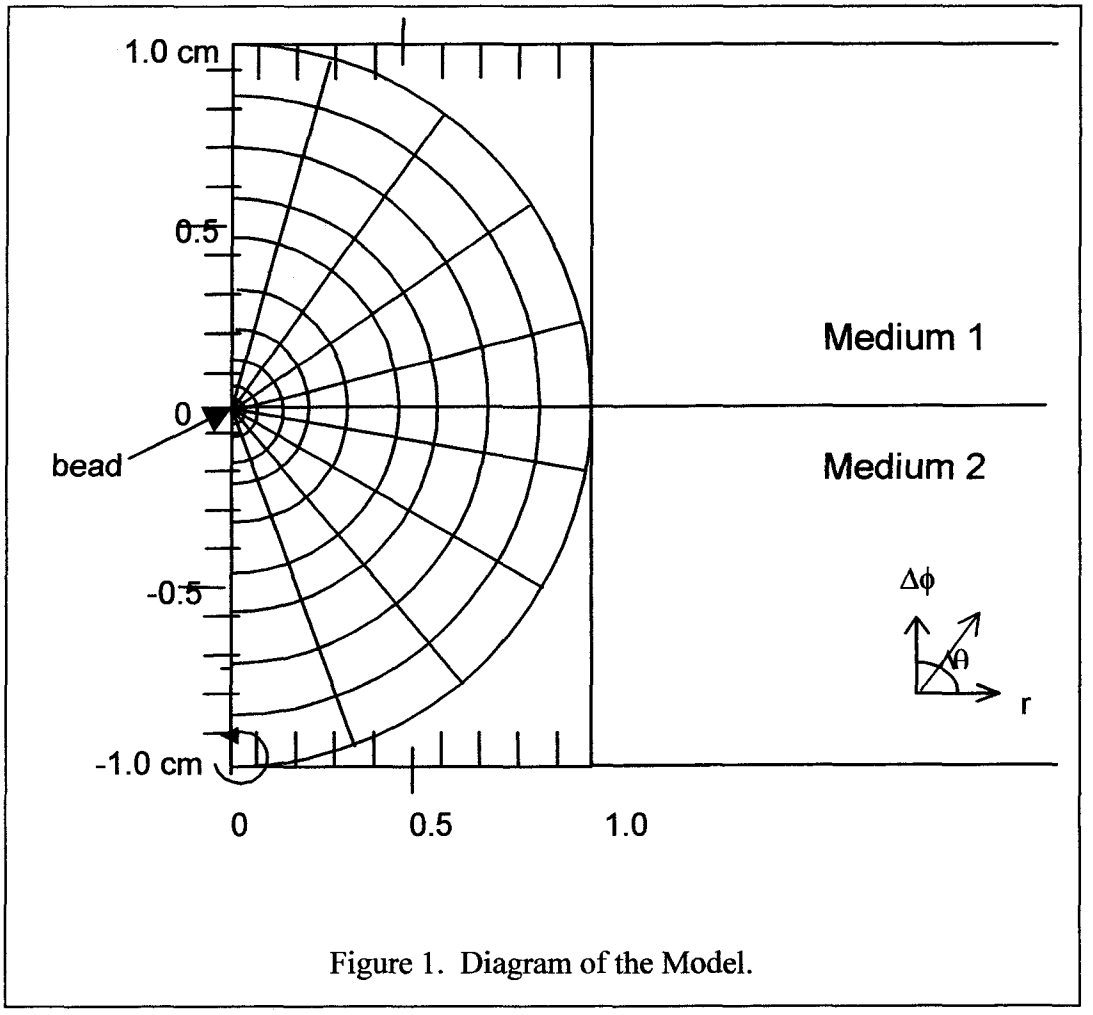

Figure 1. Diagram of the Model.

3.5 Model Parameters

3.5.1 Assumptions

Assumptions in the mathematical development of the model are summarized as follows:

(1) The Pennes' bioheat transfer equation and the conservation principles of energy governed the tissue transport.

(2) The thermistor was modeled as a uniformly heated sphere of radius a.

(3) Perfect thermal contact was assumed between the thermistor and the two adjacent media (kidney and tissue).

(4) The thermal properties of the media and thermistor were assumed constant in the volume of experimental studies.

(5) The thermal properties of the thermistor were assumed constant.

(6) The kidney and tissue were modeled as homogeneous media.

(7) The heat generation rate due to metabolism was assumed to be negligible when compared with other source terms.

(8) The effects of perfusion were accounted for in an effective thermal conductivity.

(9) Electrical power was uniformly distributed throughout the volume of the thermistor bead.

(10) An axisymmetric field as shown in Figure 1 is assumed.

3.5.2 Initial Conditions

At t=0, before power is applied to the system, the kidney, tissue and thermistor probe are in thermal equilibrium.

$T_t=T_o$

$T_k = T_o$

$T_b = T_o$

3.5.3 Boundary Conditions

The system reached unperturbed baseline conditions when the radius of the system approached infinity when the bead was used as the origin. At the probe-media interface, continuity of temperature and heat flux was assumed. When the angle in the system is equal to 0 or π, the temperatures are assumed to equal that of the thermistor bead. The media in direct contact with the thermistor probe are in thermal equilibrium with the thermistor bead at all times of t.

As the radius of the system approaches infinity the temperature is that of the initial temperature. The temperature of the bead at $t=0^+$ is at a predetermined value above the baseline temperatures measured initially. The boundaries of the kidney and tissue that are in direct contact have the same temperature as the specified for the thermistor at that time.

$T_k \rightarrow T_o$	as	$r \rightarrow \infty$
$T_t \rightarrow T_o$	as	$r \rightarrow \infty$
$T_k = T_t = T_b$		$r = a$
$k_b \cdot \frac{\partial T_s}{\partial r} = 0$	as	$r \rightarrow 0$
$T_m(r,\theta) = T_t(r,\theta)$	at all r	$\theta = 0, \pi$
$k_b \cdot \left(\frac{1}{r}\right) \cdot \frac{\partial T_b}{\partial \theta} = k_t \cdot \left(\frac{1}{r}\right) \cdot \frac{\partial T_t}{\partial \theta}$	at all r	$\theta = 0, \pi$

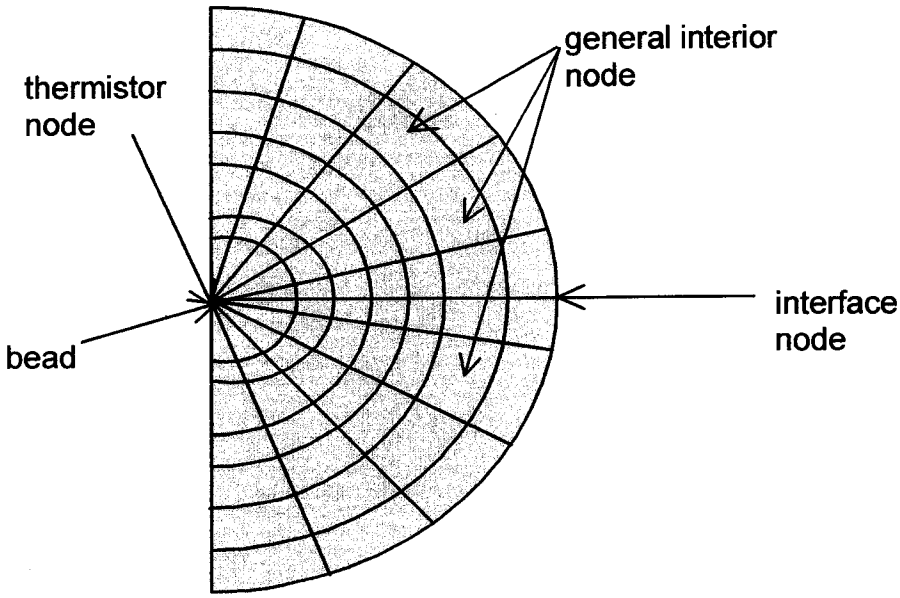

Figure 2. Diagram of Model with Nodal Locations defined.

Interface Node

$$\left[\left(\frac{k_t + k_k}{2}\right) \cdot \left(\left(r_m + \frac{\Delta r}{2}\right) \cdot 2 \cdot \pi \cdot \left(r_m + \frac{\Delta r}{2}\right) \cdot (\Delta\theta)\right)\right] \cdot \frac{T(m+1, n) - T(m, n)}{\Delta r}$$
$$+ \left[\left(\frac{k_t + k_k}{2}\right) \cdot \left(\left(r_m - \frac{\Delta r}{2}\right) \cdot 2 \cdot \pi \cdot \left(r_m - \frac{\Delta r}{2}\right) \cdot (\Delta\theta)\right)\right] \cdot \frac{T(m-1, n) - T(m, n)}{\Delta r}$$
$$+ \left[k_t \cdot \left(2 \cdot \pi \cdot r_m \cdot \sin(n \cdot \Delta\theta - \frac{\Delta\theta}{2}) \cdot \Delta r\right)\right] \cdot \frac{T(m, n-1) - T(m, n)}{r_m \cdot \Delta\theta} \qquad (6)$$
$$+ \left[k_t \cdot \left(2 \cdot \pi \cdot r_m \cdot \sin(n \cdot \Delta\theta + \frac{\Delta\theta}{2}) \cdot \Delta r\right)\right] \cdot \frac{T(m, n+1) - T(m, n)}{r_m \cdot \Delta\theta}$$
$$+ q_{met} \cdot (r_m \cdot 2 \cdot \pi \cdot \Delta r \cdot r_m \cdot \Delta\theta) - q_{per} \cdot (r_m \cdot 2 \cdot \pi \cdot \Delta r \cdot r_m \cdot \Delta\theta)$$
$$= \frac{T'(m, n) - T(m, n)}{\Delta t} \cdot \left[\left(2 \cdot \pi \cdot r_m^2 \sin(n \cdot \Delta\theta) \cdot \Delta r \cdot \Delta\theta\right) \cdot (\rho \cdot c_p)\right]$$

Thermistor Node

$$\left[k \cdot \left(\pi \cdot \left(r_m + \frac{\Delta r}{2} \cdot \sin\left(\frac{\Delta\theta}{2}\right)\right)^2\right)\right] \cdot \frac{T(m+1,\, n) - T(m,\, n)}{\Delta r}$$
$$+ \left[k \cdot \left(\Delta r \cdot 2 \cdot \pi \cdot \sin\left(\frac{\Delta\theta}{2}\right) \cdot r_m\right)\right] \cdot \frac{T(m,\, n+1) - T(m,\, n)}{r_m \cdot \Delta\theta}$$
$$+ \left[k \cdot \left(\Delta r \cdot 2 \cdot \pi \cdot \sin\left(\frac{\Delta\theta}{2}\right) \cdot r_m\right)\right] \cdot \frac{T(m,\, n-1) - T(m,\, n)}{r_m \cdot \Delta\theta} \qquad (7)$$
$$+ q_{met} \cdot \left[\left(r_m \cdot \sin\left(\frac{\Delta\theta}{2}\right)\right)^2 \cdot \pi \cdot \Delta r\right] - q_{met} \cdot \left[\left(r_m \cdot \sin\left(\frac{\Delta\theta}{2}\right)\right)^2 \cdot \pi \cdot \Delta r\right]$$
$$= \frac{T'(m,\, n) - T(m,\, n)}{\Delta t} \cdot \left[\left(\left(r_m \cdot \sin\left(\frac{\Delta\theta}{2}\right)\right)^2 \cdot \pi \cdot \Delta r\right) \cdot (\rho \cdot c_p)\right]$$

General Interior Node

$$\left[k \cdot \left(\left(r_m + \frac{\Delta r}{2}\right) \cdot \Delta\theta\right) \cdot 2 \cdot \pi \cdot \left(r_m + \frac{\Delta r}{2}\right) \cdot \sin(n \cdot \Delta\theta)\right] \cdot \frac{T(m+1,\, n) - T(m,\, n)}{\Delta r}$$
$$+ \left[k \cdot \left(\left(r_m - \frac{\Delta r}{2}\right) \cdot \Delta\theta\right) \cdot 2 \cdot \pi \cdot \left(r_m - \frac{\Delta r}{2}\right) \cdot \sin(n \cdot \Delta\theta)\right] \cdot \frac{T(m-1,\, n) - T(m,\, n)}{\Delta r} \qquad (8)$$
$$+ \left[k \cdot \left(2 \cdot \pi \cdot r_m \cdot \left(\sin\left(n \cdot \Delta\theta + \frac{\Delta\theta}{2}\right)\right) \cdot \Delta r\right)\right] \cdot \frac{T(m,\, n+1) - T(m,\, n)}{r_m \cdot \Delta\theta}$$
$$+ \left[k \cdot \left(2 \cdot \pi \cdot r_m \cdot \left(\sin\left(n \cdot \Delta\theta - \frac{\Delta\theta}{2}\right)\right) \cdot \Delta r\right)\right] \cdot \frac{T(m,\, n-1) - T(m,\, n)}{r_m \cdot \Delta\theta}$$
$$+ q_{met} \cdot \left[r_m \cdot 2 \cdot \pi \cdot \Delta r \cdot r_m \cdot \Delta\theta \cdot \sin(n \cdot \Delta\theta)\right] - q_{per} \cdot \left[r_m \cdot 2 \cdot \pi \cdot \Delta r \cdot r_m \cdot \Delta\theta \cdot \sin(n \cdot \Delta\theta)\right]$$
$$= \frac{T'(m,\, n) - T(m,\, n)}{\Delta t} \cdot \left[r_m \cdot 2 \cdot \pi \cdot \Delta r \cdot r_m \cdot \Delta\theta \cdot \sin(n \cdot \Delta\theta)\right]$$

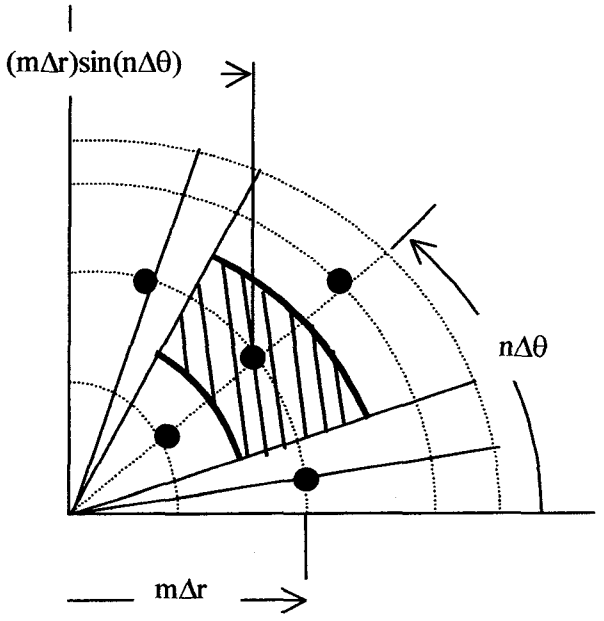

Figure 3. Finite Difference Nodal Diagram of the System.

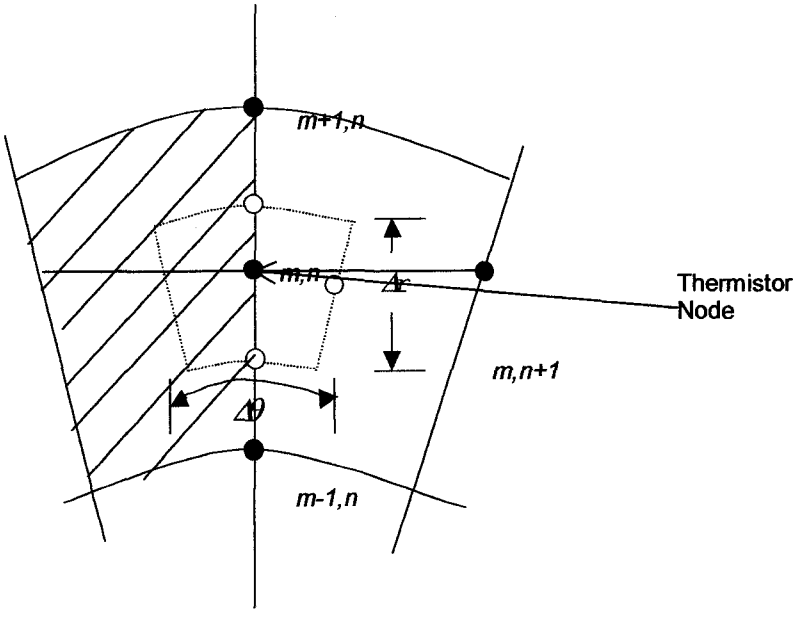

Figure 4. Thermistor node for Finite Difference Formulation.

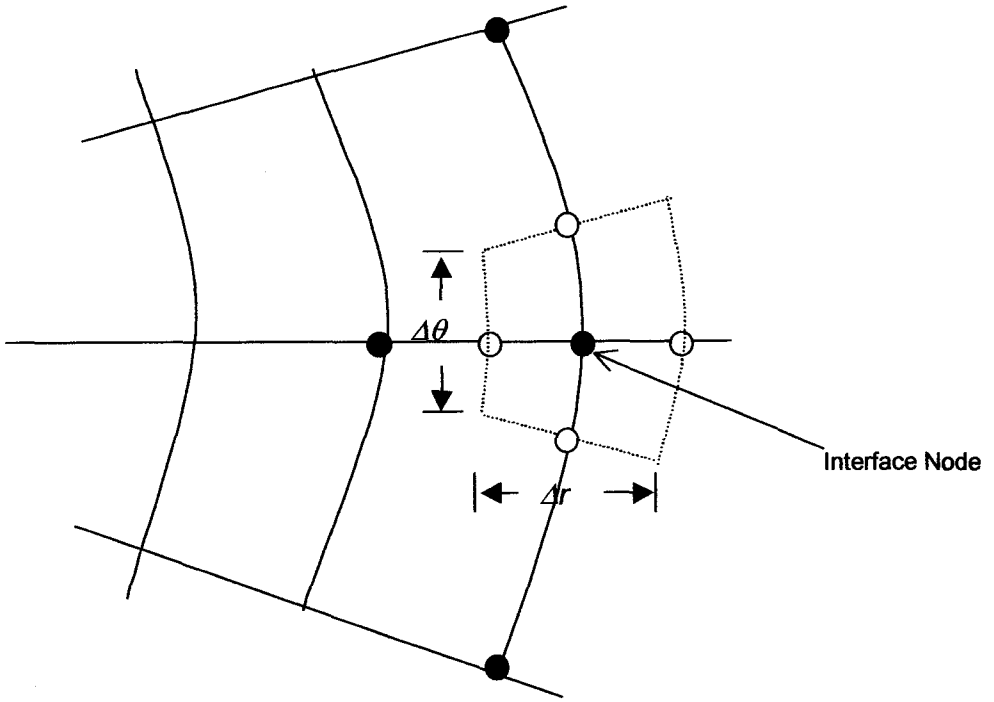

Figure 5. Interface node for finite difference formulation.

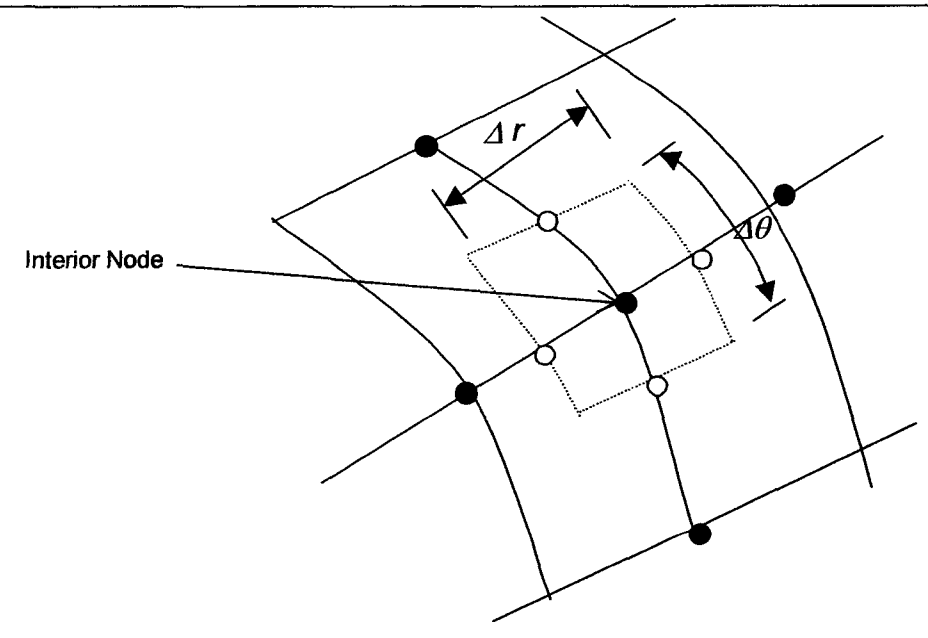

Figure 6. Interior Node for Finite Difference Formulation.

The following explicitly formulated finite difference equations were derived for interface nodes, boundary nodes, and interior nodes in the system.

Interface Node

$$
\begin{aligned}
T'(m,n) = & \left[\begin{array}{l} 1-\left(\alpha_{kt}\cdot\frac{\Delta t}{\Delta r^2}\right)\cdot\frac{\left(r_m+\frac{\Delta r}{2}\right)^2}{r_m^2}-\left(\alpha_{kt}\cdot\frac{\Delta t}{\Delta r^2}\right)\cdot\frac{\left(r_m-\frac{\Delta r}{2}\right)^2}{r_m^2} \\ -\left(\alpha_k\cdot\frac{\Delta t}{(r_m\cdot\Delta\theta)^2}\right)\cdot sin\left(n\cdot\Delta\theta+\frac{\Delta\theta}{2}\right) \\ -\left(\alpha_t\cdot\frac{\Delta t}{(r_m\cdot\Delta\theta)^2}\right)\cdot sin\left(n\cdot\Delta\theta-\frac{\Delta\theta}{2}\right) \end{array}\right]\cdot T(m,n) \\
& +\left[\left(\alpha_{kt}\cdot\frac{\Delta t}{\Delta r^2}\right)\cdot\frac{\left(r_m+\frac{\Delta r}{2}\right)^2}{r_m^2}\right]\cdot T(m+1,n)+\left[\left(\alpha_{kt}\cdot\frac{\Delta t}{\Delta r^2}\right)\cdot\frac{\left(r_m-\frac{\Delta r}{2}\right)^2}{r_m^2}\right]\cdot T(m-1,n) \\
& +\left[\left(\alpha_k\cdot\frac{\Delta t}{(r_m\cdot\Delta\theta)^2}\right)\cdot sin\left(n\cdot\Delta\theta+\frac{\Delta\theta}{2}\right)\right]\cdot T(m,n+1) \\
& +\left[\left(\alpha_t\cdot\frac{\Delta t}{(r_m\cdot\Delta\theta)^2}\right)\cdot sin\left(n\cdot\Delta\theta-\frac{\Delta\theta}{2}\right)\right]\cdot T(m,n-1) \\
& +q_{met}\cdot\frac{\Delta t}{\left(\rho\cdot c_{p_k}+\rho\cdot c_{p_t}\right)}-q_{per}\cdot\frac{\Delta t}{\left(\rho\cdot c_{p_k}+\rho\cdot c_{p_t}\right)}
\end{aligned}
\tag{9}
$$

Boundary Node

$$T'(m,n) = \left[1 - \left(\alpha \cdot \frac{\Delta t}{\Delta r^2}\right) \cdot \frac{\left(r_m + \frac{\Delta r}{2}\right)^2}{r_m^2} - \left(\alpha \cdot \frac{\Delta t}{\Delta r^2}\right) \cdot \frac{\left(r_m - \frac{\Delta r}{2}\right)^2}{r_m^2} - 4 \cdot \left(\alpha \cdot \frac{\Delta t}{(r_m \cdot \Delta\theta)^2}\right)\right] \cdot T(m,n)$$

$$+ \left[\left(\alpha \cdot \frac{\Delta t}{\Delta r^2}\right) \cdot \frac{\left(r_m + \frac{\Delta r}{2}\right)^2}{r_m^2}\right] \cdot T(m+1,n) + \left[\left(\alpha \cdot \frac{\Delta t}{\Delta r^2}\right) \cdot \frac{\left(r_m - \frac{\Delta r}{2}\right)^2}{r_m^2}\right] \cdot T(m-1,n) \qquad (10)$$

$$+ 4 \cdot \left(\alpha \cdot \frac{\Delta t}{(r_m \cdot \Delta\theta)^2}\right) \cdot T(m,n+1) + q_{met} \cdot \frac{\Delta t}{\rho \cdot c_p} - q_{per} \cdot \frac{\Delta t}{\rho \cdot c_p}$$

Interior Node

$$T'(m,n) = \begin{bmatrix} 1 - \left(\alpha \cdot \frac{\Delta t}{\Delta r^2}\right) \cdot \frac{\left(r_m + \frac{\Delta r}{2}\right)^2}{r_m^2} - \left(\alpha \cdot \frac{\Delta t}{\Delta r^2}\right) \cdot \frac{\left(r_m - \frac{\Delta r}{2}\right)^2}{r_m^2} \\ - \left(\alpha \cdot \frac{\Delta t}{(r_m \cdot \Delta\theta)^2}\right) \cdot \frac{\sin\left(n \cdot \Delta\theta + \frac{\Delta\theta}{2}\right)}{\sin(n \cdot \Delta\theta)} \\ - \left(\alpha \cdot \frac{\Delta t}{(r_m \cdot \Delta\theta)^2}\right) \cdot \frac{\sin\left(n \cdot \Delta\theta - \frac{\Delta\theta}{2}\right)}{\sin(n \cdot \Delta\theta)} \end{bmatrix} \cdot T(m,n)$$

$$+ \left[\left(\alpha \cdot \frac{\Delta t}{\Delta r^2}\right) \cdot \frac{\left(r_m + \frac{\Delta r}{2}\right)^2}{r_m^2}\right] \cdot T(m+1,n) + \left[\left(\alpha \cdot \frac{\Delta t}{\Delta r^2}\right) \cdot \frac{\left(r_m - \frac{\Delta r}{2}\right)^2}{r_m^2}\right] \cdot T(m-1,n)$$

$$+ \left[\left(\alpha \cdot \frac{\Delta t}{(r_m \cdot \Delta\theta)^2}\right) \cdot \frac{\sin\left(n \cdot \Delta\theta + \frac{\Delta\theta}{2}\right)}{\sin(n \cdot \Delta\theta)}\right] \cdot T(m,n+1) \qquad (11)$$

$$+ \left[\left(\alpha \cdot \frac{\Delta t}{(r_m \cdot \Delta\theta)^2}\right) \cdot \frac{\sin\left(n \cdot \Delta\theta - \frac{\Delta\theta}{2}\right)}{\sin(n \cdot \Delta\theta)}\right] \cdot T(m,n-1)$$

$$+ q_{met} \cdot \frac{\Delta t}{\rho \cdot c_p} - q_{per} \cdot \frac{\Delta t}{\rho \cdot c_p}$$

3.6 Stability Criterion

The explicit method of solution was used to determine temperatures at nodal locations throughout the system. This method was used to evaluate unknown nodal temperatures for the new time by using known nodal temperatures at the previous time. The explicit method is not unconditionally stable. Numerically induced oscillations could cause the numerical solution to diverge from the actual steady state conditions that would normally be achieved. This can be avoided by maintaining Δt below a certain limit that is determined by certain factors in the numerical model such as Δr, $\Delta\theta$, and other parameters of the system. Determining a stability criterion prevents these numerically induced oscillations.

The stability criterion of the solution was mathematically determined by using the limiting case, which was numerically determined to be that of the thermistor node. This was done to avoid instabilities in the program.

$$\Delta t_{max} = \frac{1}{\left(\frac{4\alpha}{(\Delta r)^2}\cdot\left(\frac{\left(\left(r_m+\frac{\Delta r}{2}\right)\cdot\frac{\Delta\theta}{2}\right)^2}{\left(r_m\cdot\Delta\theta\right)^2}\right)+\left(\frac{\left(\left(r_m-\frac{\Delta r}{2}\right)\cdot\frac{\Delta\theta}{2}\right)^2}{\left(r_m\cdot\Delta\theta\right)^2}\right)\right)+\frac{8\alpha}{\left(r_m\cdot\Delta\theta\right)^2}}$$

3.7 Numerical Validation

A grid independence study was done to determine whether the numerically determined temperatures where dependent on grid spacing in the directions of $\Delta\theta$ and Δr. In this study, when a 60x60 nodal network of the system was compared with that of a more refined 100x100 nodal network of the system, the same amount of accuracy in

numerically determined temperatures was found to exist between the two nodal networks of the system. Since the 60x60 nodal region took considerably less computational time than the 100x100 nodal region, the 60x60 nodal region was used to determine numerical solutions of the system.

Steady state and transient numerical solutions were compared with analytical solutions in an effort to validate the numerical model. The steady state model solutions were compared with that of the analytical solution of the heat equation for one-dimensional conduction (Incropera and DeWitt 1996). The transient numerical model solutions were compared with the analytical solution for a region internally bounded by the sphere r=a (Carslaw and Jaeger 1959).

3.7.1 Steady State

Steady state temperatures are calculated using Mathcad and the numerical code developed in Fortran 90. The steady state solution of temperature distribution and heat dissipation throughout the system was determined using simultaneously solved steady state equations in the numerical code and MathCad. These solutions were in turn compared to determine the validity of the numerical code. There was found to be less than 10^{-4} percent difference when the numerical and analytical solutions were compared.

The heat equation used for one-dimensional conduction in the thermistor was $\frac{1}{r}\frac{d}{dr}\left(r^2\frac{dT}{dr}\right) = 0$. The temperature distribution in a sphere was given as

$T_{s,1} - \Delta T \cdot \left[\frac{1 - \frac{r_1}{r}}{1 - \frac{r_1}{r2}}\right]$. The heat flux (q") is given by $\frac{k \cdot \Delta T}{r^2 \cdot \left[\frac{1}{r_1} - \frac{1}{r_2}\right]}$. The heat rate (q) is given by $\frac{4 \cdot \pi \cdot k \cdot \Delta T}{\left(\frac{1}{r_1}\right) - \left(\frac{1}{r_2}\right)}$.

3.7.2 Transient

The transient solutions for heat dissipation and temperature distribution throughout the system were compared with the analytical solutions for a region bounded internally by the sphere r=a (Carslaw and Jaeger 1959). This was in turn used to determine the validity of the numerical code in the transient case.

For 0 initial, V step on boundary

Good for the entire time the temperature is stepped up.

$$v = \frac{a \cdot V}{r} erfc\left(\frac{r - a}{2 \cdot \sqrt{\alpha \cdot t}}\right)$$

$$v = T - T_{initial}$$

$$V = T_{step} - T_{initial}$$

$$\frac{T - T_{initial}}{T_{step} - T_{initial}} = \frac{a}{r} erfc\left(\frac{r - a}{2 \cdot \sqrt{\alpha \cdot t}}\right)$$

This gives the temperature distribution throughout the system. The heat dissipation throughout the system is given by the following

$$q = -k \cdot A \cdot \frac{\partial T}{\partial r} = -k \cdot 4 \cdot \pi \cdot r^2 \cdot \left(T_{step} - T_{initial}\right) \cdot \left(-\frac{1}{r} - \frac{1}{\sqrt{\pi \cdot \alpha \cdot t}}\right)$$

3.7.3 Model Calibration

The thermal conductivity properties used to calibrate the model were those for the human kidney and tissue. These properties are located in Table 1. Alternating Region 1 thermal properties are also provided (Table 1). Baseline temperatures were assumed to be 33°C.

Several sets of data were analyzed comparing the numerical model to the analytical results. Generally temperature distributions were determined with the numerical model and heat transfer values from the thermistor were found. Then the heat transfer results were compared to the analytical model. Typical of this type of comparison is shown in Figure 7. Here a uniform thermal conductivity is assumed (0.42 W/m°C), and the heat dissipated as a function of time is shown for a 0.5°C increase in sphere temperature. Excellent agreement between the two methods is shown for a 60 x 60-node numerical model representation.

To show the effects of different thermal conductivity, a series of numerical evaluations were performed. Two sets of results are shown in Figures 8 and 9. In these cases, the thermal conductivity for region 2 was held at 0.42 W/m°C, and the value for the other region, region 1, was varied from case to case. Figure 8 shows the typical heat dissipation functions for three specific values of thermal conductivity for region 1. These curves were then fit to polynomial functions and integrated analytically. A plot of the integrated values as a function of the varied thermal conductivity is shown in Figure 9.

Table 1. Model Parameters [Bowman 1975]

	Thermal Conductivity (W/m °C)	Density (kg/m^3)	Specific Heat (J/kg °C)
Kidney (whole) Perfused (Region 1)	0.543	1050	3787.76
Kidney (whole) Non-perfused Lower bound (Region 1)	0.49	1050	3787.76
Region 1	0.46	1050	3787.76
Region 1	0.60	1050	3787.76
Region 1	0.70	1050	3787.76
Region 1	0.80	1050	3787.76
Region 1	0.84	1050	3787.76
Tissue (Region 2) *remains constant	0.42	1050	3787.76

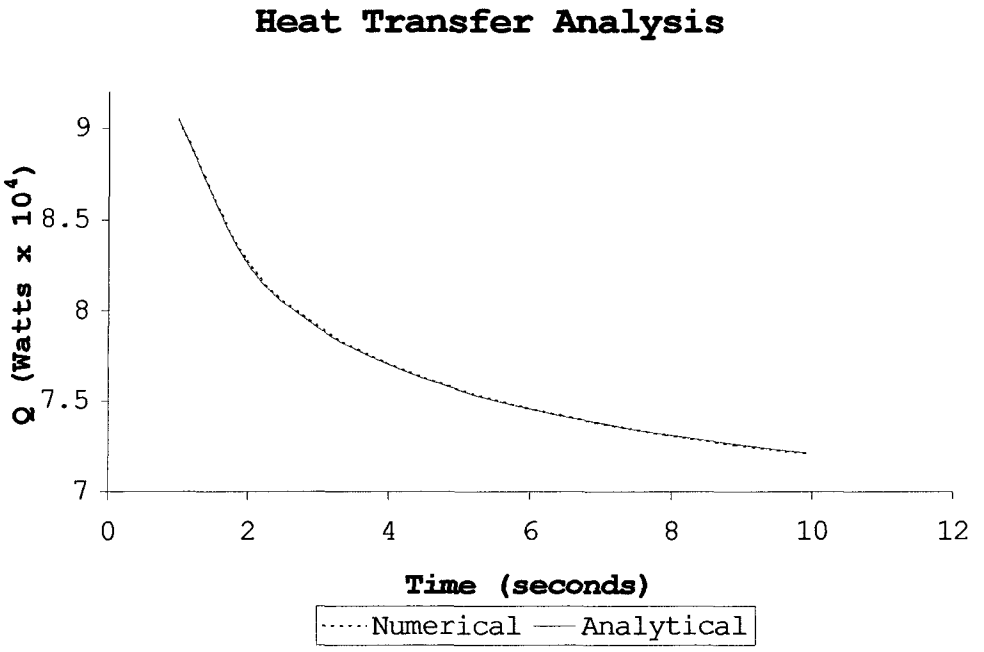

Figure 7. Numerical versus analytical power results for a uniform system of 0.42 W/m °C thermal conductivity.

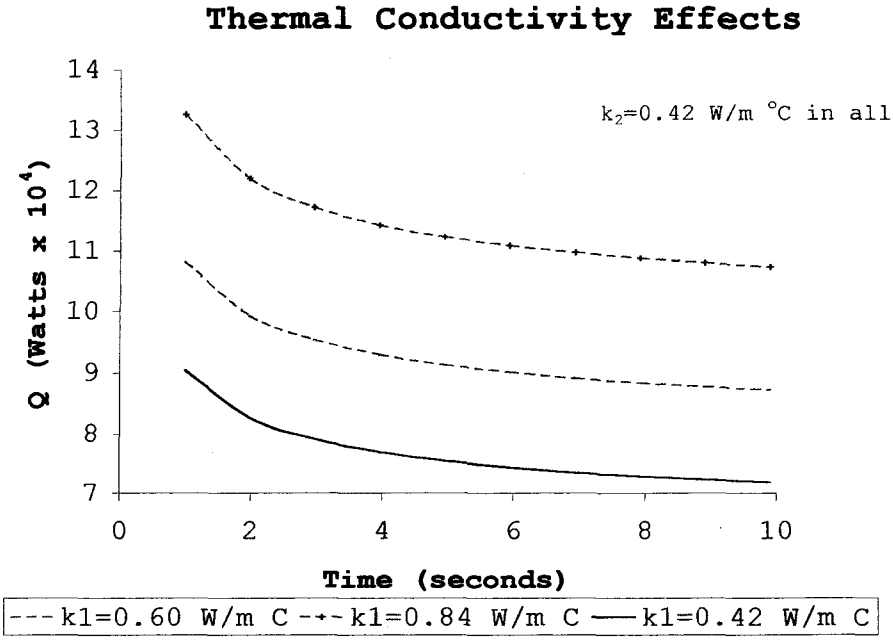

Figure 8. Heat dissipation of thermistor bead in select cases of thermal conductivity shown in table 1.

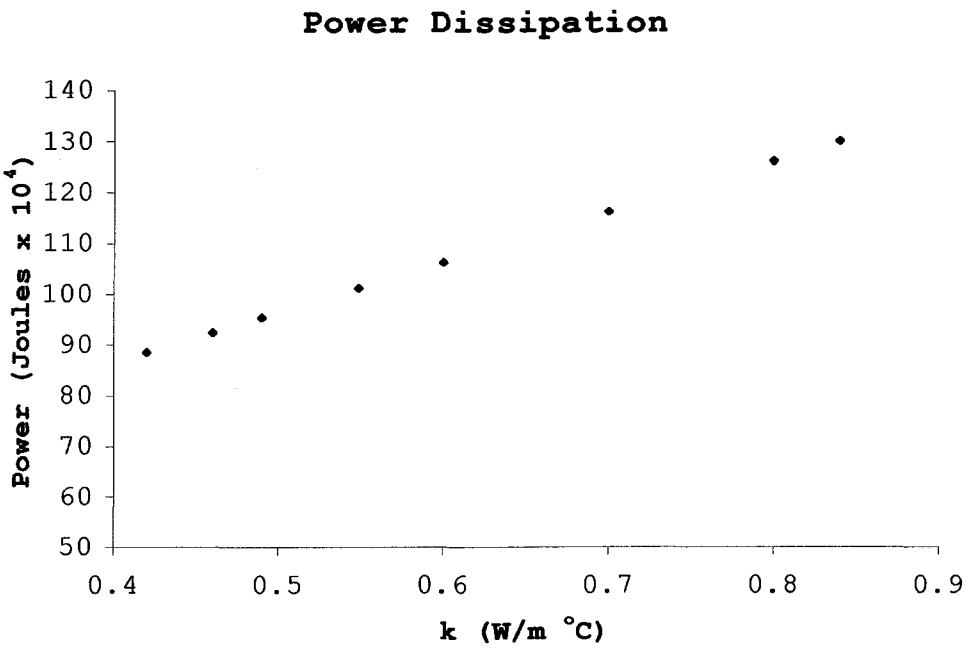

Figure 9. Power Dissipation for Varying Thermal Conductivity Values in Region 2 with a constant Value of 0.42 W/m°C in Region 1.

CHAPTER 4

EXPERIMENTAL PROCEDURE

4.1 Introduction

The experimental procedure performed is that of the measuring bead with step change in temperature. In this procedure a thermistor bead is utilized as a temperature sensor and a thermal heat source. As a temperature sensor, the thermistor bead is used to determine baseline temperatures of the adjacent system. As a thermal heat source, the thermistor bead is used to apply a specified temperature to the adjacent system. This specified temperature is one that has been increased in value over that of the predetermined baseline temperature of the system. The thermistor is operated with a constant temperature step where electrical energy is generated inside the bead to maintain its temperature at a constant predetermined value above the initial equilibrium temperature. The temperature of the thermistor bead is related to the thermal properties of the media that it is located in.

The experimental application of the self-heating thermistor bead method with a step change in temperature was achieved with the use of following apparatus: a thermistor bead, controller box, and data acquisition hardware and software. The experiments were used to determine the power output values based on the thermal conductivity of the materials.

4.2 Experimental Apparatus

4.2.1 Hardware

4.2.1.1 Thermistor

The thermistor bead method utilizes a thermistor as a point source of heat. Heat emanates from the bead into the surrounding media. A thermistor is a temperature dependent electronic component. It exhibits a change in resistance with a change in its body temperature. It has various uses in industry such as temperature measurement, temperature control, and determination of thermal properties.

The type of thermistor used in this study is a NTC (negative temperature coefficient) thermistor. This means that with an increase in temperature there is a decrease in resistance. When a NTC thermistor is connected in an electrical circuit, power is dissipated as heat and the body temperature of the thermistor rises above the ambient temperature of the environment. In this circuit the rate at which energy is supplied must equal the rate at which energy is lost plus the rate at which energy is absorbed. The rate at which thermal energy is supplied to the thermistor in an electrical current is equal to the power dissipated in the thermistor. The rate at which thermal energy is lost from the thermistor to its surroundings is proportional to the temperature rise of the thermistor. When a significant amount of power is dissipated in a thermistor, its body temperature will rise above the ambient temperature as a function of time. The self-heated thermistor exhibits a body temperature rise that is a function of time. A self-heated thermistor is heated above the ambient temperature by the power being dissipated

in the thermistor and can reach a condition of equilibrium. Once a self-heated thermistor has reached a condition of equilibrium, the rate of heat loss from the device will be equal to the power supplied.

The self-heated thermistor chosen for this study was an Omega Precision 44004. It is a NTC precision thermistor with a resistance of 2252 ohms @ 25°C. It has a maximum operating temperature of 150°C (300°F) with a time constant of 1 second. It has a minimum dissipation constant of 8mW/°C with a maximum diameter of 0.095". The approximate temperature coefficient, α_{approx} is 0.041/°C. It was chosen because of the ease of interchangeability, +0.2 °C; its bead size; and its high stability.

The thermistor bead is used in this study to increase its body temperature above that of the ambient temperature and for temperature measurement purposes. The interchangeability and large resistance change eliminate any significant error from switches or lead length. The accuracy of measured values is limited in most applications only by the readout device. Table 2 shows supplied resistance vs. temperature curve between the values of 20 and 40 °C. from information given by the vendor.

Table 3 shows measured values of resistance at known temperatures. Tests were performed to determine if the box was performing correctly. This was done calibrating the box at known temperatures. The calibration process was performed to make resistance measurements of the thermistor located in series with the control box by heating water approximately 60°C and taking resistance and temperature measurements over the range of 20 and 40°C as the water decreased in temperature. Instrumentation used in the calibration process was a Tek Stir Hotplate model H2395-1 manufactured by American Hospital Supply Corporation, b a 250 ml Pyrex (No.1000) glass beaker, a

Fluke 189 digital multimeter, and an 80TK- thermocouple model with a K type thermocouple to convert the digital multimeter signal to temperature. The Tek Stir Hotplate was used to heat the water located in the 250 ml Pyrex glass beaker. Temperature measurements were collected using the Fluke 189 digital multimeter and the 80 TK-thermocouple. Resistance measurements of the thermistor were collected using LabVIEW.

Table 2. Temperature vs. Resistance curve for OMEGA 44004 thermistor.
(From Omega Operator's Manual: M-0069/10/01)

Resistance versus Temperature 20 °C to 40 °C	
Temperature °C	Resistance (Ω)
20	2814
21	2690
22	2572
23	2460
24	2354
25	2252
26	2156
27	2064
28	1977
29	1894
30	1815
31	1739
32	1667
33	1599
34	1533
35	1471
36	1412
37	1355
38	1301
39	1249
40	1200

Table 3. Temperature vs. Resistance curve for OMEGA 44004 thermistor. (Determined during thermistor bead calibration)

Resistance versus Temperature 20 °C to 40 °C	
Temperature °C	Resistance (Ω)
20	2800
21	2686
22	2576
23	2471
24	2370
25	2273
26	2180
27	2091
28	2006
29	1924
30	1845
31	1770
32	1698
33	1629
34	1562
35	1498
36	1436
37	1378
38	1322
39	1268
40	1216

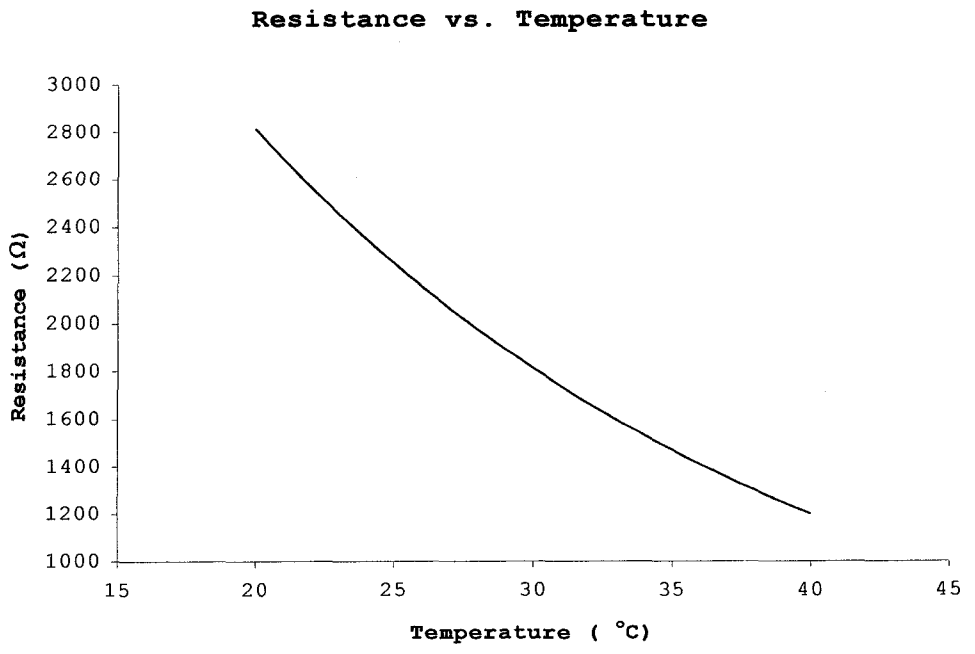

Figure 10. Resistance vs. Temperature for Omega 44004 thermistor. (From Omega Operator's Manual: M-0069/10/01)

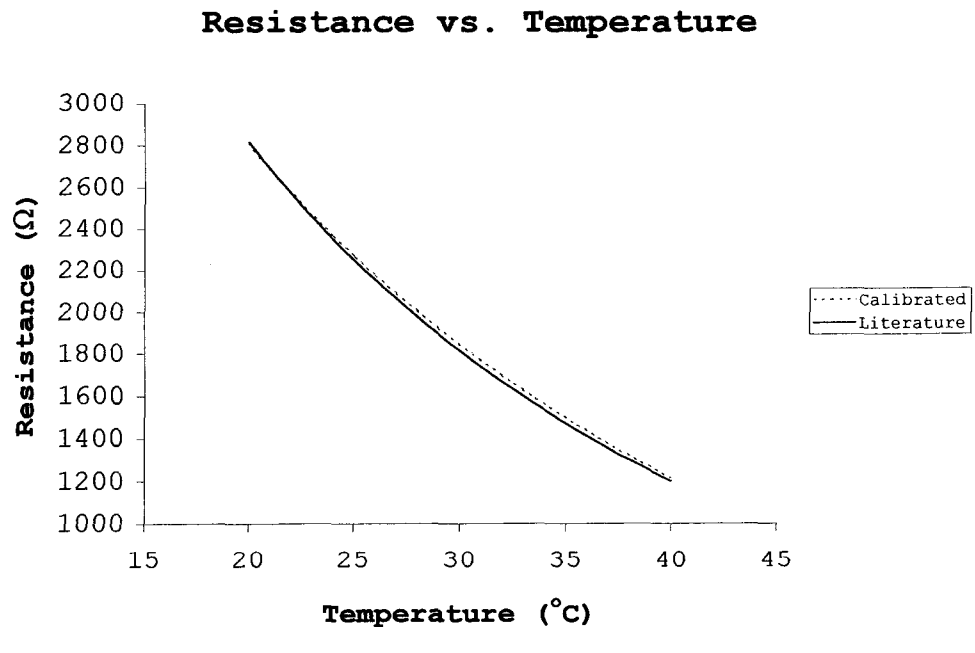

Figure 11. Comparison of Literature and Calibrated Resistance vs. Temperature for Omega 44004 thermistor.

4.2.1.2 Control Box[1,2]

Thermal property measurements were performed with a fixed temperature step of the thermistor. The temperature of the bead was almost instantaneously elevated to the temperature step for the duration of each experimental case. This was accomplished with the control box.

The control box was a 7.39" x 4.72" x 3.06" cast aluminum box that housed the electronic components used to control the heating and measure temperature using a self-heated thermistor. The self-heated thermistor was used to form one leg of an AC bridge and a variable resistor calibrated in temperature was used to form another leg. When the resistor was set to a desired temperature by the turn dial (potentiometer) located on the front of the box, bridge unbalance occurred. This unbalance was fed into an amplifier that actuated a relay to provide a source of heat by varying the current and voltage applied. When the thermistor sensed the desired temperature, the bridge was balanced, the relay opened and the increased amount of heat was turned off.

---

[1] Bill O'Donnell, a research associate in UNLV's department of Physics, designed the control box.

[2] The control box design was loosely based on a thermal property measurement circuit created by Maarten F. van Gelder (1998).

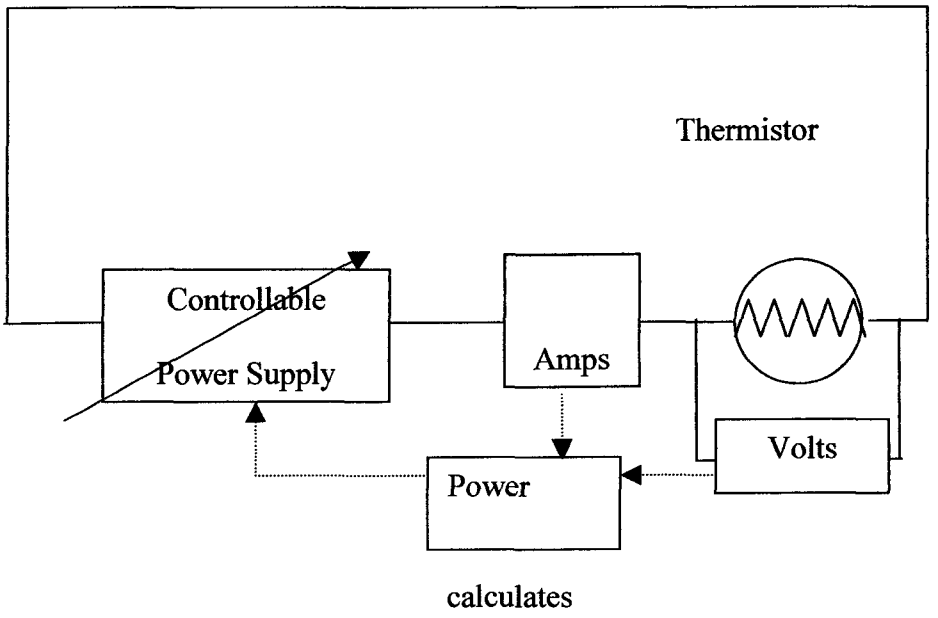

Figure 12. Basic Instrumentation Design for Experiment.

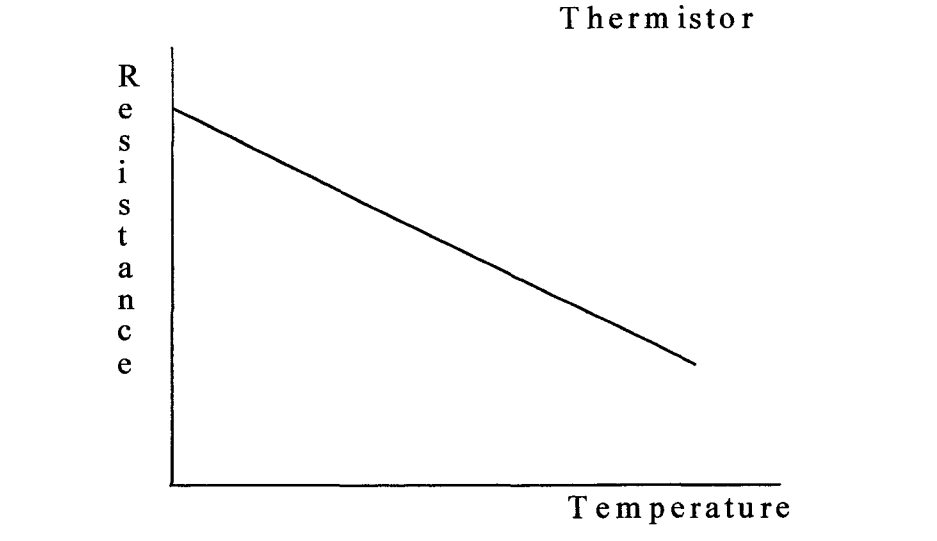

Figure 13. Typical Resistance vs. Temperature of a Thermistor.

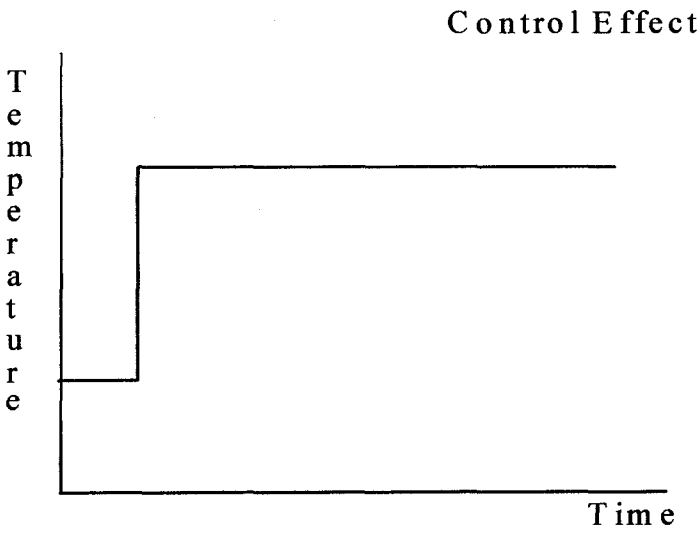

Figure 14. Ideal Box Control Effect on Thermistor

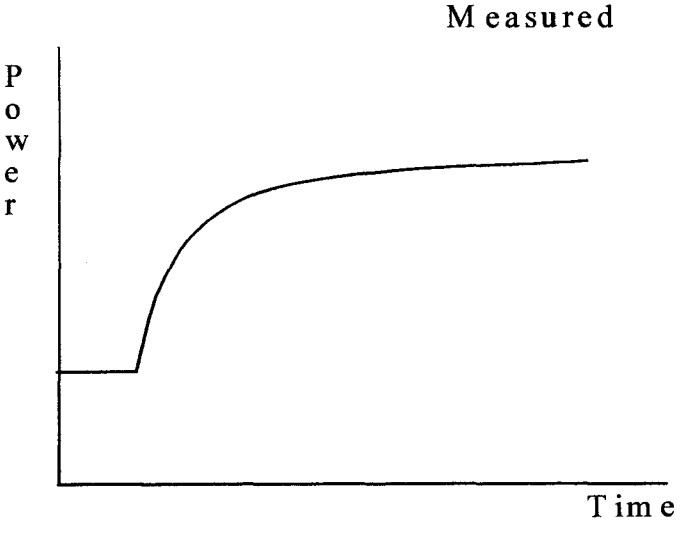

Figure 15. Typical Power vs. Time Curve

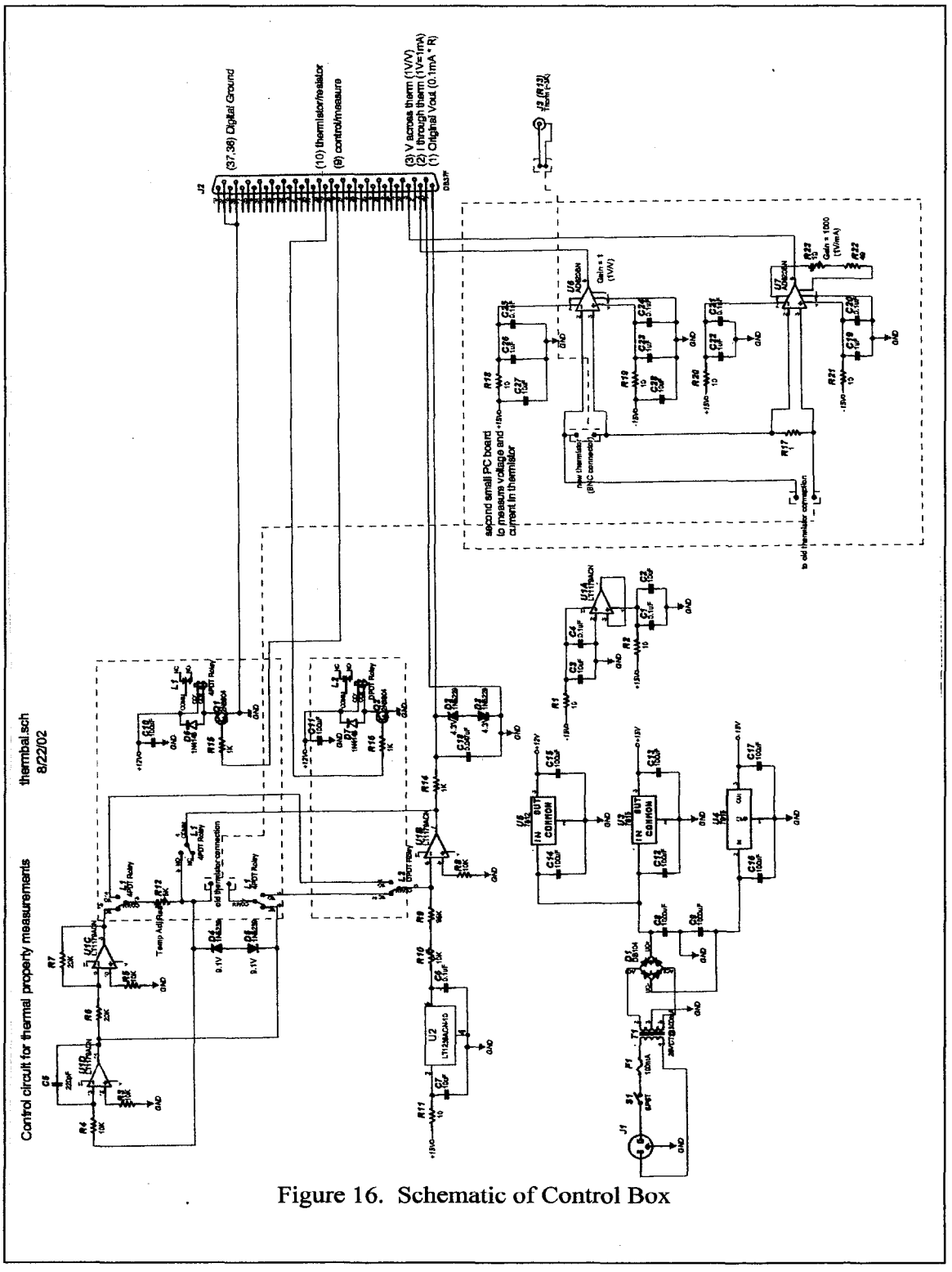

Figure 16. Schematic of Control Box

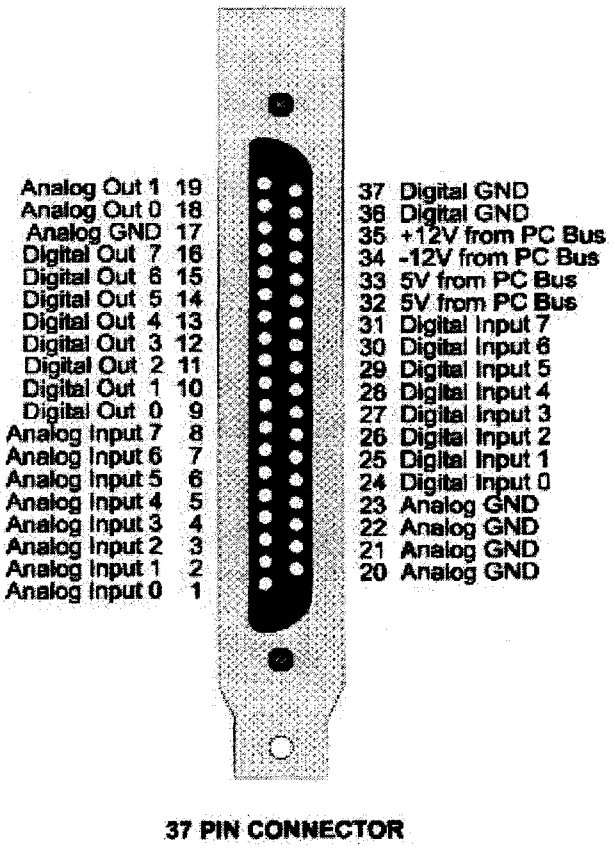

Figure 17. Diagram of the connector used for communication from the control box and the computer.

4.2.1.3 Data Acquisition and Control Board

The I/O card chosen was a Measurement Computing Board, CIO-DAS 08/JR-16. It has Analog I/O and Digital I/O analog inputs and outputs capability. It contained 16 digital channels, 8 for output, and 8 for sensing and controlling devices. The board supported 8 single ended analog inputs and could supply two analog voltage outputs with 16-bit resolution. The board has an A/D non-programmable range of +/- 5 V.

The I/O card is connected to the control box with a 37-pin connector. This allowed the box to be controlled by the 2 digital outputs and collected data from the box from the three analog inputs. Analog Input 0 is the measured voltage output when the thermistor is in measure mode. Analog Input 1 is the measured voltage across the thermistor when in control mode. Analog Input 2 is the measured current across the thermistor when in control mode. Digital Output 0 is the control/measure switch that sets the box to heating or sensing modes. Digital Output 1 is the thermistor/resistor switch that determines if the data collected from the box is related to the thermistor or the adjustable resistor.

4.2.2 Software

4.2.2.1 LabVIEW

LabVIEW is a program developed by National Instruments (2002) that uses a graphical development environment to create programs in block diagram form. It has several uses, some which are signal and data acquisition, measurement analysis, measurement control, data logging, and data presentation. It contains libraries of functions and development tools designed specifically for data acquisition and control. A VI (virtual instrument) was developed in LabVIEW to control/measure the temperature of the thermistor bead, display data, and log and collect data of the thermistor bead or the potentiometer in the system. A VI consists of an interactive user interface, a data flow diagram that serves as the source code, user interface, a data flow diagram that serves as the source, and icon connections that allow the VI to be called by higher level VI's.

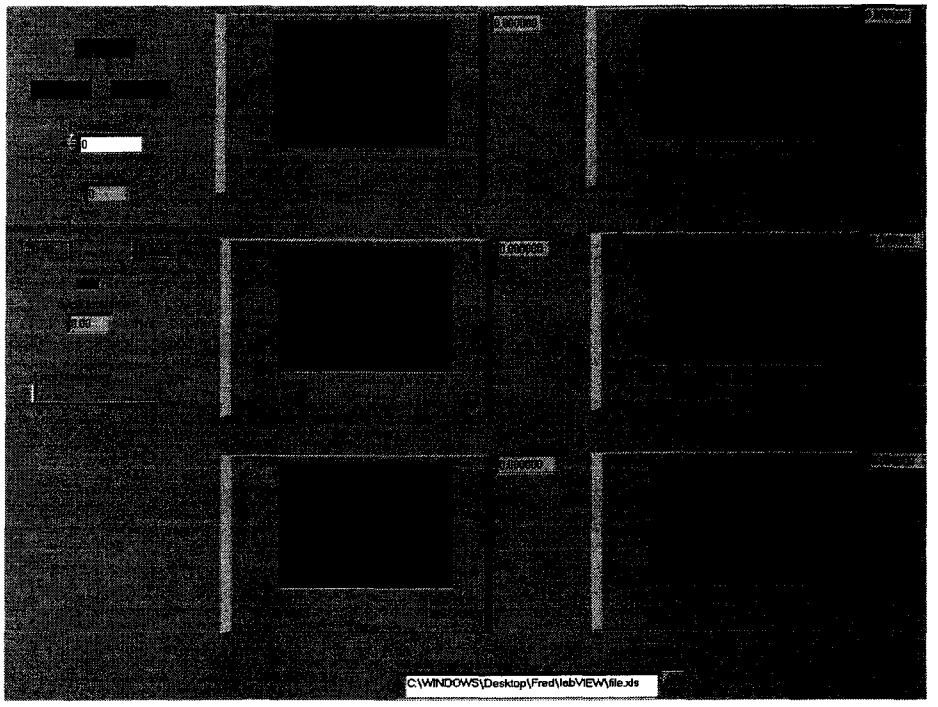

Figure 18. LabVIEW front panel designed to communicate and collect data

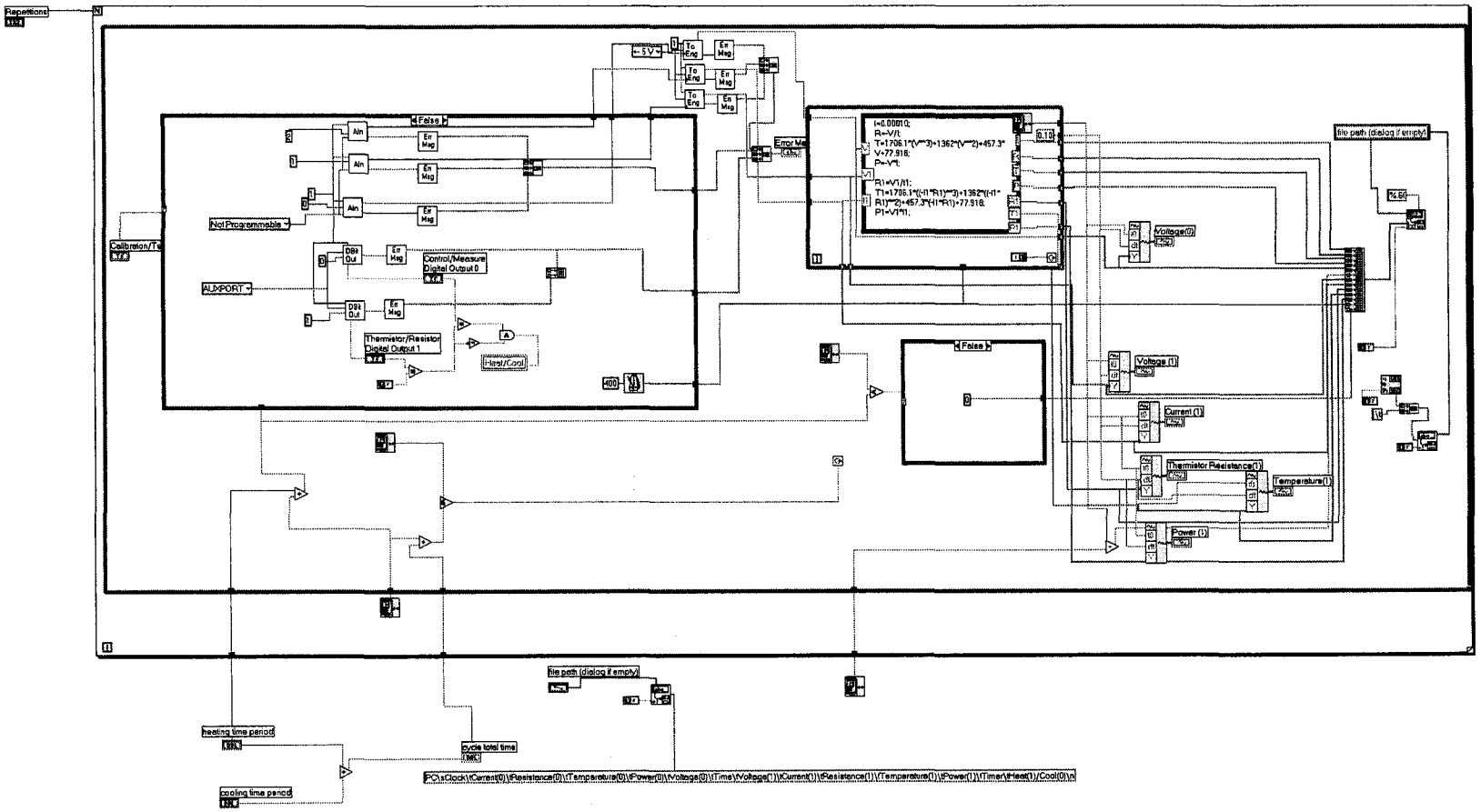

Figure 19. Flow Diagram created in LabVIEW to communicate with and collect data from the control box.

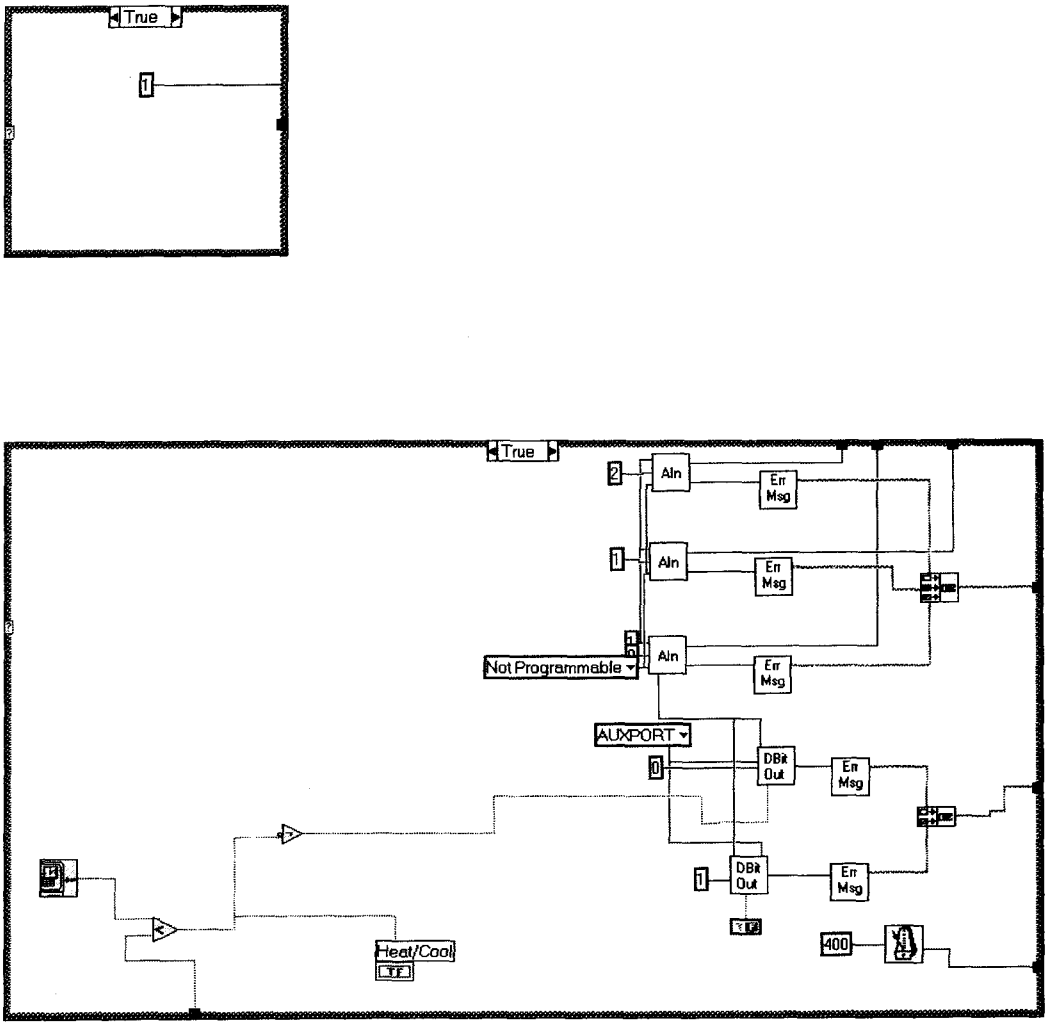

Figure 19. Extension of previous LabVIEW flow diagram.

4.2.2.2 UL (Universal Library) for LabVIEW

The LabVIEW Computer Boards Universal Library extensions contained the virtual instruments needed to construct programs in LabVIEW that would communicate with the Computer Boards data acquisition and control board. It consisted of lower lever VI's that were wired together to form the application. The main VI's used from these were Analog I/O VI's and Digital I/O VI's. This allowed LabVIEW to communicate with the data acquisition board and to collect data from the control box.

The UL VI's used to import and export data were:

- AIn.VI-reads an A/D input channel, reads the specified A/D channel form the specified board. The raw A/D value is converted to an A/D value and returned to Data Value that is the output value of A/D sample.
- Dout.VI-writes a byte to a digital output port. Port # specifies with digital I/O port to read.
- DataValue-digital output value input here
- Board #-configured as 1

Also used was the following Vi's to convert incoming data.

- ToEng.VI-converts A/D count value to an equivalent voltage (or current) value.

Used the SubVI's in the program.

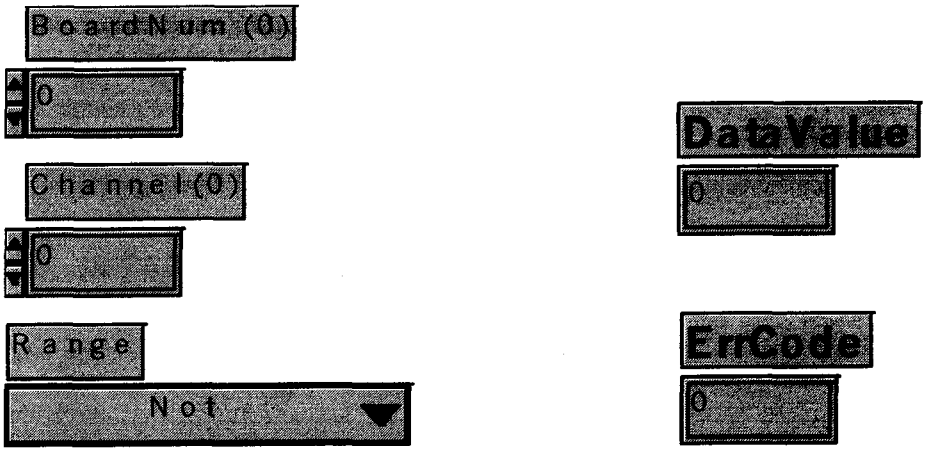

Figure 20. LabVIEW Ain. Vi Front Panel.

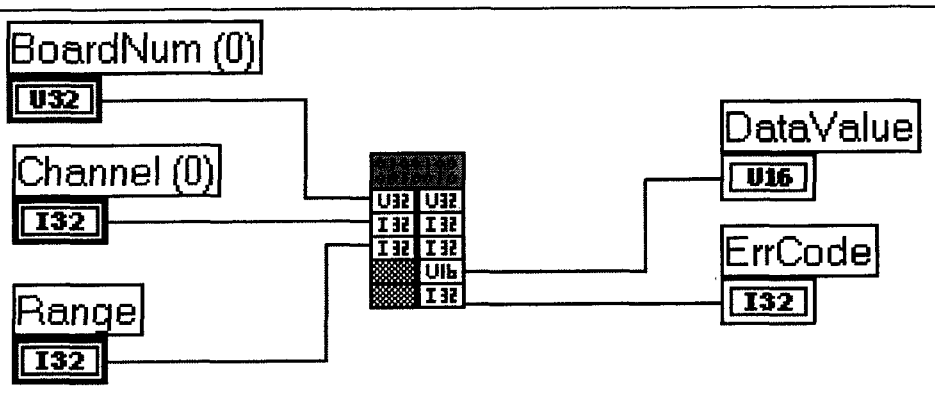

Figure 21. LabVIEW Ain. Vi Diagram.

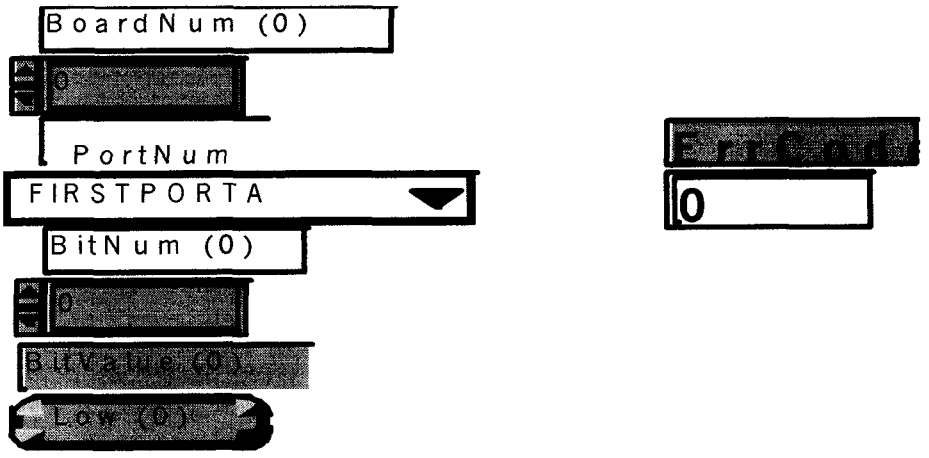

Figure 22. LabVIEW DbitOut.vi Front Panel.

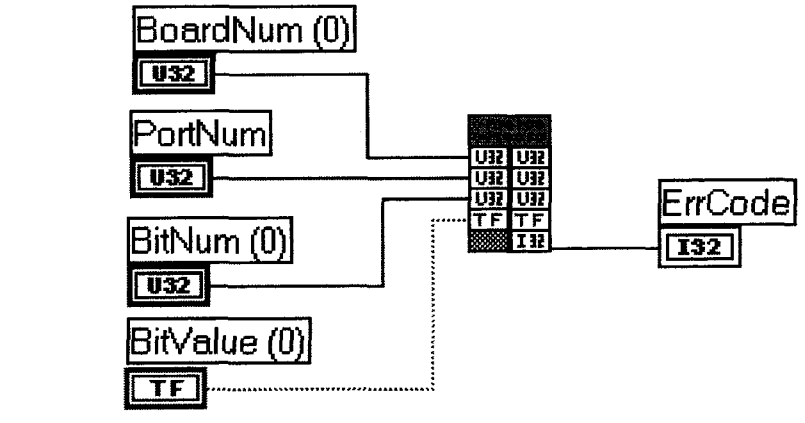

Figure 23. LabVIEW DbitOut. Vi Diagram.

4.3 Measurement System

The measurement system was composed of the thermistor bead, the attached cable to the control box and the control box. Resistances vs. temperature calibrations were performed on the measurement system to determine the additional resistance added to the thermistor due to the cable configuration and control box attachments.

4.3.1 Resistance vs. Temperature Calibration

The system was calibrated by immersing it in a well-stirred water bath and recording the water bath temperature and thermistor resistance (as recorded with the data acquisition software and hardware) at increments of 1°C between 23°C and 41°C. A constant current of 0.1 milliamps was applied across the thermistor bead. Temperature is measured with a Fluke 189 True RMS Multimeter with a Fluke 80TK Thermocouple Module to read temperature with a precision of better than +/.5% +/- 2°C. Converts any Fluke DMM to a thermometer via standard banana plugs. Uses Type-K thermocouple with mini-connector (one included). Switch selectable for °C or °F.

The voltage of the box was read in LabView. The 80TK accepted the output of the K type thermocouple and converted it to 1 millivolt per °Celsius. The thermistor resistance versus temperature calibration for a thermistor probe in the measurement system is presented in Table 1.

Table 4. The Resistance versus Temperature Calibration for OMEGA 44004 resistor attached to control box.

Resistance versus Temperature 22°C to 40°C		
Temperature (°C)	Voltage (V)	Resistance (Ω)
22	0.2496181	2496
23	0.2390963	2390
24	0.2290043	2290
26	0.2193244	2193
27	0.2100399	2100
28	0.2011346	2011
29	0.192593	1925
30	0.1844003	1844
31	0.1736459	1765
32	0.1661712	1690
33	0.1590182	1617
34	0.1521731	1548
35	0.1456226	1481
36	0.1393541	1418
37	0.1333555	1356
38	0.1276151	1298
39	0.1221217	1241
40	0.1168649	1187
41	0.1118343	1136

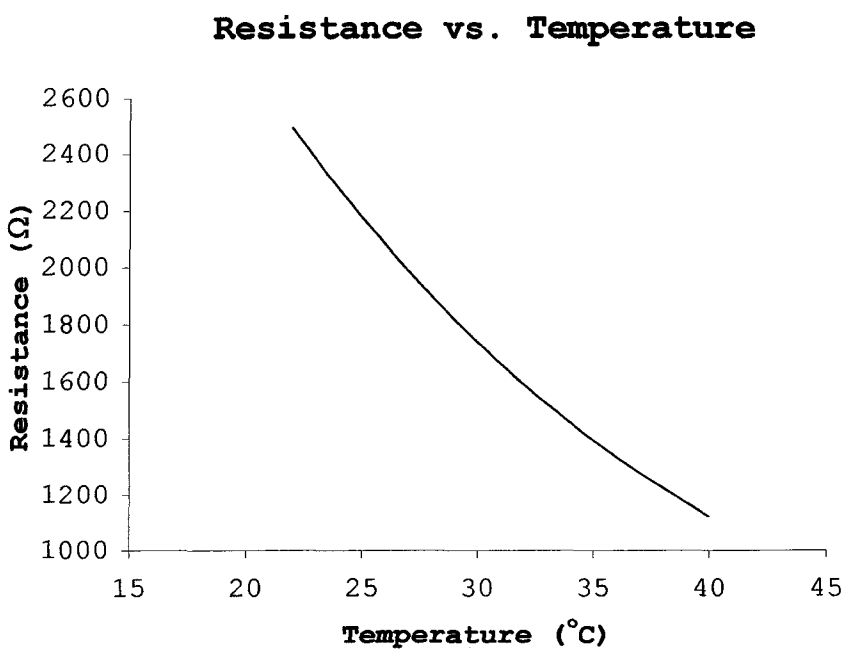

Figure 24. Resistance versus Temperature calibration for OMEGA 40044

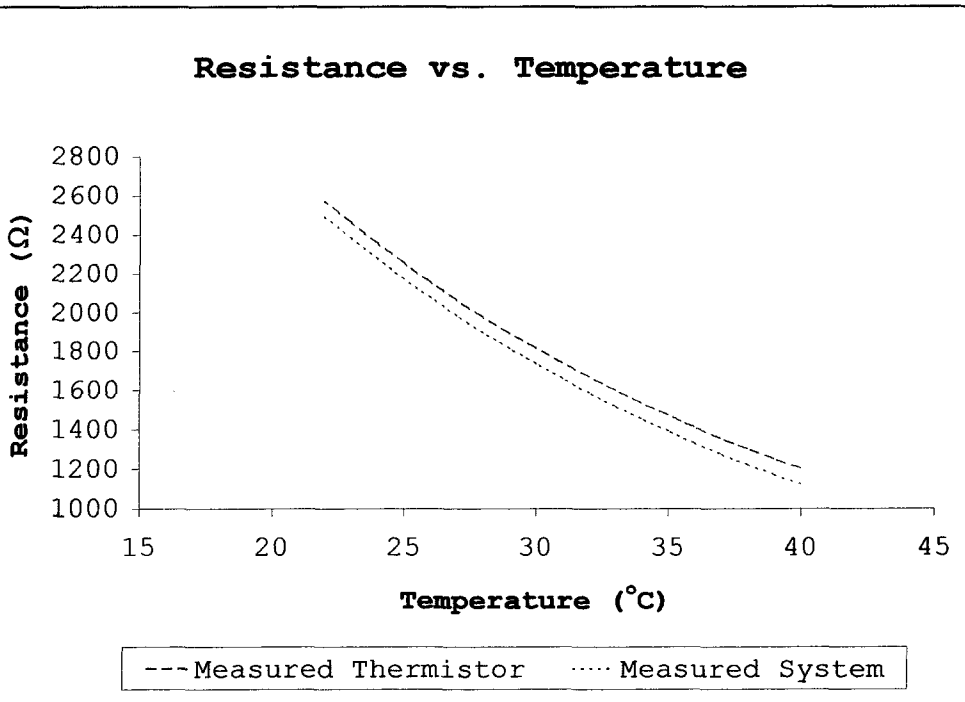

Figure 25. Resistance versus Temperature Graph for the Thermistor and Measurement System when calibrated.

4.3.2 Test of Calibration

After the determination of the resistance versus temperature curve, the next step was to test the accuracy with which the probe can measure the thermal properties of media of known thermal properties. This was an important step because for a heated thermistor in spherical geometry the accurate qualification of perfusion follows directly from the accurate measurement of thermal conductivity of the media adjacent to the thermistor bead.

The ability of the measurement system to determine thermal conductivity was evaluated using two liquids and a plastic of known thermal properties. Two liquid standards were used: ethylene glycol and glycerol. Lexan was the plastic used in this study. Thermal properties are taken at approximately 24°C.

Approximately one hundred milliliters of each liquid was poured into individual 250 milliliter beakers. The beakers were surrounded by a protective encasing to isolate them from outside thermal effects. The thermistor bead was then placed inside the beaker and located in the fluid. The thermistor bead was placed between two blocks of Lexan with a depth of 1/2" with a length of 6" and width 3". Thermal properties were derived from measurements of the applied electrical power required to maintain the volume average thermistor temperature at some predetermined increment above the initial baseline.

Table 5. Source data for liquids and plastic.

Item	Source	Amount
Etylene Glycol	Fisher Scientific	100 ml
Glycerin	Fisher Scientific	100 ml
Lexan 9034	GE (General Electric) Plastics Resin Division	1/2 " thick

Table 6. Thermal Data for Ethylene Glycol ($C_2H_4(OH)_2$) [Incropera 1996].

T (K)	ρ (kg/m^3)	C_p (kJ/kg*K)	$k*10^3$ (W/m*K)
273	1130.8	2.294	242
280	1125.8	2.323	244
290	1118.8	2.368	248
300	1114.4	2.415	252
310	1103.7	2.460	255
320	1096.2	2.505	258
330	1089.5	2.549	260
340	1083.8	2.592	261
350	1079.0	2.637	261
360	1074.0	2.682	261
370	1066.7	2.728	262
373	1058.5	2.742	263

Table 7. Thermal Data for Glycerin ($C_3H_5(OH)_3$) [Incropera 1996].

T (K)	ρ (kg/m^3)	C_p (kJ/kg*K)	k*10^3 (W/m*K)
273	1276.0	2.26	282
280	1271.9	2.298	284
290	1265.8	2.367	286
300	1259.9	2.427	286
310	1253.9	2.490	286
320	1247.2	2.564	287

Table 7. Thermal Data for Glycerin ($C_3H_5(OH)_3$) [Incropera 1996].

T (K)	ρ (kg/m^3)	C_p (kJ/kg*K)	k*10^3 (W/m*K)
273	1276.0	2.26	282
280	1271.9	2.298	284
290	1265.8	2.367	286
300	1259.9	2.427	286
310	1253.9	2.490	286
320	1247.2	2.564	287

Table 8. Thermal Data for Lexan 9034 Polycarbonate (GE) [General Electric Company 2002].

T (K)	ρ (kg/m^3)	C_p (kJ/kg*K)	k*10^3 (W/m*K)
273	1200.0	1.25	195

CHAPTER 5

RESULTS

5.1 Numerical

Numerically determined values of heat dissipation throughout the chosen media were determined using the Fortran 90 program.

Table 9. Numerically derived power values for Glycerin ($C_3H_5(OH)_3$).

Glycerin1.dat (k=0.286) ΔT=0.5°C	
Time (seconds)	Q (Watts x 10^4)
3.210366	-5.4017623
4.012499	-5.2893162
5.215700	-5.1721750
6.017833	-5.1144644
7.221034	-5.0466676
8.023162	-5.0102145
9.226068	-4.9647369
10.02800	-4.9390789
11.23091	-4.9058750
12.03285	-4.8865628
13.23575	-4.8609549
14.03769	-4.8457438
15.24060	-4.8252195

Table 10. Numerically derived power values for Ethylene Glycol ($C_2H_4(OH)_2$).

Ethylene Glycol1.dat (k=0.2537) ΔT=0.5°C	
Time (seconds)	Q (Watts x 10^4)
3.204440	-4.8057747
4.005050	-4.7045475
5.206108	-4.5990816
6.006813	-4.5471240
7.207870	-4.4860868
8.008574	-4.4532679
9.209632	-4.4123162
10.01034	-4.3892124
11.21139	-4.3593155
12.01210	-4.3419265
13.21316	-4.3188702
14.01386	-4.3051748
15.21492	-4.2866959

Table 11. Numerically derived power values for Lexan 9034 Polycarbonate (GE).

Lexan1.dat (k=0.195) ΔT=0.5°C	
Time (seconds)	Q (Watts x 10^4)
3.207952	-3.57972
4.009573	-3.51394
5.212004	-3.44543
6.013624	-3.41167
7.216055	-3.37202
8.017675	-3.3507
9.220106	-3.32409
10.02173	-3.30908
11.22416	-3.28966
12.02578	-3.27836
13.22821	-3.26338
14.02983	-3.25449
15.23226	-3.24248

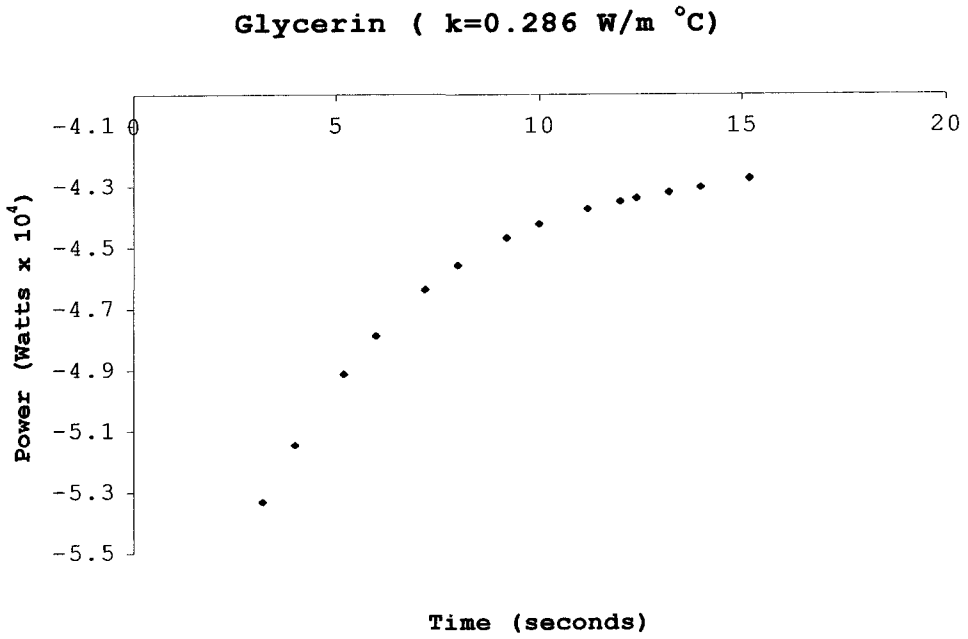

Figure 26. Numerically determined Power vs. Time Curve for Glycerin.

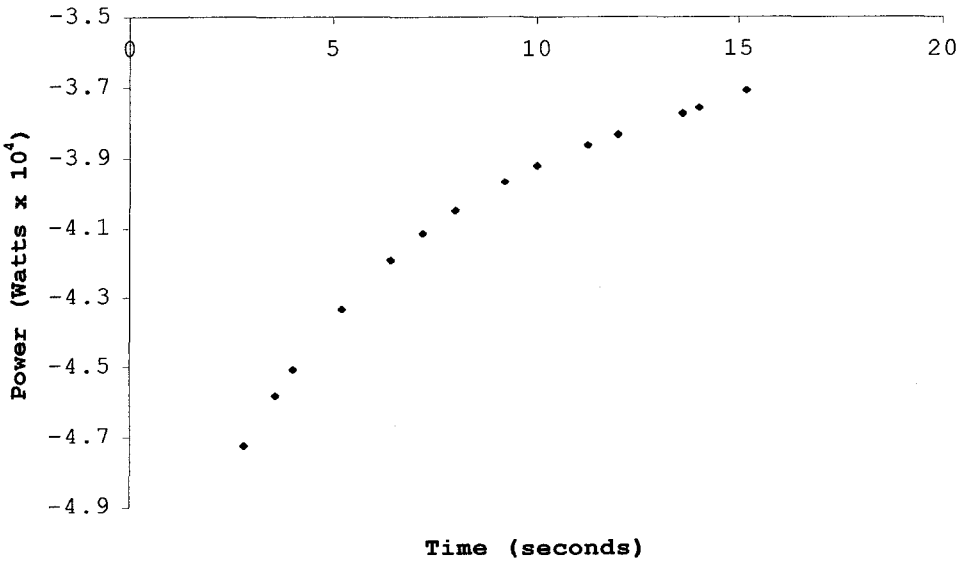

Figure 27. Numerically determined Power vs. Time Curve for Ethylene Glycol.

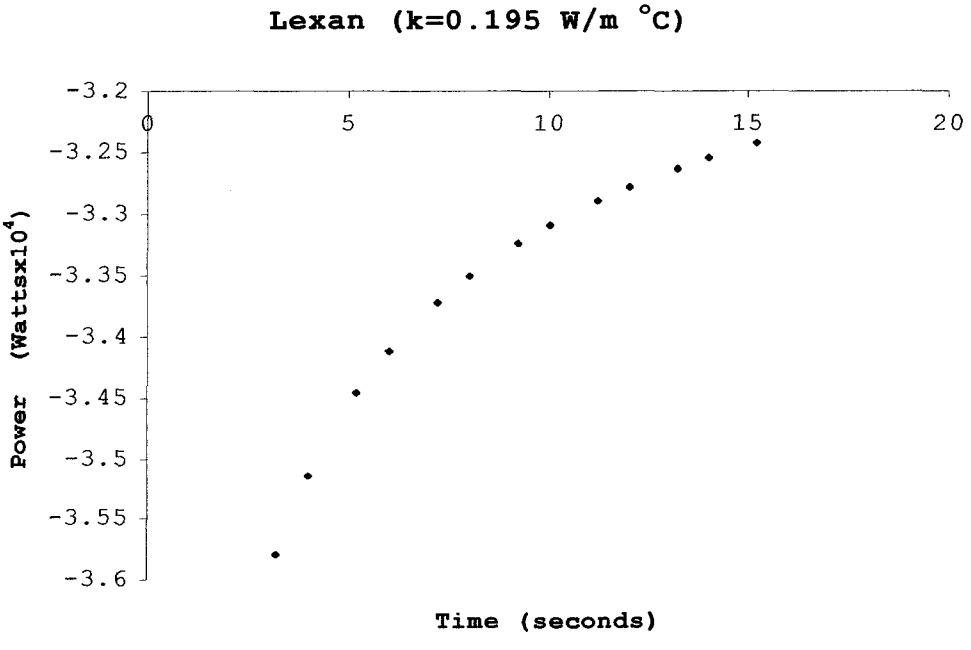

Figure 28. Numerically determined Power vs. Time Curve for Lexan.

5.2 Experimental

Twelve experiments were run in each of the media, recording voltage and current outputs. The amount of power dissipated in each medium due to thermistor heating was determined analyzing the experimentally determined voltage and current data. The energy dissipation was determined by summing the area under the power dissipation curve.

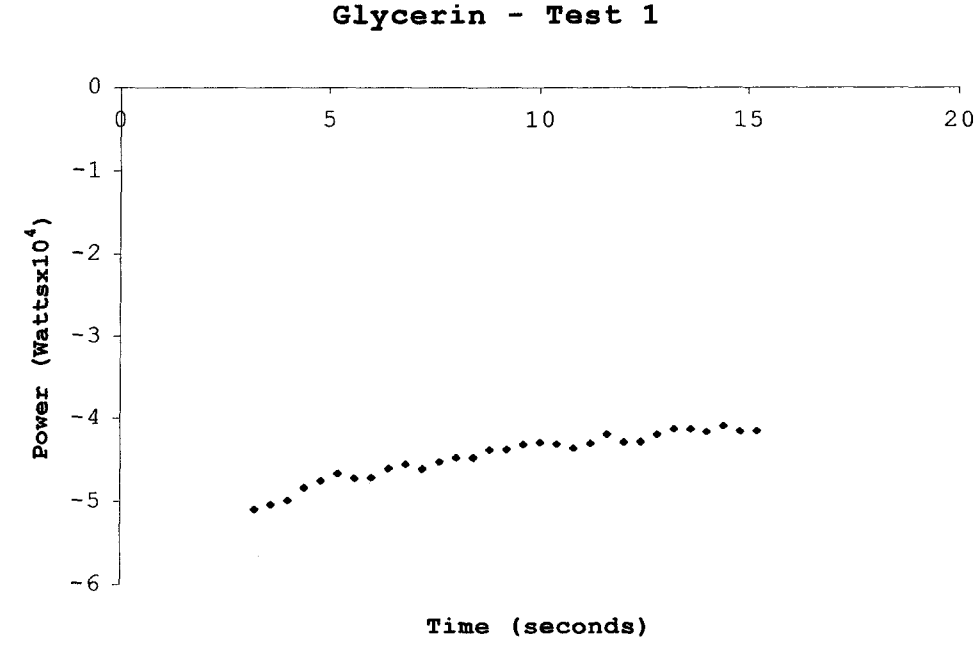

Figure 29. Experimental Power vs. Time Curve for Glycerin - Test 1.

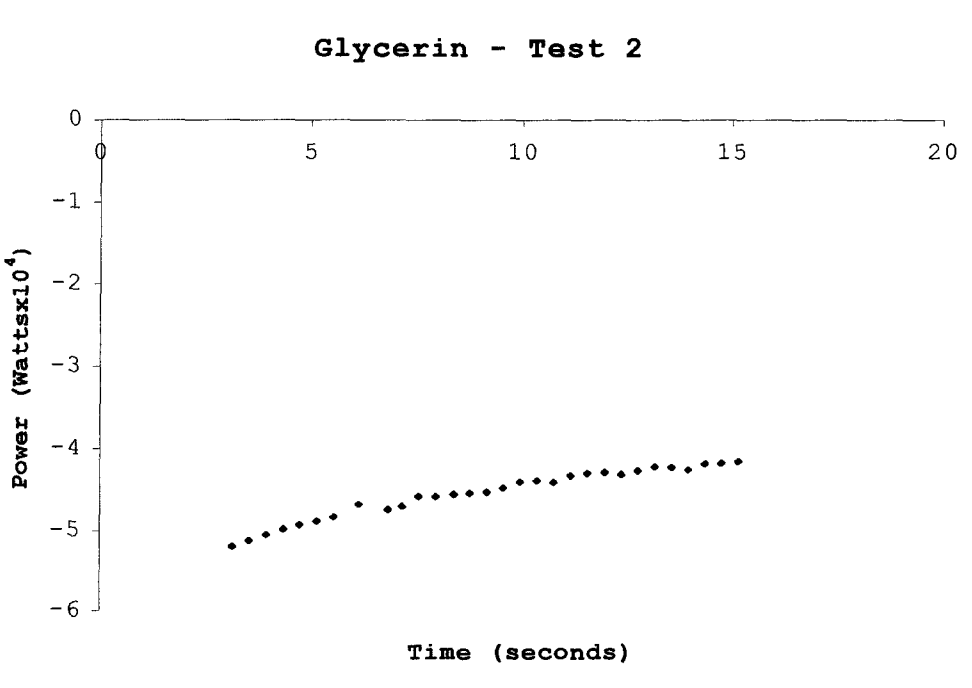

Figure 30. Experimental Power vs. Time Curve for Glycerin - Test 2.

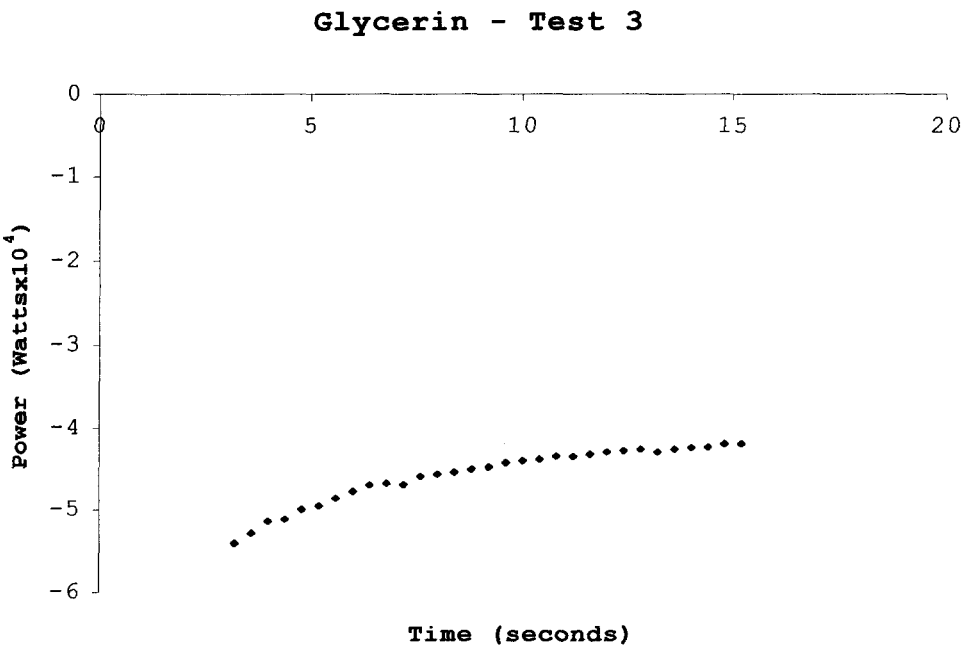

Figure 31. Experimental Power vs. Time Curve for Glycerin - Test 3.

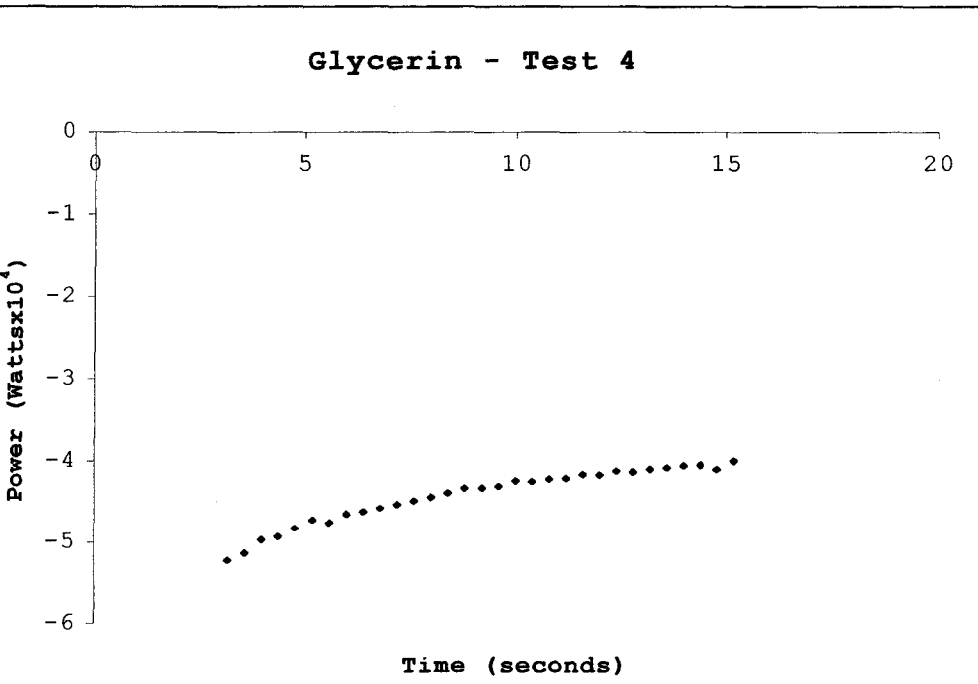

Figure 32. Experimental Power vs. Time Curve for Glycerin - Test 4.

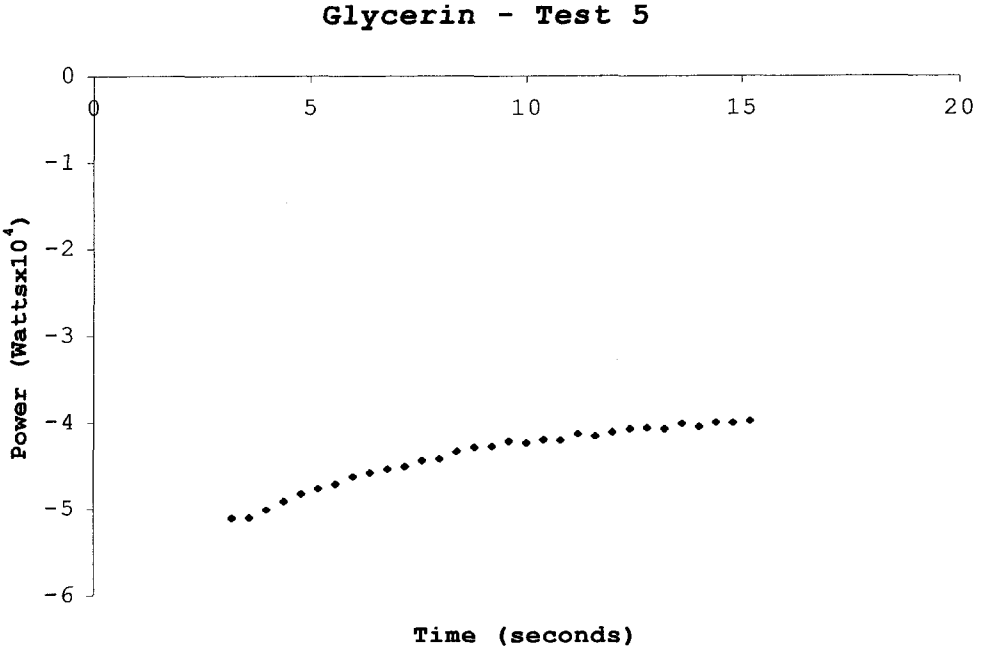

Figure 33. Experimental Power vs. Time Curve for Glycerin - Test 5.

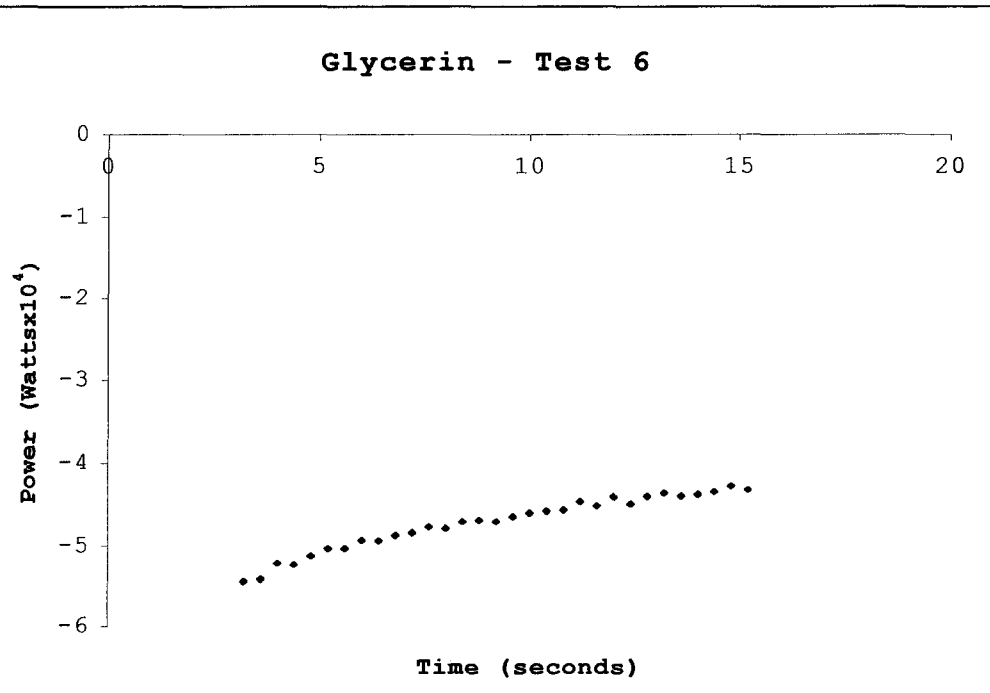

Figure 34. Experimental Power vs. Time Curve for Glycerin - Test 6.

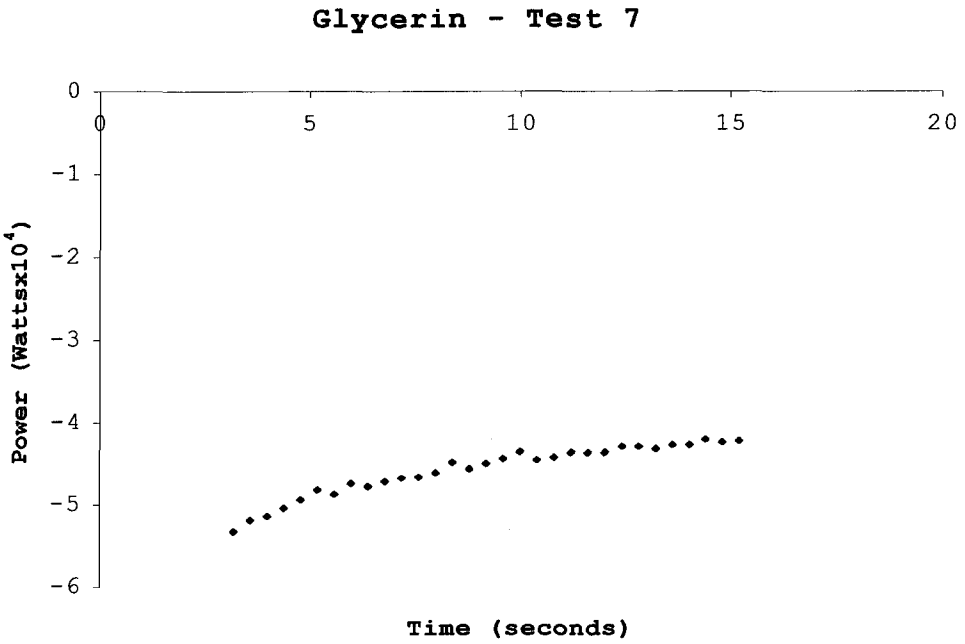

Figure 35. Experimental Power vs. Time Curve for Glycerin - Test 7.

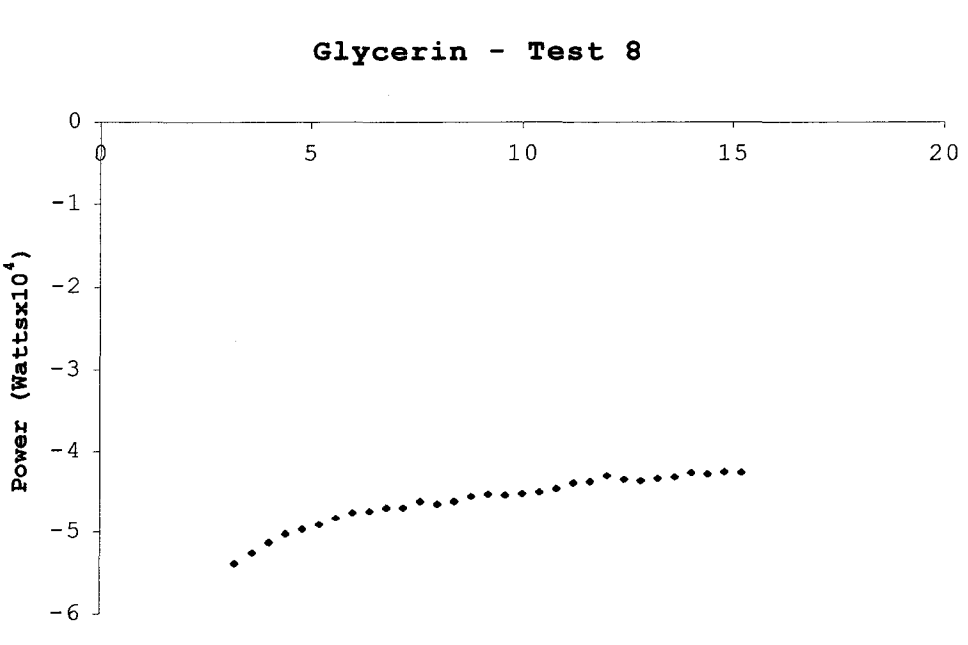

Figure 36. Experimental Power vs. Time Curve for Glycerin - Test 8.

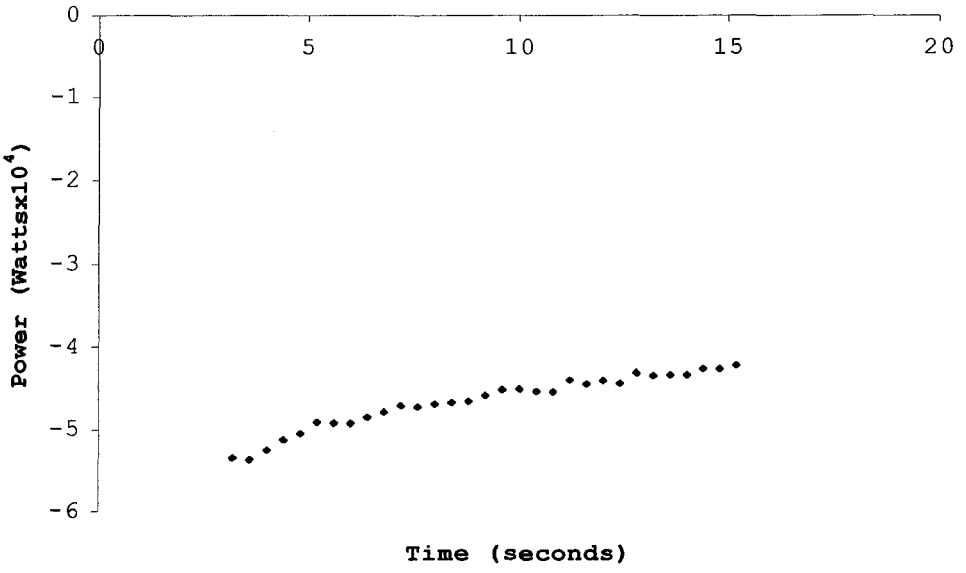

Figure 37. Experimental Power vs. Time Curve for Glycerin - Test 9.

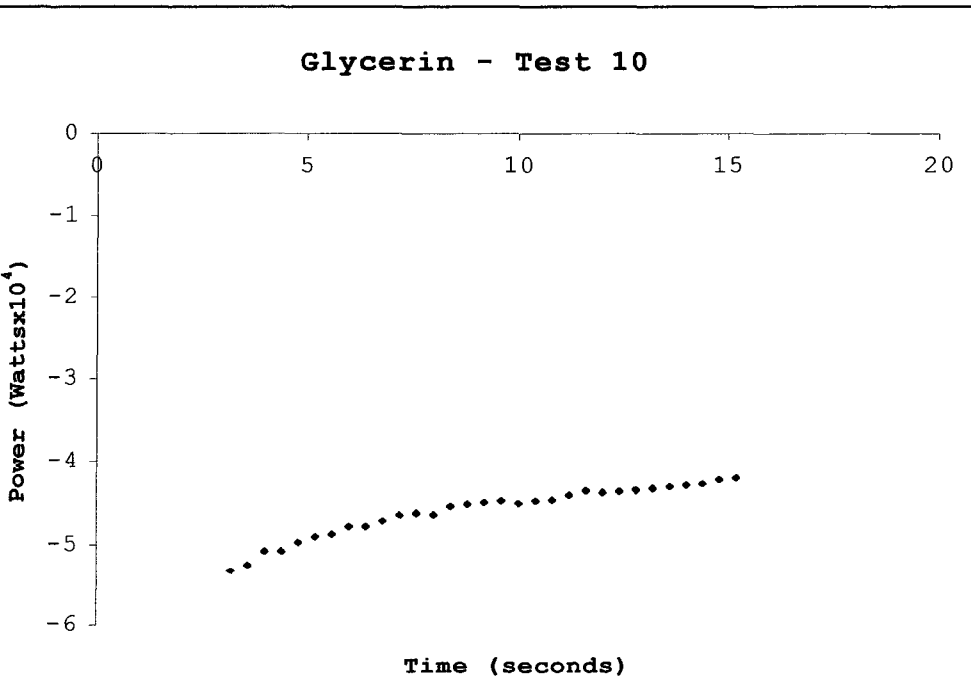

Figure 38. Experimental Power vs. Time Curve for Glycerin - Test 10.

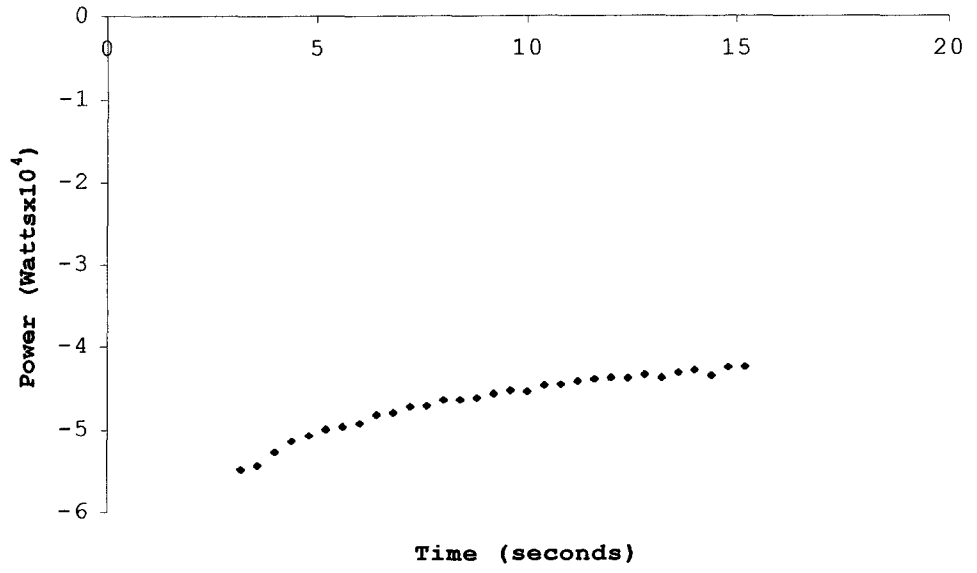

Figure 39. Experimental Power vs. Time Curve for Glycerin - Test 11.

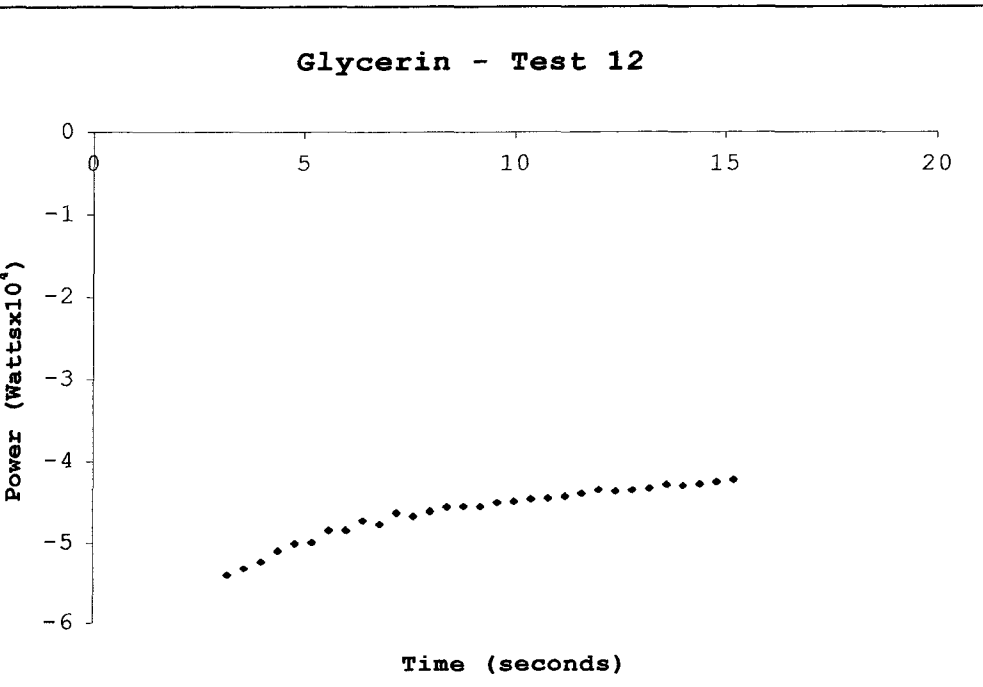

Figure 40. Experimental Power vs. Time Curve for Glycerin - Test 12.

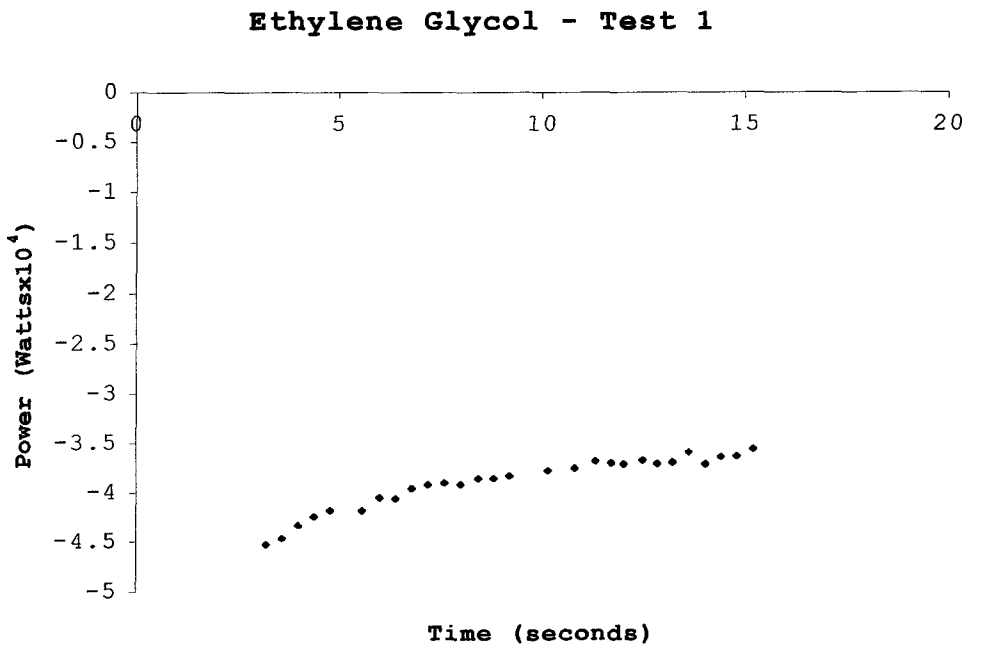

Figure 41. Experimental Power vs. Time Curve for Ethylene Glycol - Test 1.

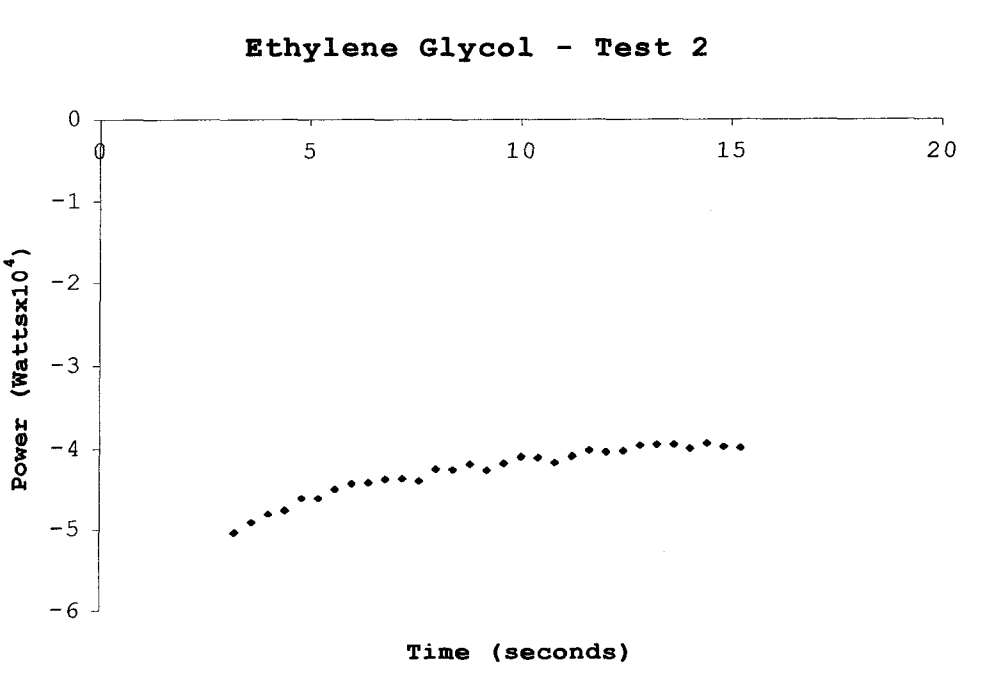

Figure 42. Experimental Power vs. Time Curve for Ethylene Glycol - Test 2.

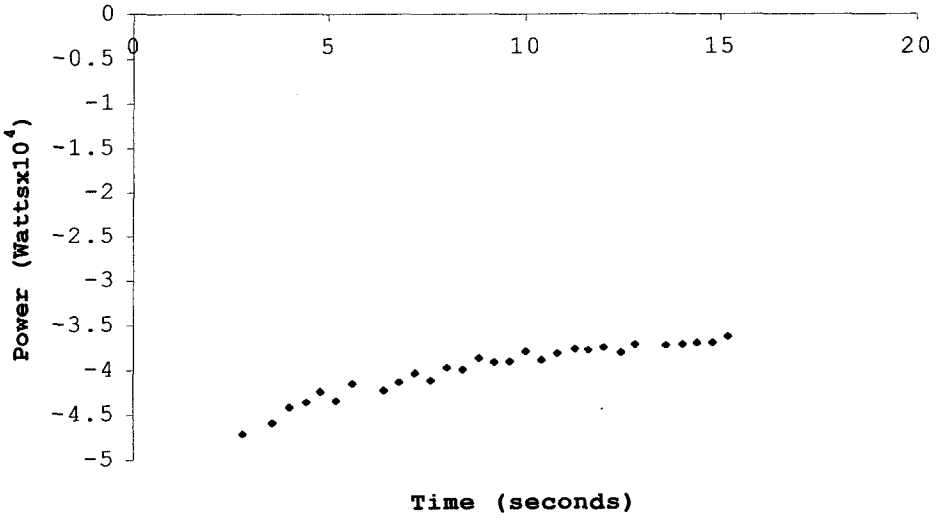

Figure 43. Experimental Power vs. Time Curve for Ethylene Glycol - Test 3.

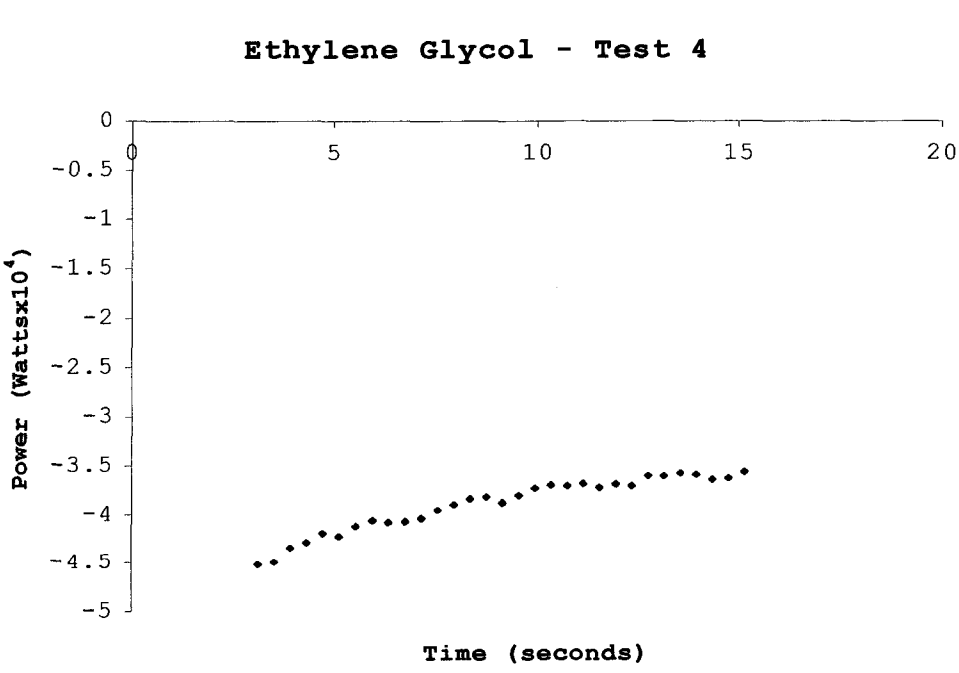

Figure 44. Experimental Power vs. Time Curve for Ethylene Glycol - Test 4.

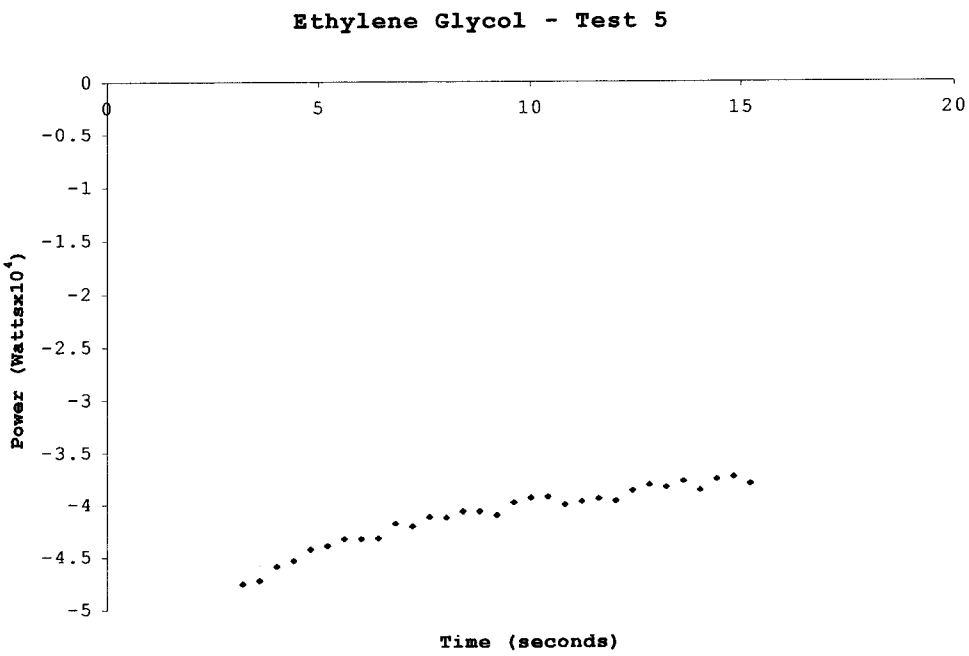

Figure 45. Experimental Power vs. Time Curve for Ethylene Glycol - Test 5.

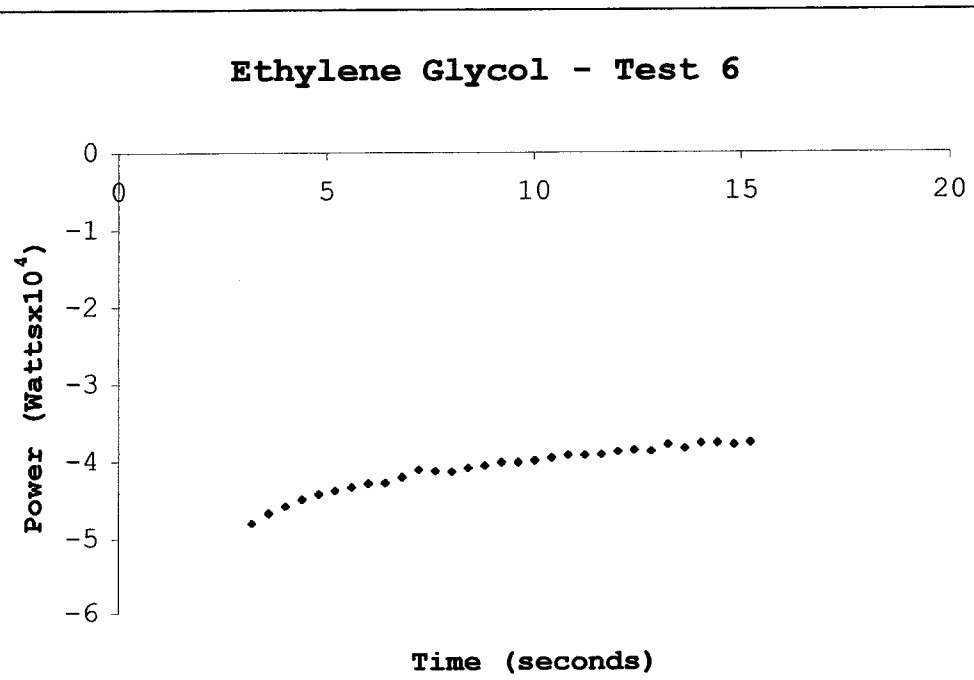

Figure 46. Experimental Power vs. Time Curve for Ethylene Glycol - Test 6.

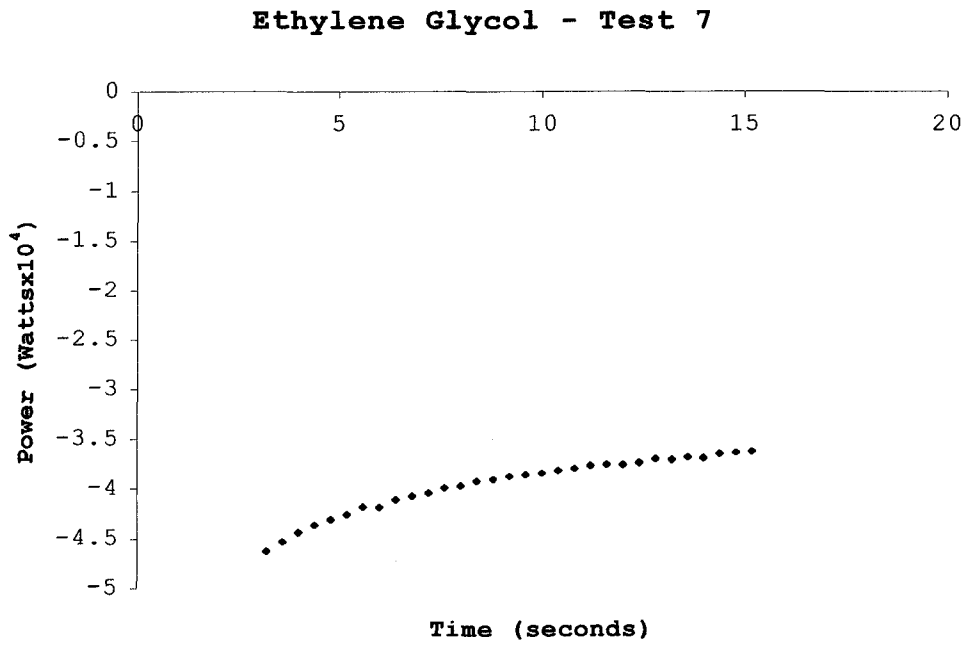

Figure 47. Experimental Power vs. Time Curve for Ethylene Glycol - Test 7.

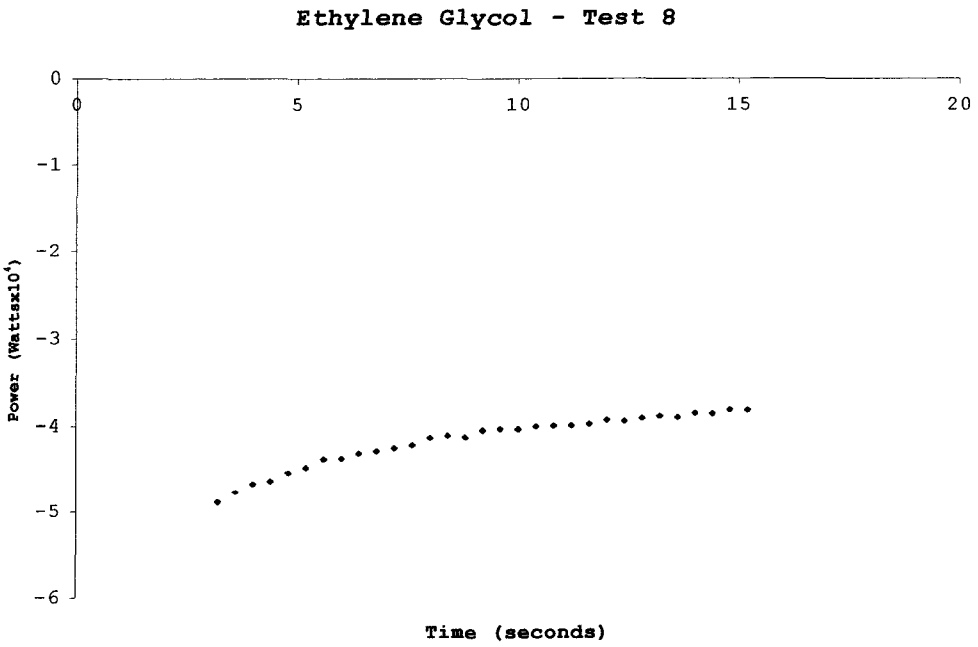

Figure 48. Experimental Power vs. Time Curve for Ethylene Glycol - Test 8.

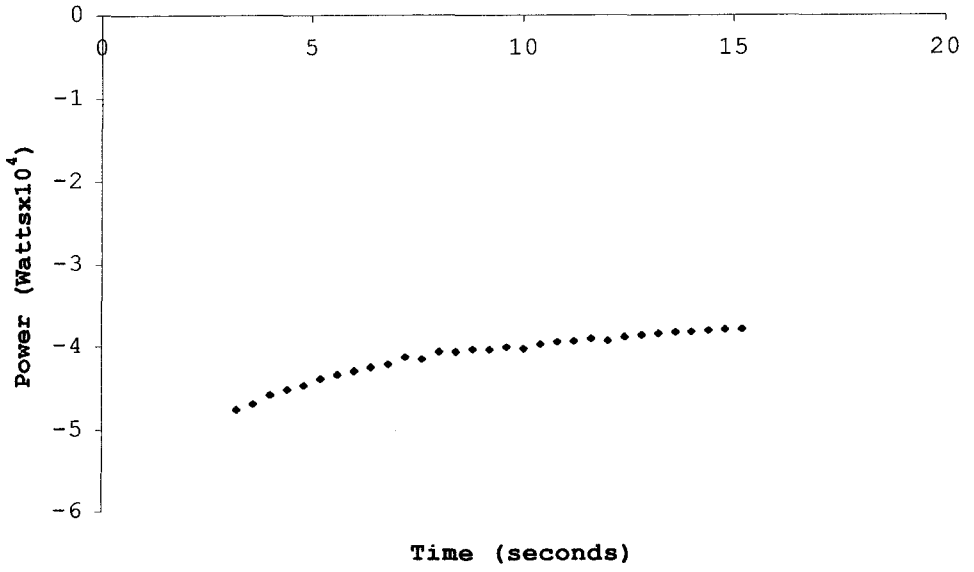

Figure 49. Experimental Power vs. Time Curve for Ethylene Glycol - Test 9.

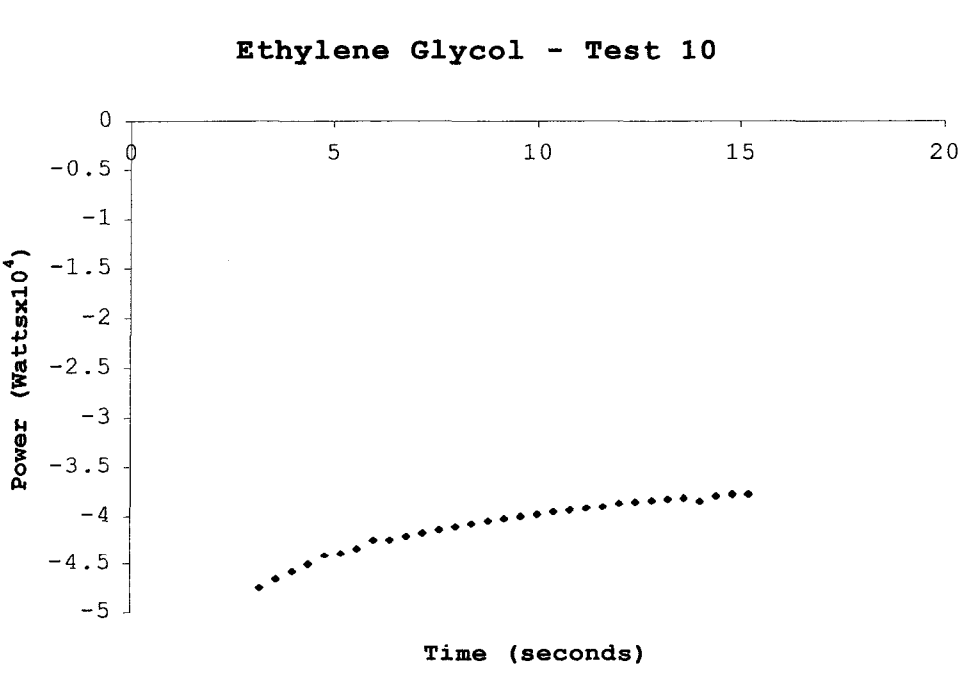

Figure 50. Experimental Power vs. Time Curve for Ethylene Glycol - Test 10.

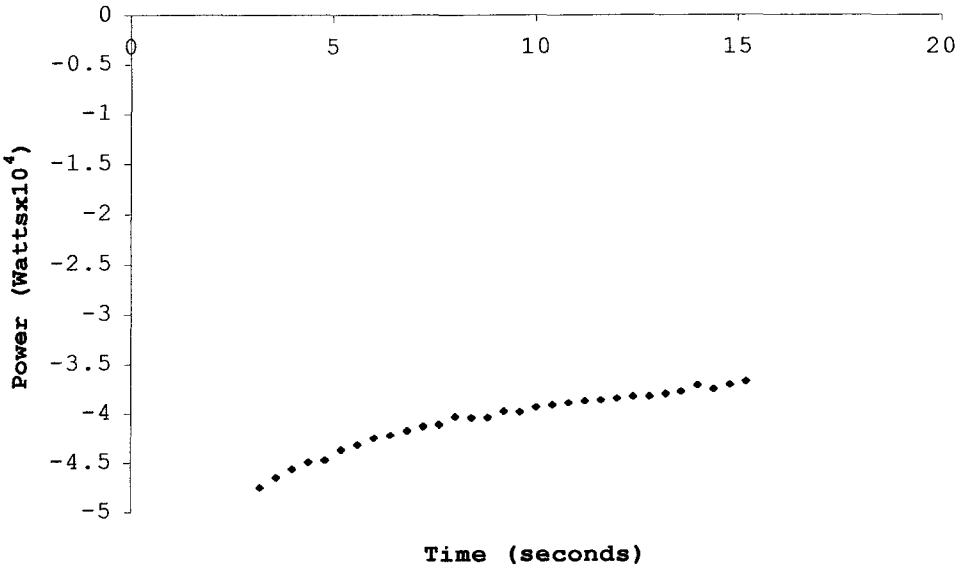

Figure 51. Experimental Power vs. Time Curve for Ethylene Glycol - Test 11.

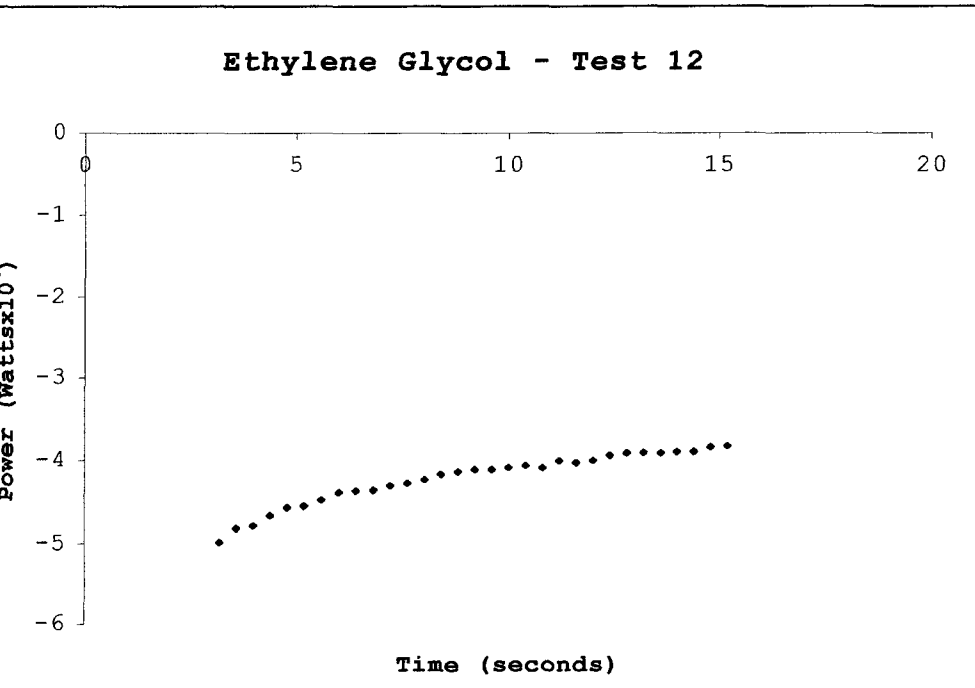

Figure 52. Experimental Power vs. Time Curve for Ethylene Glycol - Test 12.

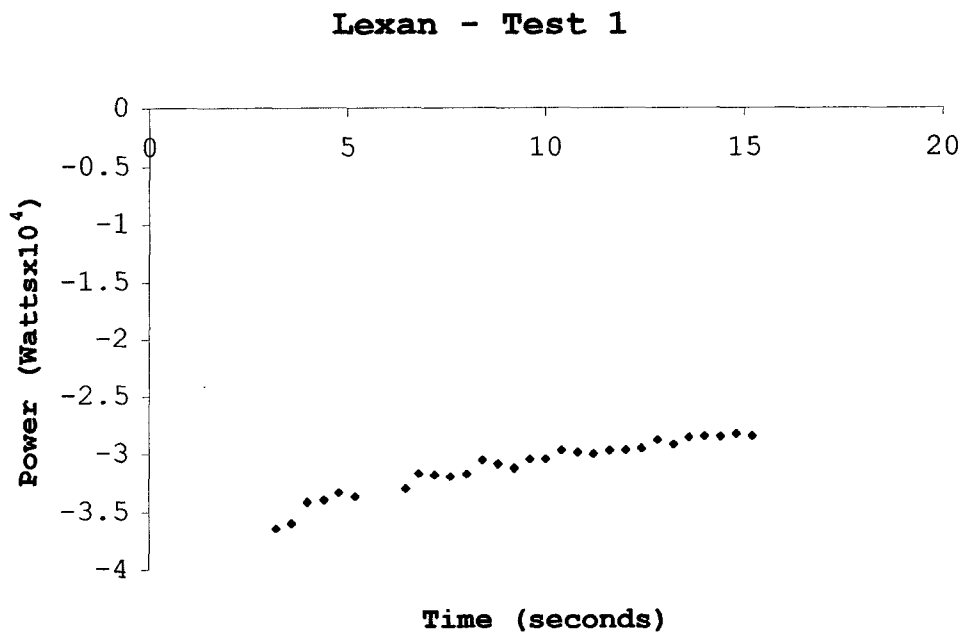

Figure 53. Experimental Power vs. Time Curve for Lexan - Test 1.

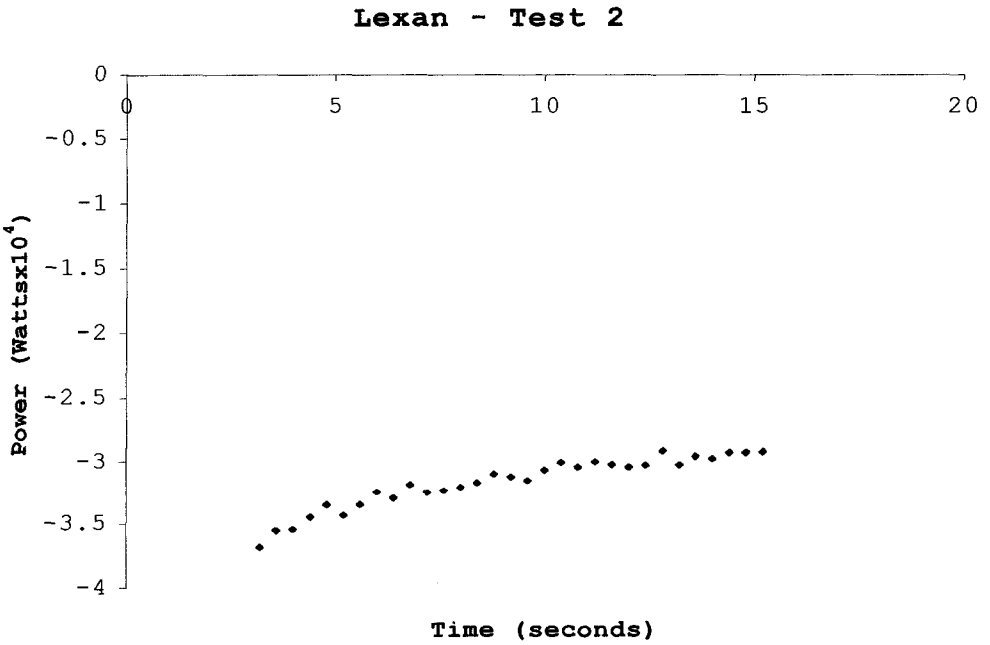

Figure 54. Experimental Power vs. Time Curve for Lexan - Test 2.

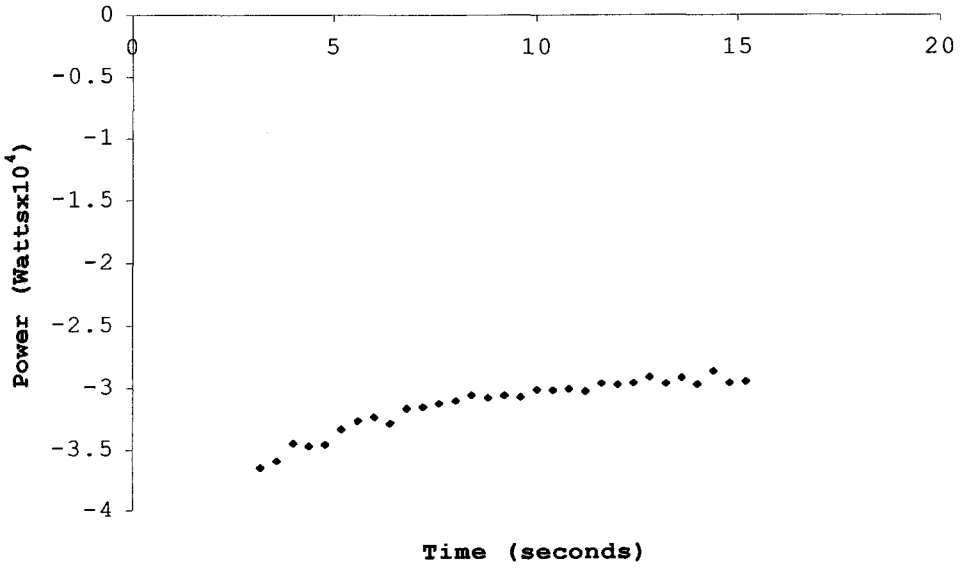

Figure 55. Experimental Power vs. Time Curve for Lexan - Test 3.

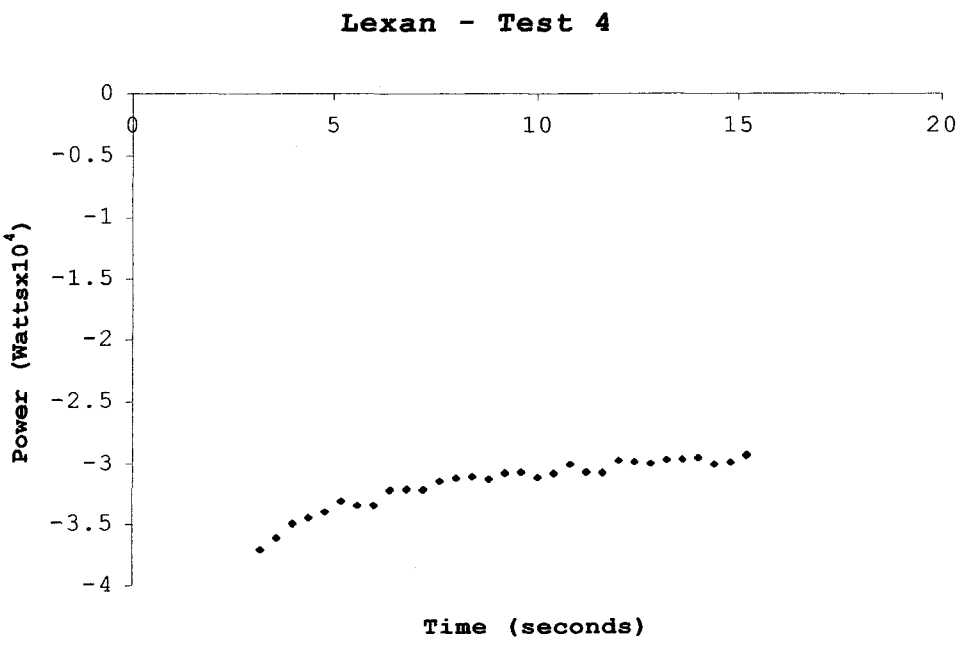

Figure 56. Experimental Power vs. Time Curve for Lexan - Test 4.

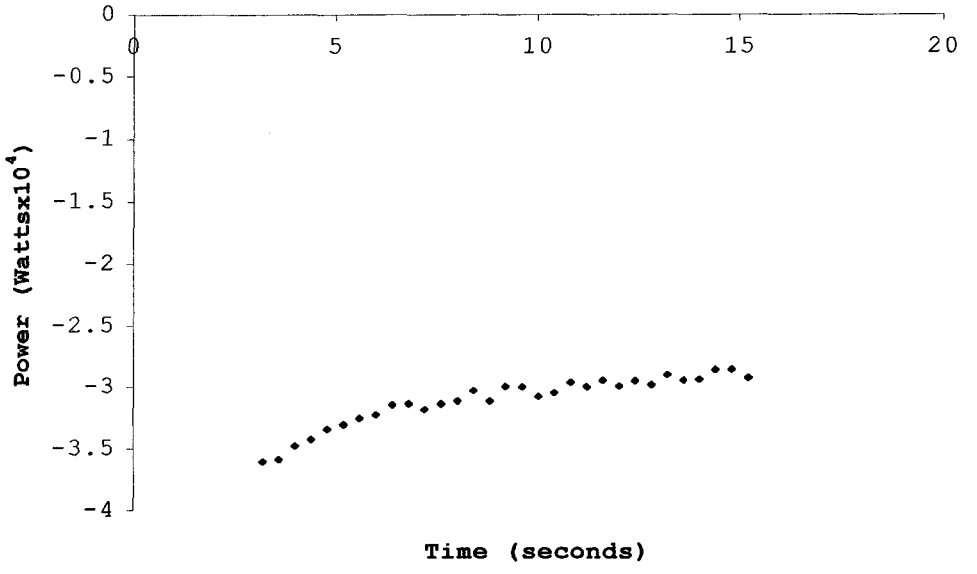

Figure 57. Experimental Power vs. Time Curve for Lexan - Test 5.

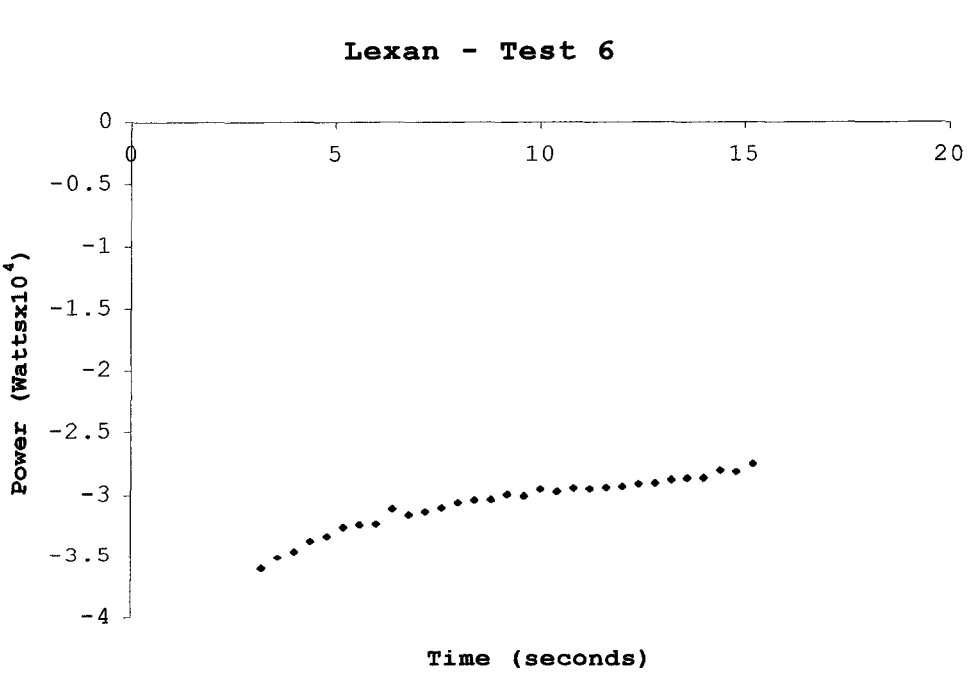

Figure 58. Experimental Power vs. Time Curve for Lexan - Test 6.

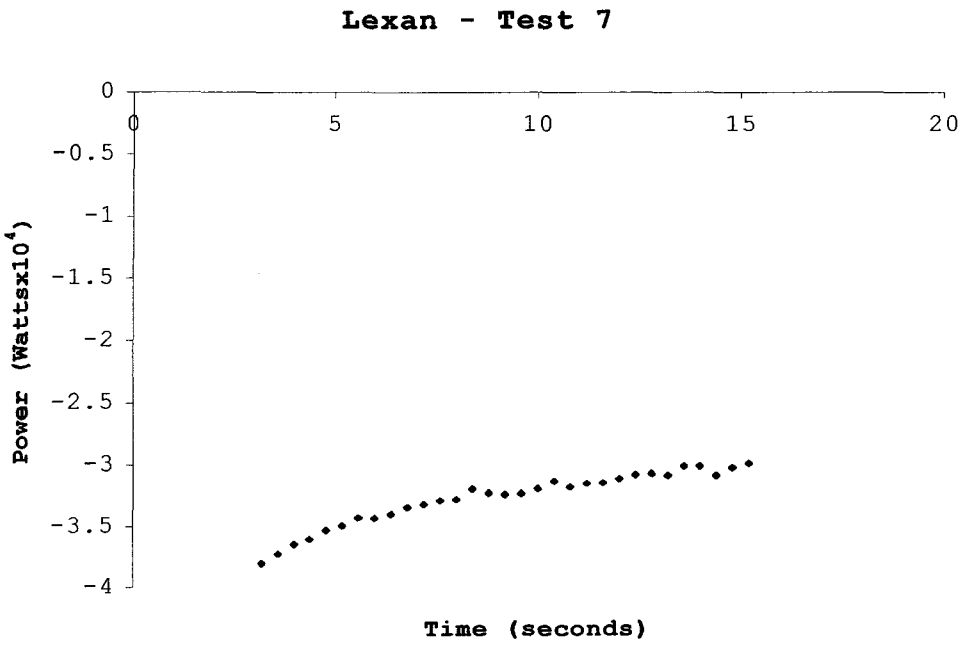

Figure 59. Experimental Power vs. Time Curve for Lexan - Test 7.

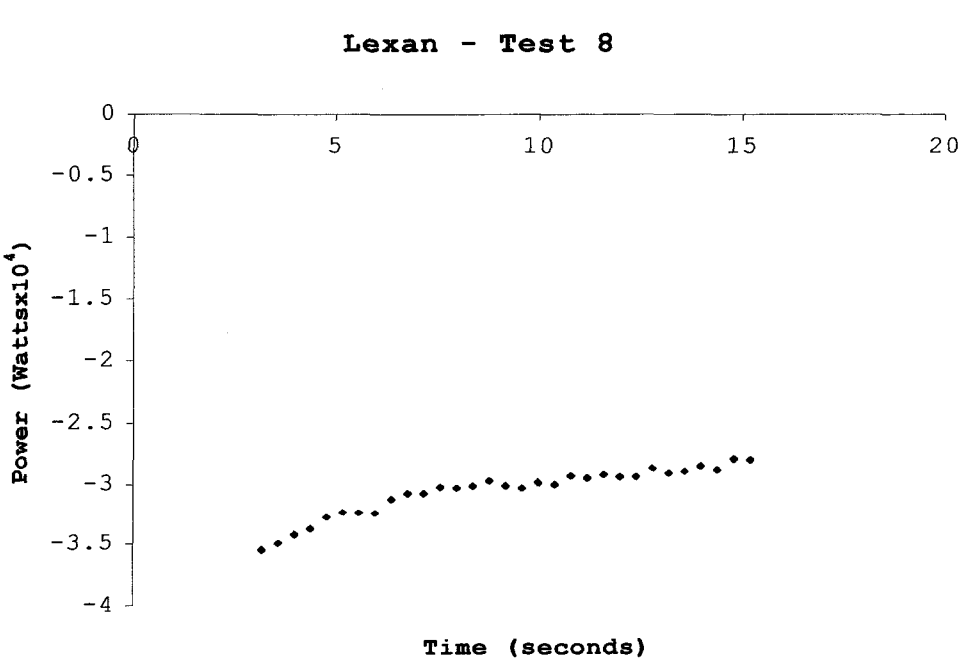

Figure 60. Experimental Power vs. Time Curve for Lexan - Test 8.

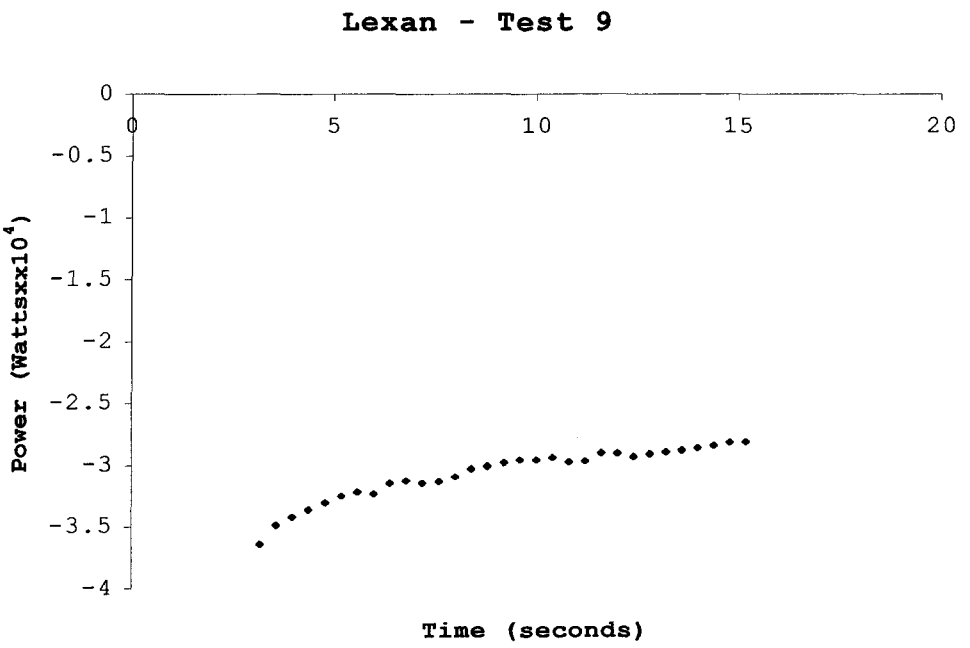

Figure 61. Experimental Power vs. Time Curve for Lexan - Test 9.

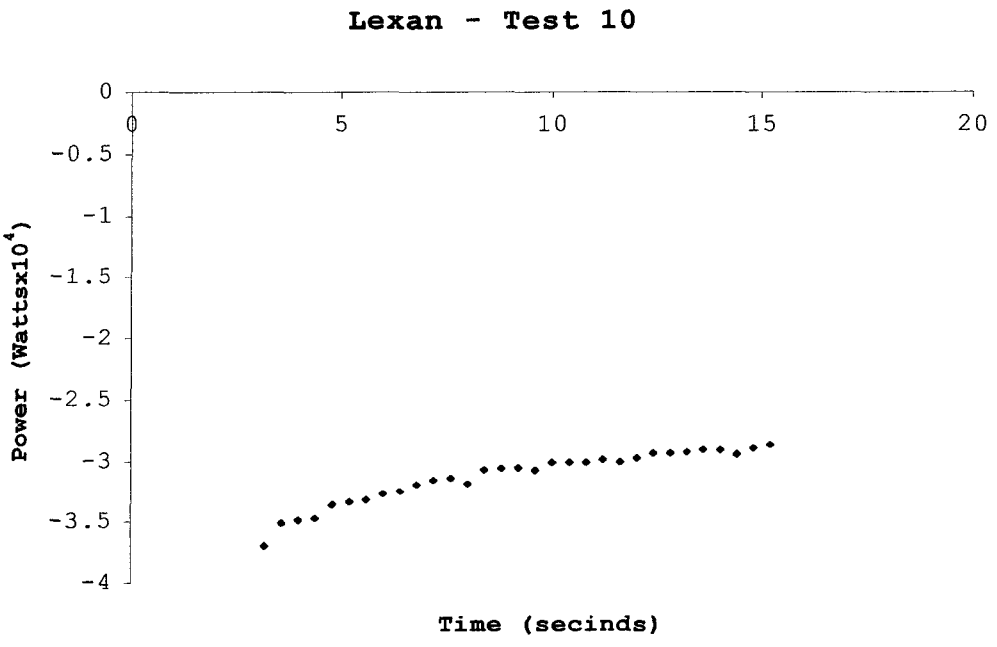

Figure 62. Experimental Power vs. Time Curve for Lexan - Test 10.

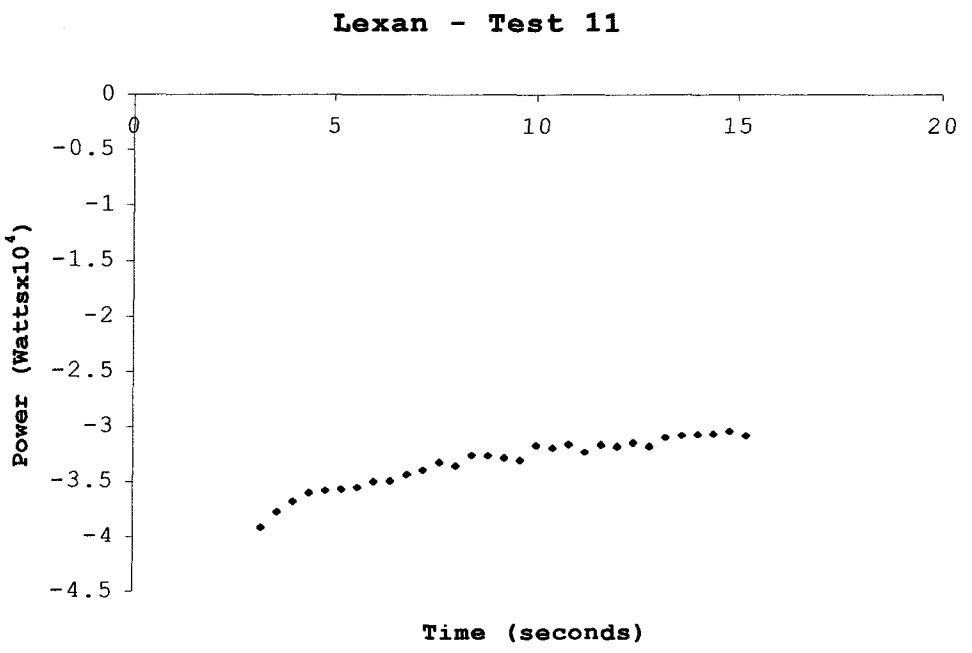

Figure 63. Experimental Power vs. Time Curve for Lexan - Test 11.

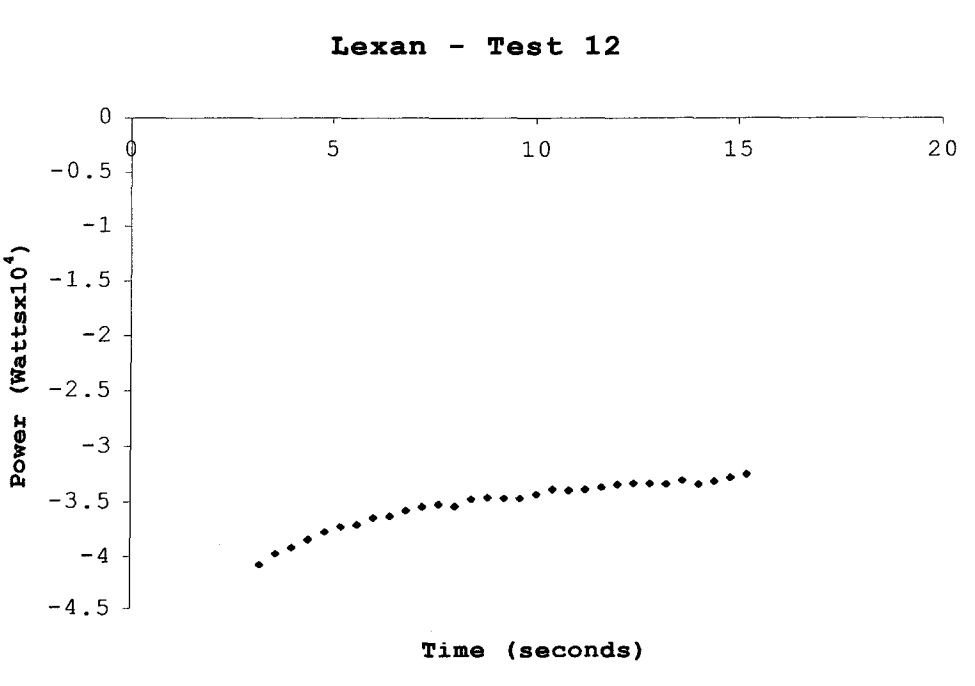

Figure 64. Experimental Power vs. Time Curve for Lexan - Test 12.

6.3 Experimental vs. Numerical Results

The amount of power dissipation due to thermistor heating as determined by the experimental and numerical program is shown in Figures 65, 66, and 67.

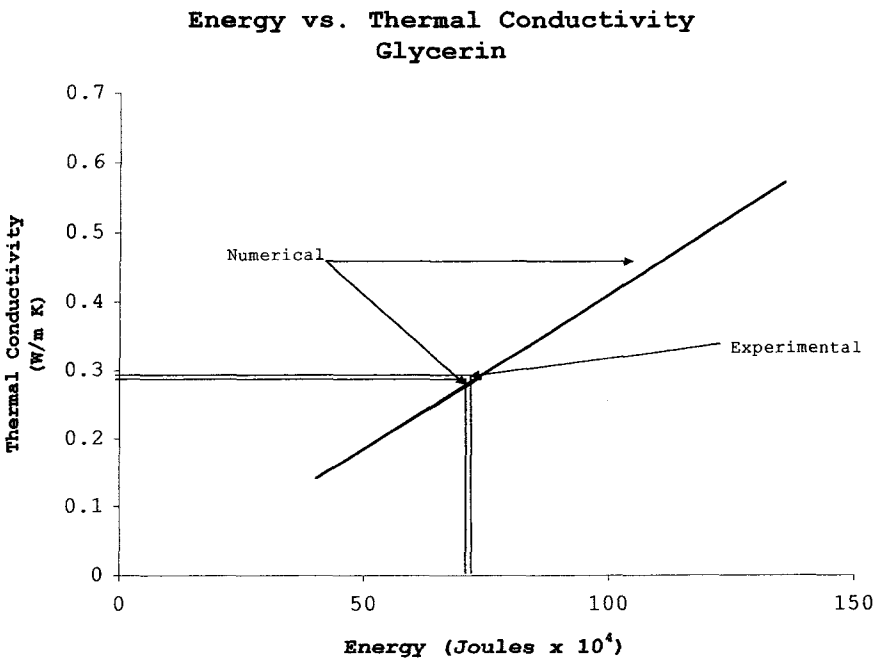

Figure 65. Comparison of numerically predicted energy dissipation and experimentally measured energy dissipation.

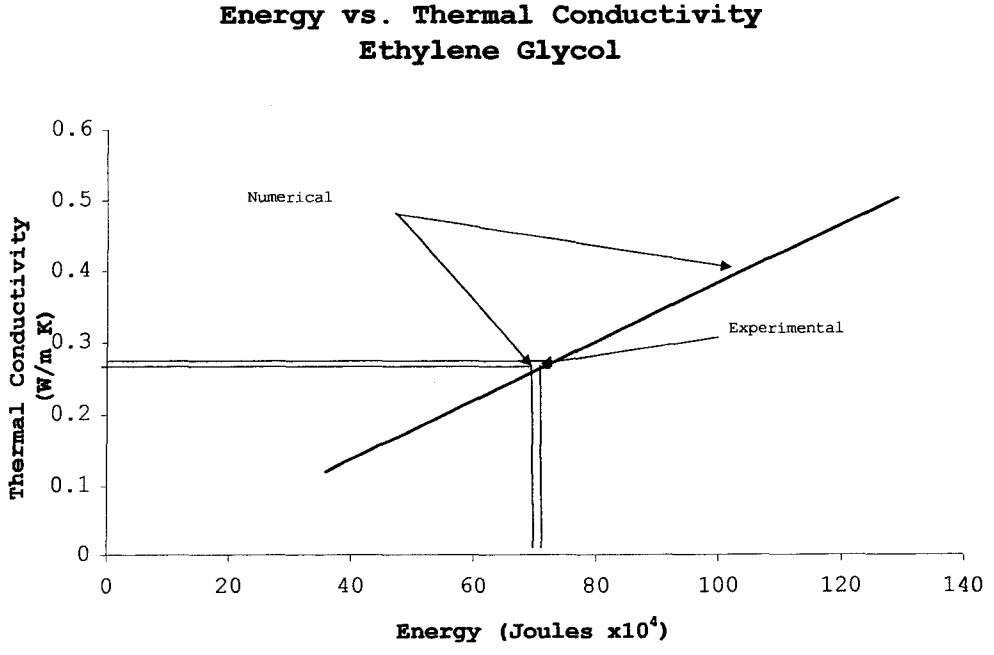

Figure 66. Comparison of numerically predicted energy dissipation and experimentally measured energy dissipation.

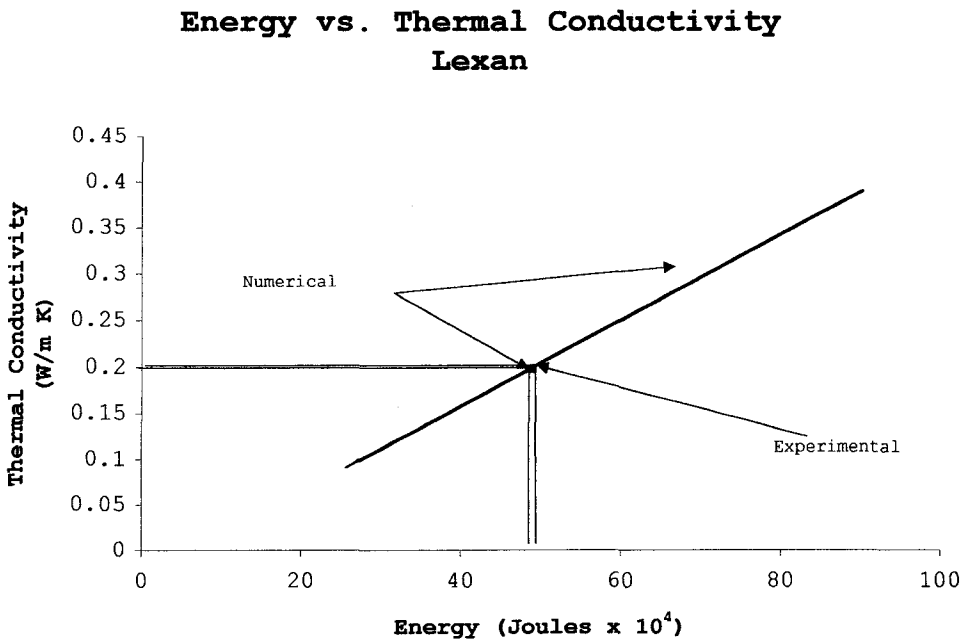

Figure 67. Comparison of numerically predicted energy dissipation and experimentally measured energy dissipation.

CHAPTER 6

FUTURE EXPERIMENTAL STUDIES

6.1 Introduction

Additional experimental studies were planned to determine how the experimental system would function during in situ evaluations of the self-heated thermistor method approach. These experimental studies have been postponed due to problems that arose from the evaluation of the protocol for animal care and use review procedure by the IACUC (Institutional Animal Care and Use Committee) of the University of Nevada Las Vegas. The initial submission of the Protocol for Animal Care and Use was in February 2003. Additional submissions of the Protocol for Animal Care and Use were made in March, April and May 2003.

The objective of this portion of the study is to assess the potential of the thermistor probe method in determining the perfusion in the kidney of Sprague Dawley Outbred rats. In this case, the analysis of blood flow will be relevant to the non-invasive measurement of blood perfusion after kidney transplant surgery, re-implantation surgery, cancer surgery, plastic surgery, microsurgery, and reconstructive surgery.

Each animal would be involved in three kidney perfusion experiments. These experiments would involve either a perfused kidney or non-perfused kidney and a perfused abdominal wall or non-perfused abdominal wall. These experiments would

occur in succession and no multiple survival surgeries would be performed. The first phase would involve the perfused kidney/perfused abdominal wall, the second phase would involve non-perfused kidney/perfused abdominal wall, and the third phase would involve non-perfused kidney/non-perfused abdominal wall. The first two phases of the experimentation (perfused kidney/perfused abdominal wall and non-perfused kidney/perfused abdominal wall) would take approximately four hours, this would allow approximately two hours per phase. The first two phases of the experimentation would be done while the animal is anaesthetized. The last phase of the experimentation (non-perfused kidney/non-perfused abdominal wall) will be done after the animal is euthanized this phase will take approximately two hours.

The heating power needed to maintain temperature elevation in each of the above perfusion experiments is evaluated to assess the feasibility of the thermistor bead method in the determination of blood flow in the kidney.

6.2 White Rat

Rats breed easily, profusely and continuously during their normal reproductive lifespan in the laboratory, are easily handled with practice, and can be housed in large numbers in a relatively confined area. They are both economic and practical to use in large numbers in an experiment and thereby lend greater statistical validity to the results. Much is known about this physiology, anatomy, genetics and behavior, and meaningful results can be obtained in rates, if interpreted with care, can be extrapolated to man. Rats are readily available, and are the main species used to evaluate new methods before human studies.

The male Sprague Dawley Outbred rat between the age of 10-12 weeks was chosen for this study. Six male Sprague Dawley Outbred rats are requested because this number was thought to be a minimum compromise between accuracy range estimates and the minimization of animal use. The Sprague Dawley species is a widely accepted and dependable general research model that is used in virtually all disciplines of biomedical research. Below is a list of biodata related to this type of animal.

Table 12. Bio data on the adult male Sprague Dawley Outbred rat.

Life Span	3 yrs. avg, 4 yrs. max
Weight, Adult Male	237- 264 grams
Rectal Temperature	37.5°C
Respiration rate	92 avg., 80-150
Heart rate	350 avg., 260-450
Kidney (R) weight	0.38 - 0.52 grams/100 grams
Kidney (L) weight	0.37 - 0.56 grams/100 grams

6.3 Pre-operative Evaluation and Care

The animals would be received from a virus free distributor (Animal Technologies Limited) and visually checked for health. This would be done by evaluating whether the animal has rapid respiration, very slow, shallow and labored respiration, rapid weight loss, ruffled fur (rough hair coat), hunched posture, hypothermia or hyperthermia, alertness, and clear eyes. Food and water were provided per normal protocol. The animals would be housed at the UNLV Animal Housing Facility in White Hall.

6.4 Researcher Preparation for Surgery

A basic set of instruments comprised of a scalpel (size 3), with a number 10 blade, a pair of blunt ended Mayo scissors, a pair of vascular scissors for blunt dissection, and a pair of pointed dressing scissors would be on hand to perform the surgical procedure.

All instruments would be sterilized and disinfected. The surgery area and board would be sanitized and sterilized with a Betadine scrub. The area chosen would free of clutter, clean and away from heavy traffic. The researcher would thoroughly scrub her hands with a Betadine scrub. Sterile gloves would be cleaned with a Betadine scrub and would be worn throughout the procedure. The researcher would wear a clean lab coat throughout the procedure. Surgical instruments, gloves, and other paraphernalia would be carefully cleaned and disinfected between animals. The operating area and board would be wiped down with a Betadine solution.

6.5 Animal Preparation for Surgery

The animal would be brought to a clean surgical area in White Hall Room 122C that was wiped down with a Betadine scrub. Pentobarbital would be the pre-operative and inter-operative medication administered to the animals. Before beginning the surgical procedure, the animals would be given 50 mg/kg of Pentobarbital through IP (intraperitoneal) using a 21-gauge needle and a 3ml syringe. This dosage would be administered once at the beginning. Regular monitoring would occur every 10 minutes throughout the surgery, the animals would be evaluated for pain and discomfort by monitoring their respiratory rate, palpebral (ear pinch) and pedral (toe pinch) response. If determined that additional anesthesia would be needed, an additional 10 mg/kg of Pentobarbital would administered IP as required PRN.

A water-circulating blanket would be used to prevent dehydration and hypothermia of the animals during surgery.

6.6 Animal Surgical Procedure

The data will be collected with the aid of a PC, data acquisition board, and LabVIEW software. At the end of the three perfusion studies, the kidney is excised and weighed.

The animal would be brought to a clean surgical area that is wiped down with a Betadine scrub. The animal would be anaesthetized with 50 mg/kg Pentobarbital IP. The animal would be placed in a supine position on the surgical board. The mid-abdomen would be shaved with sterilized instruments. The mid-abdomen would be scrubbed with

a Betadine scrub while being careful to scrub from the center of the site toward the periphery.

The anaesthetized rat would be placed on its back with its tail towards the investigator. Once the skin had been prepared with the antiseptic, the mid-abdomen would be shaved. The skin incision would be made with a scalpel extending from the xipoid to the pubis to enter the abdomen. The scalpel would be held at an angle of approximately 30^{o} to the skin. The kidney would be identified. The thermistor probe would then inserted between the outer cortex of the kidney and the abdominal wall and secured with a suture of 4-0 Vicryl (polyglactic acid suture). The abdomen would then be closed with sterilized clips. A stabilization period would be allowed after the closure of the abdomen. The thermistor would function as a self-heated and sensing device. The baseline temperatures of the organ and the surrounding tissues would be determined with the thermistor bead. A constant current source would be used to pass a small (< 100 mA) current through the thermistor. The generated voltage would be proportional to the thermistor resistance, measured by a precision analog to digital converter. Based on the voltage detected, the temperature would be calculated via the curve fitted data that was obtained from the thermistor/analog to digital converter resistance characteristics. The blood flow measurements and thermal properties would be determined when the thermistor was placed in the self-heated mode. A fixed temperature increment above that of the measured baseline temperatures ($0.5^{o}C$ to $2.0^{o}C$) would be achieved by ohmic heating (<10 mW). The heating power necessary to maintain the elevated temperature would be related to the local tissue thermal properties. The thermistor would function the same in all phases of the experimentation process.

In the case of the nonperfused kidney/perfused abdominal wall, the renal arteries would be dissected out. Sterilized vascular clips would be placed on the renal artery to temporarily stop perfusion to the kidney. The thermistor functions as previously stated.

In the nonperfused kidney/nonperfused abdominal wall case, the animal is euthanized with a drug overdose of Pentobarbital (10 mg/kg) that would be delivered through IP. The thermistor functions as previously stated.

CHAPTER 7

DISCUSSION

This dissertation had as its objective to evaluate an easy-to-use, relatively non-intrusive technique to infer perfusion in human organs subsequent to their implantation. As was pointed out earlier, knowledge of abnormal levels of perfusion can prompt the surgeon to remedial techniques that otherwise would not be used.

The general approach examined here is to use a time-varying, heated-and-unheated thermistor bead to infer perfusion in a qualitative manner. While reports of studies where the heated thermistor technique has been applied previously are found in the literature, the emphases of the present study are somewhat different. Here the concern is on using a single probe that is easily inserted adjacent to the organ, operating it in a fairly simple way, and then easily extracting it after perfusion is noted. The system cost, including expendable sensors, should not be inordinately large. As a simple-to-use approach that is inexpensive, the technique should be applicable to surgery rooms anywhere.

Generally, the project was two-pronged in its approach. Included was the development of the physical apparatus, consisting of a box of electronic components for control of the probe (Figure 16) and processing of data. Also included was an assessment of the accuracy of the results. Calibration measurements were made and evaluated using a finite difference simulation of the effect of possible perfusion effects on the thermal

environment formed (Figure 25). Additionally, animal studies were anticipated, but only the former was performed for reasons beyond the writer's control. Discussion of each of these aspects is given below.

While the dissertation includes an extensive numerical analysis of the heat transfer situation, a point should be noted in passing. It should be emphasized that the clinical application the technique investigated here would not require the use of the numerical code. This is only used as a tool in the evaluation of the range of sensitivities that the technique might demonstrate. The surgeon and assistants would only deal with a probe, a control box and a simple readout of energy absorbed. For further simplification, the latter could be developed into a "likely perfusing/not likely perfusing" meter.

7.1 Experimental Technique

The development of the experimental technique involved using a thermistor and a system both to monitor and to control the thermistor. Of these two aspects, the system design offers the more significant challenge.

Thermistors are readily available commercially, so this aspect presented little problem. The issues in selecting a thermistor are primarily ones of choosing an appropriate size and resistance. Related to its size, the thermistor should not be too intrusive when placed next to the transplanted organ. This would suggest that it should be very small. However, the size should be large enough that the thermistor can be extracted successfully at the completion of its useful application period -- usually one or two days. It is anticipated that the leads of the thermistor would be inside the drainage tube normally put in place at the end of surgery. This would allow the thermistor to be

removed at the same time as the tube. If the leads are too small, they might break during the probe removal. The resistance of the thermistor does not enter into the selection process in a significant way. Ideally the temperature coefficient of resistance would be quite large, as this will benefit the control function of the experimental apparatus.

The controller box (Figure 16) is really the heart of this off/on system. Initially power dissipation in the probe is insignificant, and the thermistor acts simply as a temperature-measuring device. After a period (set by the operator or generally preset) for the determination of the baseline condition, the heating mode begins. A set-point increase in temperature is programmed into the system. This enables the controller to determine the change in resistance that the thermistor will have to undergo to achieve the correct temperature increase. The controller maintains the thermistor resistance at this predetermined value by adjusting the applied power. Heat is dissipated from the thermistor to the surrounding tissue to achieve this necessary set point temperature. The controller is designed to be driven by a constant voltage, and the current is varied to achieve the necessary heat dissipation to maintain the desired thermistor resistance (set-point temperature).

The controller operated in an almost flawless manner. The only possible drawback was that there was some variation in the smoothness of the power-dissipated-versus-time curves shown in the Results section. This was due to some noise that is inherent in system with small signals like found in this one. Attempts to isolate the system from the noise were partially successful, but some variations can still exist.

LabVIEW, the data acquisition and interface system used with the controller allowed a great deal of flexibility and operational latitude. While the system is very

powerful, it does take some experience to access the various operational aspects available.

Tests had been planned on both simulants and animals. For the simulants, a number of materials were used. All of these materials had well documented thermal conductivity values so that comparisons could easily be made to the measured values. We did not have a way to assess thermal conductivity on an independent basis, so we relied on published values for the basic material.

Although thermal conductivity values were available on the simulants used, the manufacturer only documented the properties of Lexan at a single temperature value. Therefore these were the only thermal properties used in the evaluation of Lexan.

A key element in the measurements was determination of the total energy dissipated to achieve a specific set point temperature. Since LabVIEW outputted essentially the power versus time, these values needed to be integrated. It was determined that including the initial milliseconds of the transient could have a profound effect on the results. This is because the variation of power with time is the highest of any series at the beginning of the temperature-change period. Since data access rates could render slightly different values for essentially the same test at these earliest times, it could render slightly different values for essentially the same test at these earliest times, and it was decided to eliminate the very early portion of the transient from the evaluation.

Initially, an empirically based curve fit was used to match the power-versus-time data. This curve fit was then integrated analytically to find the energy. Too much variation was found in how well the fit represented the data. As a result, a Simpson's Rule numerical integration scheme was used directly on the acquired data.

One final experimental element was planned. It was hoped at the end of the program to perform animal studies on Sprague Dawley rats. Generally the approach was to be the reverse of the one used in human transplant application. The first step would be the placement of the probe beside the perfusing kidney of an anesthetized animal. The off-on protocol would then be performed for a period of time. Then blood flow would be ceased to the kidney. Another off-on protocol would be performed. Finally, the animal would be sacrificed and the protocol performed a final time. This approach would allow the assessment of effects of blood flow for the following combination of organ and surrounding tissue: both perfusing, surrounding tissue perfusing, and neither perfusing.

Initially plans were made to use rats that had been subjected to various tests in another laboratory. Many times, the function we were seeking would not have been impaired in these rats as a result of the prior work. At the point in time where we wished to perform our studies, the other laboratory was performing other work that made the rats unsatisfactory for our studies. We then pursued performing studies on rats we would purchase for this purpose. All of the procedures to be used were described and submitted in the form of a Protocol for Animal Care and Use to the IACUC (Institutional Animal Care and Use Committee) of the University of Nevada Las Vegas. After having the procedures rewritten three times, two of the IACUC Committee members who work with animals regularly in the lab admitted that they rejected the procedure because they thought that they knew better ways of measuring blood flow. One of the ways involved the use of chemical dilutants. While these other approaches could be quite appropriate in the lab, they were not harmonious with the objectives of this dissertation work. Animal

studies were eliminated from this work because of the impasse over approval with the IACUC committee.

7.2 Numerical Analysis

Although the experimental part of the project was the heart of the dissertation work, a numerical study was devised to allow the evaluation of the possible applicability of the approach. In this, the interface region, centered at the probe, was analyzed. As described earlier, a two-dimensional, axisymmetric, transient heat conduction model was developed. The Pennes equation was used for the analysis, and the probe was treated as a finite diameter heat source at the center of the region of interest. In essence Pennes equation (Equation 1) allows for complex perfusion effects to be included quite simply as an effective thermal conductivity. This greatly decreased the amount of analysis required while still representing the general influences we were seeking. We opted to develop our own code (an explicit finite difference approach) instead of using a commercially--available code.

When writing codes for complicated analysis, one major issue is the evaluation of the accuracy of the output. Recognizing this fact, we applied several tests to the code results. Comparisons were made to simpler cases where analytical solutions are known.

What is in reality a two-region semi-infinite volume required for analysis, a constant temperature boundary condition was applied. It is not desirable for this boundary condition to unrealistically influence the analysis. The impact of this assumption was evaluated in the course of the analysis by examining the temperatures in the region two nodes in toward the probe from this outer boundary. No temperature

change was witnessed there, satisfying our concern about the appropriateness of this boundary condition.

Most of the accuracy evaluations performed on the code used the simpler case of constant properties in all portions of the analysis region. Two kinds of evaluations were performed. In one, a transient, infinite region solution tabulated by Carlsaw and Jaeger (1959) was used. Good agreement was found. In addition, steady-state conduction across a spherical shell (Incropera and DeWitt 1996) was used to compare to our steady-state asymptotic solution. Again, good agreement was found.

With the use of the functioning code, we were able to determine the changes in power dissipated as a function of an imbalance in thermal conductivity between the two regions. From this we found that the technique is not as sensitive to this imbalance as we would like to have it, but it appears it might still be useful in clinical applications. The use of animal studies would have allowed us to assess this aspect.

CHAPTER 8

CONCLUSION

One of the most important tasks encountered in the fields of medicine and physiological sciences is the assessment of blood perfusion rates. The determination of blood perfusion rates has been widely used to ascertain normal or abnormal physiological states. This could include the determination of infection, viability of ischemic or re-implanted tissue or the viability of skin flaps. Despite the notable importance of inferring blood perfusion in clinical situations, there is no current method that is non-invasive to the tissue of interest, cost-effective, allows for continuous monitoring, accurately predicts values, and is reproducible. In theory, if a method was available to non-invasively, inexpensively, and continuously monitor tissue perfusion, this may allow timely therapeutic maneuvers to correct an abnormality in blood flow.

Critical to this study is the determination of the clinical validity of a non-invasive to the organ method of inferring the presence of satisfactory perfusion. Numerical and experimental analysis were performed to analyze whether or not the presence of tissue perfusion in an organ could be assessed using a non-invasive self-heated thermal diffusion probe. The determination of power dissipation in the experimental and numerical studies was related to the perfusion rate. Increases in power dissipation signified an increase in perfusion whereas a decrease in power dissipation depicted a decrease in perfusion. Self-heated thermal diffusion probe experiments were performed

with an OMEGA 44044 thermistor that was connected in series with a control box. The thermistor was located in three media of interest with different thermal properties. Media were chosen with different thermal properties because this was indicative of the effective thermal conductivity that would be measured in "in vivo" tissue. The effective thermal conductivity term was used in the numerical analysis as a way to account for the additional convective effects that would be presence in a perfused situation. A change in effective thermal conductivity would occur when the tissue was perfused or non-perfused. It was very important to determine the sensitivity of the thermistor bead to the changes in thermal conductivity.

A numerical model was created using the finite difference method to thermally depict the processes occurring in the system. A two-dimensional axisymmetric model was developed to predict the presence of regional blood perfusion. The system modeled consisted of two adjacent semi-infinite tissues, the kidney and the connecting tissue. The thermistor bead was modeled located between the kidney and the connecting tissue in such a way that it was in direct contact with both media. The thermistor bead was taken as a point source that began out in thermal equilibrium with the surrounding media and then increased to a predetermined temperature over a specified amount of time. The amount of energy dissipated within the system during the heating phase of the thermistor was indicative of a perfused or non-perfused state. The validity of the numerical data collected from the program was determined by benchmarking of the code. The code was benchmarked using analytical solutions from Incropera and DeWitt (1996) and Carslaw and Jaeger (1959). Good agreement was obtained. Thermal properties of characteristic

media were taken from published data. The results of the numerical model were used as a way to determine the efficacy of the experimental system.

Experimental procedures where performed on three characteristic materials. These materials were Lexan, Ethylene Glycol, and Glycerin. The experimental apparatus was comprised of a thermistor bead, a controller box, and data acquisition and control hardware and software. Calibration studies were performed on the experimental apparatus to make resistance measurements of the thermistor and correlate that with accurate temperature measurements over a range of 20°C to 40°C. The experiments were used to determine the power output values based on the thermal conductivity of the materials.

It was found that the non-invasive thermistor bead method could measure changes in perfusion (changes in effective thermal conductivity). The sensitivity with which the probe could measure changes in perfusion would be better determined with "in vivo" experiments with a perfused vs. a non-perfused kidney. The additional "in vivo" experiments would prove valuable in further analyzing the experimental apparatus. "In vivo" studies are planned in Sprague Dawley rats. The experimental procedure to determine a perfused or non-perfused case of the kidney of these animals was discussed in a preceding chapter. It is thought that this validation will prove the practicality of using this stand alone experimental apparatus in the determination of blood perfusion in the kidney after it has been transplanted.

APPENDIX

```
Program Perfusion Model

double precision T(0:2000,0:2000)
double precision TP(0:2000,0:2000)
double precision Ta(0:2000,0:2000)
double precision Tt(0:2000,0:2000)
double precision q(0:2000,0:2000)

real fodra,fodrab,rhoa,cpa,alphaab,dt,qmet,qper,alpha,Tinf
real dr,dtheta,r,ka,kb,iprint,rhob,cpb
real mtotal,ntotal,nodemax,ttime,qa
real timea,timeb,area,timeheat,ttimeheat
real alphaa,alphab,rt
real sum,qaa,deltaT
double precision pi, theta,p
parameter (r=0.01,ro=(0.0002413),rhoa=1050.0,rhob=1050.0)
parameter (ka=(0.42),kb=(0.42))
parameter (cpa=3787.76,cpb=3787.76)
parameter (qmet=0.0,qper=0.0,theta=(3.141592653589793))
parameter (mtotal=60.0,ntotal=60.0)
parameter (pi=3.141592653589793)
parameter (deltaT=0.5)

*     r= complete radius of the region                    (m)
*     ro= radius of thermistor                            (m)
*     rhoa= density of material a                         (kg/m3)
*     rhob= density of material b                         (kg/m3)
*     ka= thermal conductivity of material a              (W/m C)
*     kb= thermal conductivity of material b              (W/m C)
*     cpa= specific heat of material a                    (J/kg C)
*     cpb= specific heat of material b                    (J/kg C)
*     qmet= metabolic heat flow rate                      (W)
*     qper= perfusion heat flow rate                      (W)
*     theta= angle                                        (C)

*     mtotal= total number of divisions in the m-direction (radians)
```

```
*     Tinf=  temperature as the media approach infinite       (C)
*     ntotal= total number of divisions in the n-direction

open(unit=1,file='FILE.dat',STATUS='new')
dr = ((r-ro)/mtotal)
write(1,*) 'The value for dr is: ',dr
dtheta = ((theta)/(ntotal))
write(1,*) 'The value for dtheta is: ',dtheta
alphaa=ka/(rhoa*cpa)
write(1,*) 'The value for alphaa is: ',alphaa
alphab= kb/(rhob*cpb)
write(1,*) 'The value for alphab is: ',alphab
alphaab=(ka+kb)/(rhoa*cpa+rhob*cpb)

write(1,*) 'The value for alphaab is: ',alphaab
write(1,*) 'The value for ka is:  ',ka
write(1,*) 'The value for kb is:  ',kb
write(1,*) 'The value for rhoa is:  ',rhoa
write(1,*) 'The value for rhob is:  ',rhob
write(1,*) 'The value for cpa is:  ',cpa
write(1,*) 'The value for cpb is:  ',cpb
write(1,*) 'The value for mtotal is:  ',mtotal
write(1,*) 'The value for ntotal is:  ',ntotal
write(1,*) 'The value for deltaT is:  ',deltaT
*     calculate time step
rt=ro+1*dr
*     surface area of thermistor
area=4.0*pi*(ro*ro)
timea=1/((4*alphaa/((dr**2)*(rt**2)))*(((rt+dr/2)**2)+((rt-dr/2)**2
   +     ))+8*alphaa/((rt*dtheta)**2))
timeb=1/((4*alphaa/((dr**2)*(rt**2)))*(((rt+dr/2)**2)+((rt-dr/2)**2
   +     ))+8*alphaa/((rt*dtheta)**2))
write(1,*) 'The value for timeb is: ',timeb
if (timea.lt.timeb) then
dt = timea
else
dt = timeb
endif
write(1,*) 'The value for dt is: ',dt
fodra=alphaa*dt/((dr)**2)
write(1,*) 'The value for fodra is: ',fodra
fodrb=alphab*dt/((dr)**2)
write(1,*) 'The value for fodrb is: ',fodrb
fodrab=alphaab*dt/((dr)**2)
write(1,*) 'The value for fodrab is: ',fodra
diva=(dt/(rhoa*cpa))
```

```
write(1,*) 'The value for diva is: ',diva
divb=(dt/(rhob*cpb))
write(1,*) 'The value for divb is:  ',divb
divab=dt/((rhoa*cpa+rhob*cpb)/2)
write(1,*) 'The value for divab is:  ',divab

time=0
ttime=0
setpoint=1.0
count=0
iprint=0.0
ssetpoint=20.0
timeheat=0
ttimeheat=0
endtime=0
finaltime=21.1

do 20 m = 0,mtotal,1
do 10 n = 0,ntotal,1
Ta(m,n)=32.0
T(m,n)=Ta(m,n)
10     continue
20   continue
60   iprint=iprint+dt
ttime=ttime+dt
time=time+dt
count=count+1
endtime=endtime+dt

do 70 m = 0,mtotal,1
rm=ro+m*dr
diff1=rm+dr/2
diff2=rm-dr/2
fodthetaa=alphaa*dt/((rm*dtheta)**2)
fodthetab=alphab*dt/((rm*dtheta)**2)
do 65 n = 0,ntotal,1
angle3=SIN(n*dtheta)
angle4=SIN(n*dtheta+(dtheta/2))
angle5=SIN(n*dtheta-(dtheta/2))

if (m.eq.0) then
TP(m,n)=Ta(m,n)
else
if (m.eq.mtotal) then
TP(m,n)=Ta(m,n)
else
```

```
if ((n.eq.0)) then
TP(m,n)=(1.0-fodra*((diff1**2)/(rm**2))
+       -fodra*((diff2**2)/(rm**2))
+       -4*fodthetaa)*T(m,n)
+       +(fodra*(diff1**2)/((rm**2)))*T(m+1,n)
+       +(fodra*(diff2**2)/((rm**2)))*T(m-1,n)
+          +(4*fodthetaa)*T(m,n+1)
+       +qmet*diva-qper*diva
else
if(n.eq.((ntotal/2))) then
TP(m,n)=(1.0-
+      fodrab*((diff1**2)/(rm**2))
+      -fodrab*((diff2**2)/(rm**2))
+      -fodthetaa*angle5-fodthetab*angle4)*T(m,n)
+      +fodrab*((diff1**2)/(rm**2))*T(m+1,n)
+      +fodrab*((diff2**2)/(rm**2))*T(m-1,n)
+         +fodthetab*angle4*T(m,n+1)
+         +fodthetaa*angle5*T(m,n-1)
+      +qmet*divab-qper*divab
else
if (n.lt.((ntotal/2))) then
TP(m,n)=(1.0-fodra*(diff1**2)*(1/
+       (rm**2))-fodra*(diff2**2)*
+       (1/(rm**2))-fodthetaa*(angle4/angle3)-fodthetaa*
+        (angle5/angle3))*T(m,n)
+       +(fodra*(diff1**2)*(1/(rm**2)))*T(m+1,n)
+       +(fodra*(diff2**2)*(1/(rm**2)))*T(m-1,n)
+          +fodthetaa*(angle4/angle3)*T(m,n+1)
+          +fodthetaa*(angle5/angle3)*T(m,n-1)
+       +qmet*diva-qper*diva
          else
if (n.eq.ntotal) then
TP(m,n)=(1.0-fodrb*((diff1**2)/(rm**2))
+       -fodrb*(diff2**2)/((rm**2))
+       -4*fodthetab)*T(m,n)
+       +(fodrb*(diff1**2)/((rm**2)))*T(m+1,n)
+       +(fodrb*(diff2**2)/((rm**2)))*T(m-1,n)
+       +(4*fodthetab)*T(m,n-1)
+       +qmet*divb-qper*divb
else
if (n.gt.((ntotal/2))) then
TP(m,n)=(1.0-fodrb*(diff1**2)*(1/
+       (rm**2))-fodrb*(diff2**2)*
+       (1/(rm**2))-fodthetab*(angle4/angle3)-
+       fodthetab*(angle5/angle3))*T(m,n)
+       +(fodrb*(diff1**2)*(1/(rm**2)))*T(m+1,n)
```

```
+       +(fodrb*(diff2**2)*(1/(rm**2)))*T(m-1,n)
+          +fodthetab*(angle4/angle3)*T(m,n+1)
+          +fodthetab*(angle5/angle3)*T(m,n-1)
+       +qmet*divb-qper*divb
endif
endif
endif
endif
endif
endif
endif
endif
65  continue
70  continue
do 90 m=0,mtotal,1
do 80 n=0,ntotal,1
T(m,n)=TP(m,n)
80  continue
90  continue
do 100 n=0,ntotal,1
m=0
q(m,n)=0.0
100  continue
do 110  n=0,ntotal,1
      m=0

      rm=ro+m*dr
        if (n.eq.0) then
        q(m,n)=ka*(pi*(((rm+dr/2)*SIN(dtheta/2))**2))*
   +((T(m+1,n)-T(m,n))/dr)
        else
if (n.lt.((ntotal/2))) then
q(m,n)=ka*(2*pi*dtheta*(((rm+dr/2))**2))*((T(m+1,n)-T(m,n))
+/dr)*angle4
else
if (n.eq.((ntotal/2)))then
q(m,n)=kb*(pi*(((rm+dr/2)*SIN(dtheta/2))**2))*
+((T(m+1,n)-T(m,n))/dr)
else
if (n.eq.ntotal) then
q(m,n)=kb*(pi*(((rm+dr/2)*SIN(dtheta/2))**2))*
+((T(m+1,n)-T(m,n))/dr)
else
if (n.gt.((ntotal/2))) then
q(m,n)=kb*(2*pi*dtheta*(((rm+dr/2))**2))*((T(m+1,n)-T(m,n))
+/dr)*angle4
endif
```

```
endif
endif
endif
endif
110  continue
sum=0.0
sum1=0.0
do 115 n=0,ntotal,1
m=0
sum= sum + q(m,n)
115     continue
if (time.lt.setpoint) then
goto 60
else
write(1,*)'heating'
time=0
goto 180
endif
if (endtime.ge.finaltime) then
write(1,*)'Time elapsed'
write (1,150) (m,m=0,mtotal,1)
150             format(1x,10(6x,i2))
do 170 n=0,ntotal,1
write (1,160) n,(T(m,n),m=0,mtotal,1)
 160            format (i2,10(2x,f6.3))
 170            continue
write (1,*)'The value of q is:  ', sum
stop
endif
180  iprint=iprint+dt
j=1
ttime=ttime+dt
count=count+1
timeheat=timeheat+dt
ttimeheat=ttimeheat+dt
endtime=endtime+dt
do 200 m = 0,mtotal,1
rm=ro+m*dr
diff1=rm+dr/2
diff2=rm-dr/2
fodthetaa=alphaa*dt/((rm*dtheta)**2)
fodthetab=alphab*dt/((rm*dtheta)**2)
do 190 n = 0,ntotal,1
angle3=SIN(n*dtheta)
angle4=SIN(n*dtheta+(dtheta/2))
angle5=SIN(n*dtheta-(dtheta/2))
```

```
if (m.eq.0) then
TP(m,n)=Ta(m,n)+deltaT
else
if (m.eq.mtotal) then
TP(m,n)=Ta(m,n)
else
if (n.eq.0) then
TP(m,n)=(1.0-fodra*((diff1**2)/(rm**2))
+       -fodra*(diff2**2)/((rm**2))
+       -4*fodthetaa)*T(m,n)
+       +(fodra*(diff1**2)/((rm**2)))*T(m+1,n)
+       +(fodra*(diff2**2)/((rm**2)))*T(m-1,n)
+       +(4*fodthetaa)*T(m,n+1)
+       +qmet*diva-qper*diva
else
if(n.eq.((ntotal/2))) then
TP(m,n)=(1.0-
+        fodrab*((diff1**2)/(rm**2))
+       -fodrab*((diff2**2)/(rm**2))
+       -fodthetaa*angle5-fodthetab*angle4)*T(m,n)
+       +fodrab*((diff1**2)/(rm**2))*T(m+1,n)
+       +fodrab*((diff2**2)/(rm**2))*T(m-1,n)
+           +fodthetaa*angle5*T(m,n+1)
+       +fodthetab*angle4*T(m,n-1)
+       +qmet*divab-qper*divab
else
if (n.lt.((ntotal/2))) then
TP(m,n)=(1.0-fodra*(diff1**2)*(1/
+       (rm**2))-fodra*(diff2**2)*
+       (1/(rm**2))-fodthetaa*(angle4/angle3)-fodthetaa*
+        angle5/angle3)*T(m,n)
+       +(fodra*(diff1**2)*(1/(rm**2)))*T(m+1,n)
+       +(fodra*(diff2**2)*(1/(rm**2)))*T(m-1,n)
+           +fodthetaa*(angle4/angle3)*T(m,n+1)
+        +fodthetaa*(angle5/angle3)*T(m,n-1)
+       +qmet*diva-qper*diva
else
if (n.eq.ntotal) then
TP(m,n)=(1.0-fodrb*((diff1**2)/(rm**2))
+       -fodrb*(diff2**2)/((rm**2))
+       -4*fodthetab)*T(m,n)
+       +(fodrb*(diff1**2)/((rm**2)))*T(m+1,n)
+       +(fodrb*(diff2**2)/((rm**2)))*T(m-1,n)
+           +(4*fodthetab)*T(m,n-1)
+       +qmet*divb-qper*divb
else
```

```
if (n.gt.((ntotal/2))) then
TP(m,n)=(1.0-fodrb*(diff1**2)*(1/
+        (rm**2))-fodrb*(diff2**2)*
+        (1/(rm**2))-fodthetab*(angle4/angle3)-fodthetab*
+         (angle5/angle3))*T(m,n)
+        +(fodrb*(diff1**2)*(1/(rm**2)))*T(m+1,n)
+        +(fodrb*(diff2**2)*(1/(rm**2)))*T(m-1,n)
+        +fodthetab*(angle4/angle3)*T(m,n+1)
+         +fodthetab*(angle5/angle3)*T(m,n-1)
+        +qmet*divb-qper*divb
endif
endif
endif
endif
endif
endif
endif
endif
 190      continue
 200      continue
do 220 m=0,mtotal,1
do 210 n=0,ntotal,1
T(m,n)=TP(m,n)
 210         continue
 220           continue
sum=0.0
do 240  n=0,ntotal,1
m=0
rm=ro+m*dr
angle3=SIN(n*dtheta)
qaa=(-4.0*pi*((ka+kb)/2)*(T(mtotal,1)-T(0,1))/((1/(r))-1/ro))
qa=-4.0*pi*ro*((ka+kb)/2)*deltaT-4.0*ro*ro*deltaT
+       *(1/(timeheat**0.5))*
+       ((pi*((ka+kb)/2)*((rhoa*cpa+rhob*cpb)/2))**0.5)
if (n.eq.0) then
q(m,n)=ka*(pi*(((rm+dr/2)*SIN(dtheta/2))**2))*
+((T(m+1,n)-T(m,n))/dr)
else
if (n.lt.((ntotal/2))) then
q(m,n)=ka*(2*pi*dtheta*(((rm+dr/2))**2))*((T(m+1,n)-T(m,n))
+/dr)*angle4
else
if (n.eq.((ntotal/2)))then
q(m,n)=ka*((rm+dr/2)**2)*((T(m+1,n)-T(m,n))/dr)*2*pi+
+kb*((rm+dr/2)**2)*((T(m+1,n)-T(m,n))/dr)*2*pi       else
if (n.eq.ntotal) then
q(m,n)=kb*(pi*(((rm+dr/2)*SIN(dtheta/2))**2))*
```

```
+((T(m+1,n)-T(m,n))/dr)
else
if (n.gt.((ntotal/2))) then
q(m,n)=kb*(2*pi*dtheta*(((rm+dr/2))**2))*((T(m+1,n)-T(m,n))
+/dr)*angle4
endif
endif
endif
endif
endif
240  continue
do 245 n=0,ntotal,1
m=0
 sum= sum+q(m,n)
245     continue
if (iprint.ge.0.99) then
do 270 n=0,ntotal,1
write (1,260) (T(m,n),m=0,mtotal,1)
260   format (49(2x,f6.3))
270              continue
write(1,*)'The value of q is:  ', sum
write(1,*)'The value of qa is:  ',qa
write(1,*) 'The value of qaa is:  ', qaa
write(1,*) timeheat
iprint=0
endif
if (endtime.ge.finaltime) then
write (1,*) 'Time elapsed'
write (1,280) (m,m=0,mtotal,1)
 280             format(1x,10(6x,i2))
do 300 n=0,ntotal,1
write (1,290) n,(T(m,n),m=0,mtotal,1)
 290             format (i2,10(2x,f6.3))
 300             continue
write (1,*)'The value of q is:  ', sum
write (1,*)'The value of qa is:  ',qa
write(1,*) 'The value of qaa is:  ', qaa
write(1,*) timeheat
stop
endif
if (timeheat.ge.ssetpoint) then
write (1,*)'cooling'
timeheat=0
goto 60
else
goto 180
```

```
endif
close(unit=1)

END
```

REFERENCES

Adams T, Spielman W.S., et al., 1985, "Proposed Methods for the Measurement of Regional Renal Blood Flow Using Heat Transfer Analysis," Annals of Biomedical Engineering, Vol. 13, pp. 237-258.

Anderson G.T and Valvano J.W., 1989, "An Interlobular Artery and Vein Based Model for Self-Heated Thermistor Measurements of Perfusion in Canine Kidneys," ASME Heat Transfer Division, Vol. 126, pp. 29-35.

Anderson G.T. and Valvano J.W., 1994, "A Small Artery Heat Transfer Model for Self-Heated Thermistor Measurements of Perfusion in the Kidney Cortex," ASME Journal of Biomechanical Engineering, Vol. 116, pp. 71-78.

Anderson G.T., Valvano J.W., et al., 1988, "The Effect on Self-Heated Thermistors: A Comparison Between Pennes' Equation and an Effective Thermal Conductivity Model," ASME Bioengineering Division Publication, Vol. 9, pp. 301-312.

Anderson G.T., Valvano J.W. and Sanots R.R., 1992, "Self-Heated Thermistor Measurements of Perfusion," IEEE Transactions on Biomedical Engineering, Vol. 39, pp. 877-885.

Arkin H., Holmes K.R., and Chen M.M., 1987, "Theory on Thermal Probe Arrays for the Distinction Between the Convective and the Perfusive Modalities of Heat Transfer in Living Tissues," Transactions of the ASME - Journal of Biomedical Engineering, Vol. 109, pp. 346-352.

Baish J.W., Ayyaswamy P.S., and Foster K.R., 1986, "Small-Scale Temperature Fluctuations in Perfused Tissue Local Hyperthermia," Transactions of the ASME - Journal of Biomedical Engineering, Vol. 108, pp. 246-250.

Baish J.W., Ayyaswamy P.S., and Foster K.R., 1986, "Heat Transport Mechanisms in Vascular Tissues: A Model Comparison," Transactions of the ASME - Journal of Biomedical Engineering, Vol. 108, pp. 324-331.

Balsasubramiam T.A. and Bowman H.F., 1974, "Temperature Field due to a Time Dependent Heat Source of Spherical Geometry in an Infinite Medium," ASME Journal of Heat Transfer, pp. 296-299.

Balsasubramaniam T.A. and Bowman H.F., 1977, "Thermal Conductivity and Thermal Diffusivity of Biomaterials: A Simultaneous Measurement Technique," Transactions of the ASME - Journal of Biomedical Engineering, Vol. 99, pp. 148-154.

Bazett H.C. and McGlone B., 1927, "Temperature Gradients in the Tissue in Man," American Journal of Physiology, Vol. 82, pp. 415.

Bowman, H. F., Cravalho E.G. and Woods M, 1975, "Theory, Measurement, and Application of Thermal Properties of Biomaterials," Annual Review of Biophysics and Bioengineering, Vol. 4, pp. 43-78.

Bowman, H.F., 1985, "Estimation of Tissue Blood Flow," in Heat Transfer in Medicine and Biology, Plenum Pub., Shitzer and Eberhart (ed.), pp. 167-192.

Bowman H.F., Martin G.T., et al., 1992, "Human Tumor Perfusion Measurements during Hyperthermia Therapy," Hyperthermic Oncology 1992 Proceedings of the Sixth International Conference on Hyperthermic Oncology, Vol. I-Summary Papers Addendum.

Carslaw H.S. and Jaeger J.C., 1959, Conduction of Heat in Solids, 2 ed. Oxford University Press, Oxford, p. 483.

Carter L.P. and Atkinson J.R., 1973, "Cortical Blood Flow in Controlled Hypotension as Measured by Thermal Dilution, " Journal of Neurologic Neurosurgery Psychology, Vol. 36, pp. 906-913.

Charny C.K., Weinbaum S., Jiji L.M., and Lemons D.E., 1988, "On the Generalization of the Relation Between the Near Field and Local Average Tissue Temperatures," Transactions of the ASME - Journal of Biomedical Engineering, Vol. 110, pp. 74-81.

Charny C.K. and Levin R., 1988, "Heat Transfer Normal to Paired Arterioles and Venules Embedded in Perfused Tissue During Hyperthemia," Transactions of the ASME - Journal of Biomedical Engineering, Vol. 110, pp. 277-282.

Chato J.C., 1968, "A Method for Measurement of Thermal Properties of Biological Materials," In Thermal Problems in Biotechnology, ASME Symposium, pp. 16-25.

Chato J.C., 1980, "Measurement of Thermal Properties of Growing Tumors," Proceedings of the New York Academy of Science, Vol. 335, pp.67-85.

Chato J.C., 1985, "Measurement of Thermal Properties of Biological Materials," Heat Transfer in Medicine and Biology: Analysis and Applications, pp. 167-192.

Chen M.M. and Rupinskas V., 1977, "A Simple Method for Measuring and Monitoring Thermal Properties in Tissue," ASME Paper No. 77-WA/HT-42.

Chen M.M. and Holmes K.R., 1980, "Thermal Pulse-Decay Method for Simultaneous Measurement of Thermal Conductivity and Local Blood Perfusion Rate in Living Tissues," In Advances in Bioengineering, V.C. Mow, Ed., ASME, New York, pp. 113-115.

Chen M. M., Holmes K.R. and Rupinskas V., 1981, "Pulse-Decay Method for Measuring Thermal Conductivity of Living Tissue," ASME Journal of Biomechanical Engineering, Vol. 103, pp. 253-260.

Chen M.M. and Holmes K.R., 1980, "Microvascular Contributions in Tissue Heat Transfer," Annuals of New York Academy of Sciences, Vol. 335, pp. 137-150.

Cooper T.E. and Trezek G.J., 1970, "Thermal Properties of Human Organs via the Needle Probe Technique," Proceedings of the 23rd ACEMB, p. 155.

Coremans J., Vermareien H., et al., 1985, "Assessment of the In Vivo Recording of Local Cerebral Blood Flow Using a Thermistor Device," Advances in Experimental Medicine and Biology, Vol. 191, pp. 139-148.

Delhomme G., Dittmar A., et al., 1992, "Thermal Diffusion Probes for Tissue Blood Flow Measurements," Sensors and Actuators B, Vol. 6, pp. 87-90.

Delhomme G., Newman W.H., et al., 1994, "Thermal Diffusion Probe and Instrument System for Tissue Blood Flow Measurements: Validation in Phantoms and In Vivo Organs," IEEE Transactions on Biomedical Engineering, 41(7), pp. 656-662.

Diller K., Valvano J., et al., 2000, "Bioheat Transfer." The CRC Handbook of Thermal Engineering. CRC Press, New York, New York, pp. 4-114 - 4-187.

Dittmar A., Delhomme G., et al., 1993, "Continuous Measurement of Testicular Tissue Blood Flow by A Micro-Probe Using Thermal Diffusion," IEEE Proceedings of the Annual Conference on Engineering in Medicine and Biology, 15(2), pp. 992-993.

Dittmar A., Pauchard T., et al., 1992, "A Thermal Conductivity Sensor for the Measurement of Skin Blood Flow," Sensors and Actuators B, Vol. 7, pp. 327-331.

Fegler G., 1954, "Measurement of Cardiac Output in Anaesthetized Animals by a Thermodilution Method," Quarterly Journal of Experimental Physiology, Vol. 39, p. 153.

Ferrari M., Giannin I., et al., 1982, "Quantitative Measurements of Tissue Blood Flow by Fast Pulse Heated Thermistors," Physiological Chemistry and Physics, Vol. 14, pp. 553-560.

General Electric Company, 2002, "Lexan Datasheet," GE Plastics Design Solution Center. GE. 08 July 2002. http://www.geplastics.com/resins/datasheets/americas/lexan/103.html

Gibbs F.A., 1933, "A Thermoelectric Blood Flow Recorder in the Form of a Needle," Proceedings of the Society of Experimental Biology Medicine, Vol. 31, pp. 141-146.

Gisselsson L. and Ericsson M., 1981, "Evaluation of the Continuous Thermal Dilution Technique for Measurement of Coronary Blood Flow," Upsala Journal of Medical Science, Vol. 86, pp. 83-92.

Grayson J., 1952, "Internal Calorimetry in the Determination of Thermal Conductivity and Blood Flow," Journal of Physiology, Vol. 118, pp. 54-72.

Hansson G.A., Hauksson A., et al., 1987, "An Instrument for Measuring Endometrial Blood Flow in the Uterus, Using Two Thermistor Probes," Journal of Medical Engineering and Technology, 11(1), pp. 17-22.

Haug H.W., Shen Z.P. and Roemer R.B., 1986, "A Counter-Current Vascular Network Model of Heat-Transfer In Tissues," Journal of Biomechanical Engineering, Vol. 118, pp. 120-129.

Holmes K.R. and Chen M.M., 1983, "Local Tissue Heating: Microprobe Pulse-Decay Technique for Heat Transfer Parameter Evaluation," European Conference on Microcirculation, pp. 50-56.

Holmes K.R., Arkin H., and Chen M.M., 1989, "Tissue Blood Perfusion Measured Using the Thermal Pulse Decay (TPD) Method," IEEE Engineering in Medicine and Biology Society 11th Annual International Conference, 1(1), pp. 302-303.

Incropera F.P. and DeWitt D.P., 1996, Introduction to Heat Transfer, John Wiley and Sons, New York.

Jain R.K., 1978, "Effects of Inhomogeneities and Finite Boundaries on Temperature Distributions in a Perfused Medium, with Application to Tumors," ASME Journal of Biomechanical Engineering, Vol. 101, pp. 235-241.

Jain R.K., 1979, "Transient Temperature Distributions in an Infinite, Perfused Medium Due to a Time-Dependent, Spherical Heat Source," ASME Journal of Biomechanical Engineering, Vol. 101, pp. 82-86.

Kedem J., Acad B., and Sonn J., 1981, "Dynamic Redistribution of Coronary Blood Flow in the Dog as Measured by a Thermistor Technique," Quarterly Journal of Experimental Physiology, Vol. 66, pp. 25-37.

Klar E., Kraus T., et al., 1995, "Thermodiffusion as a Novel Method for Continuous Monitoring of the Hepatic Microcirculation after Liver Transplantation," Transplantation Proceeding, 27(5), pp. 2610-2612.

Klar E., Kraus T., et al., 1996, "First Clinical Realization of Continuous Monitoring of Liver Microcirculation after Transplantation by Thermodiffusion," Transplant International, Supplement 1, pp. S140-S143.

Kolios M.C., Worthington A. E., et al., 1998, "Experimental Evaluation of Two Simple Thermal Models Using Transient Temperature Analysis," Physics in Medicine and Biology, Vol. 43, pp. 3325-3340.

Kolis M.C., Sherar M.D., and Hunt J.W., 1995, "Large Vessel Cooling in Heated Tissues: A Numerical Study," Physics in Medicine and Biology, Vol. 40, pp. 477-494.

Kolis M.C., Sherar M.D., Worthinton A.E., and Hunt J.W., 1994, "Modeling Temperature Gradients Near Large Vessels in Perfused Tissues." Fundamentals of Biomedical Heat Transfer HTD-Vol 295, American Society of Mechanical Engineers, New York, New York, pp. 23-30.

Kraus T., Klar E., et al., 1996, "Continuous Measurement of Porcine Renal Cortex Microcirculation with Enhanced Thermal Diffusion Technology," Journal of Surgical Research, Vol. 61, pp. 531-536.

Kress R. and Roemer R., 1987, "A Comparative Analysis of Thermal Blood Perfusion Measurement Techniques," ASME Journal of Biomechanical Engineering, Vol. 109, pp. 218-225.

Kreller K.H. and Seiler L., 1971, "An Analysis of Peripheral Heat Transfer in Man," Journal of Applied Physiology, Vol. 30, p. 779.

Lagendijk J.J.W., 1990, Thermal Models: Principles and Implementation Introduction to the Clinical Aspects of Clinical Hyperthermia, Taylor and Francis, Bristol, PA, pp. 478-511.

Lemons D.E., Weinbaum S., and Jiji L.M., 1987, "Experimental Studies on the Role of the Micro and Macro Vascular System in Tissue Heat Transfer," American Journal of Physiology, Vol. 253, pp. R128-R135.

Mitchell J.W. and Myers G.E., 1968, "An Analytical Model of the Countercurrent Heat Exchange Phenomena," Biophysics Journal, Vol. 8, pp. 897-911.

Muller-Schauenburg W., Apfel H., et al., 1975, "Quantitative Measurement of Local Blood Flow with Heat Clearance," Basic Research in Cardiology, Vol. 70, pp. 547-567.

National Instruments, 2002, "Ni LabVIEW," National Instruments Products and Services Division. NI. 08 July 2002. http://www.ni.com/labview

Newman W.H., Bowman F., et al., 1995, "A Methodology In Vivo Measurement of Blood Flow in Small Tissue Volumes," ASME Heat Transfer Division, Vol. 32, pp. 99-105.

Patel P.A., Valvano J.W., and Hayes L.J., 1987, "A Finite Element Analysis of a Surface Thermal Probe," Thermodynamics, Heat, and Mass Transfer in Biotechnology, ASME Annual Winter Meeting, Boston, HTD-Vol. 90, BED. Vol. 5, edited by Diller, pp. 95-102.

Patel P.A., Valvano J.W., et al., 1987, "A Self-Heated Thermistor Technique to Measure Effective Thermal Properties form the Tissue Surface," ASME Journal of Biomechanical Engineering, Vol. 109, pp. 330-335.

Patel P.A., Valvano J.W., and Hayes L.J., 1987, "Perfusion Measurement by a Surface Thermal Probe," IEEE Engineering in Medicine and Biology, Boston.

Pennes H.H., 1948, "Analysis of Tissue and Arterial Blood Temperatures in the Resting Forearm," Journal of Applied Physiology, Vol. 1, pp. 93-122.

Robertson C.S., Contact C.F., et al., 1992, "Cerebral Blood Flow, Arteriovenous Oxygen Difference, and Outcome in Head Injured Patients," Journal of Neurology, Neurosurgery, and Psychiatry, Vol. 55, pp. 594-603.

Samara T., Regli P., and Kuster N., 2000, "Electromagnetic and Heat Transfer Computations for Non-Ionizing Radiation Dosimetry," Physics and Medicine and Biology, Vol. 45, pp. 1-14.

Scott E.P, Robinson P.S., and Diller T.E., 1998, "Development of Methodologies for the Estimation of Blood Perfusion using Minimally Invasive Thermal Probe," Measurement Science and Technology, Vol. 9, pp. 888-897.

Shitzer A. and Eberhart R., 1985, Heat Transfer in Medicine and Biology, Vol. 2, Plenum Press, New York, New York.

Song W.J., Weinbaum S., and Jiji L.M., 1987, "A Theoretical Model For Peripheral Tissue Heat Transfer Using the Bioheat Equation of Weinbaum and Jiji," Transactions of the ASME - Journal of Biomedical Engineering, Vol. 109, pp. 72-77.

Strick D.M., Fiksen-Olsen M.J., et al., 1994, "Direct Measurement of Renal Medullary Blood Flow in the Dog," American Journal of Physiology, Vol. 267, No. 1, pp. R253-R259.

Sioutos P.J., Orozco J.A., et al., 1995, "Continuous Regional Cerebral Cortical Blood Flow Monitoring in Head Injured Patients," Neurosurgery, Vol. 36, No. 5, pp. 943-950.

Valvano J.W., Patel P.A., and Hayes L.J., 1983, "A Finite Element Analysis of Self-Heated Noninvasive Thermistors," Advances in Bioengineering, pp. 149-150.

Valvano J.W., Allen J.T., and Bowman H.F., 1984, "The Simultaneous Measurement of Thermal Conductivity, Thermal Diffusivity, and Perfusion in Small Volumes of Tissue," ASME Journal of Biomechanical Engineering, Vol. 106, pp. 192-196.

Valvano J.W., Allen J.T., et al., 1984, "An Isolated Rat Liver Model for the Evaluation of Thermal Techniques to Quantify Perfusion," ASME Journal of Biomechanical Engineering, Vol. 106, pp. 187-191.

Valvano J.W., Patel P.A., and Hayes L.J., 1987, "A Finite Element Analysis of a Surface Thermal Probe," ASME Winter Annual Meeting, Boston, Massachusetts, pp. 103-107.

Valvano J.W., Nho S., and Anderson G.T., 1994, "Analysis of the Weinbaum-Jiji Model of Blood Flow in the Canine Kidney Cortex for Self-Heated Thermistors," ASME Journal of Biomechanical Engineering, Vol.116, pp. 201-207.

Van Gelder M.F., "A Thermistor Bead Method for Measurement of Thermal Conductivity and Thermal Diffusivity of Moist Food Materials at High Temperatures," Ph.D. dissertation, http://scholar.lib.vt.edu/theses/available/etd-12698-1093/unrestricted/dissall.pdf

Walsh, J.T., 1984, "A Noninvasive Thermal Method for the Quantification of Tissue Perfusion," M.S. Thesis, Massachusetts Institute of Technology, Cambridge, MA.

Wei D., Saidel G.M., and Jones S.C., 1990, "Optimal Design of a Thermistor Probe for Surface Measurement of Cerebral Blood Flow," IEEE Transactions on Biomedical Engineering, 37(12), pp. 1159-1172.

Wei D., Saidel G.M., and Jones S.C., 1994, "Thermal Method for Continuous Measurement of Cerebral Perfusion," Medical and Biological Engineering and Computing, Vol. 32, pp. 481-488.

Wei D., Saidel G.M., and Jones S.C., 1995, "Estimation of Cerebral Blood Flow from Thermal Measurement," ASME Journal of Biomechanical Engineering, Vol. 117, pp. 74-84.

Weinbaum S. and Jiji L.M., 1979, "A Two Phase Theory for the Influence of Circulation on the Heat Transfer in Surface Tissue", Advancements in Bioengineering, ASME WA/HT-72, pp. 179-182.

Weinbaum S., Jiji L.M. and Lemons D.E., 1984, "Theory and Experiment for the Effect of Vascular Microstructure on Surface Tissue Heat Transfer--Part I: Anatomical Foundation and Model Conceptualization," ASME Journal of Biomechanical Engineering, Vol. 106, pp. 312-330.

Weinbaum S., Jiji L.M., and Lemons D.E., 1984, "Theory and Experiment for the Effect of Vascular Temperature on Surface Tissue Heat Transfer. II. Model Formulation and Solution," ASME Journal of Biomechanical Engineering, Vol. 106, pp. 331-341.

Weinbaum S. and Jiji L.M., 1985, "A New Simplified Bioheat Equation for the Effect of Blood Flow on Local Average Tissue Temperature," ASME Journal of Biomechanical Engineering, Vol. 107, pp. 131-139.

Weinbaum S. and Jiji L.M., 1987, "Discussion of Papers By Wissler and Baish et al. concerning the Weinbaum-Jiji Bioheat Equation," Transactions of the ASME Journal of Biomedical Engineering, Vol. 109, pp. 234-237.

Weinbaum S. and Jiji L.M., 1989, "The Matching of Thermal Fields Surrounding Countercurrent Microvessels and the Closure Approximation in the Weinbaum-Jiji Equation," ASME Journal of Biomechanical Engineering, Vol. 111, pp. 271-275.

Wissler E.H., 1987, "Comments on the New Bioheat Equation Proposed by Weinbaum and Jiji," Transactions of the ASME - Journal of Biomedical Engineering, Vol. 109, pp. 226-233.

Weinbaum S. and Jiji L.M., 1985, "A New Simplified Bioheat Equation for the Effect of Blood Flow on Local Average Tissue Temperature," Transactions of the ASME - Journal of Biomedical Engineering, Vol. 107, pp. 131-139.

Xu L.S., Chen M.M., et al., 1991, "The Theoretical Evaluation of the Pennes, the Chen-Holmes, and the Weinbaum-Jiji Bioheat Transfer Models in the Pig Renal Cortex," ASME Heat Transfer Division, Vol. 189, pp. 15-21.

Yuan D.Y., Valvano J.W., et al., 1995, "2-D Finite Difference Modeling of Microwave Heating in the Prostate," ASME Winter Annual Meeting, Appendix 2, pp. 1-4.

Young L.S., Regan M.C., et al., 1996, "Methods of Renal Blood Flow Measurement," Urology Research, Vol. 24, pp. 149-160.

Zajic F., Brun Z., and Novotny M., 1975, "Time Constant of Thermistors and Its Role in Thermnodilution Methods," Cor Vasa, 17(3), pp. 204-211.

Zhang Y.P., Liang X.G., et al., 2000, "A Method of Determining the Thermophysical Properties and Calorific Intensity of the Organ or Tissue of a Living Body," International Journal of Thermophysics, 21(1), pp. 207-215.

VITA

Graduate College
University of Nevada, Las Vegas

Fredericka Delores Brown

Local Address:
1851 North Green Valley Parkway
#321
Henderson, Nevada 89074

Home Address:
2243 Kaufman Street
Baton Rouge, Louisiana 70807

Degrees:
Bachelor of Science, Physics, 1996
Xavier University of Louisiana

Master of Science, Mechanical Engineering, 1998
University of Nevada, Las Vegas

Special Honors and Awards:
NIH Predoctoral Fellowship
Bridges Scholar
MGE @ MSA Scholarship
Gates Millennium Scholarship
Roosevelt Fitzgerald Outstanding Student Award
Graduate Academic Heritage Achievement Award

Publications:
F. Brown, R. Kozak, B. O'Toole, and R. Boehm, "Replicating the Thermal Environment in a Simulated Thermoplastic Pultrusion Process," SAMPE 2001 Symposium and Exposition, 2001.